ВИДАВНИЧИЙ ДІМ
АКАДЕМ ПЕРІОДИКА

3 **DARK MATTER:** OBSERVATIONAL MANIFESTATION AND EXPERIMENTAL SEARCHES

DARK ENERGY AND DARK MATTER IN THE UNIVERSE

3 VOLUME

DARK MATTER:

OBSERVATIONAL MANIFESTATION AND EXPERIMENTAL SEARCHES

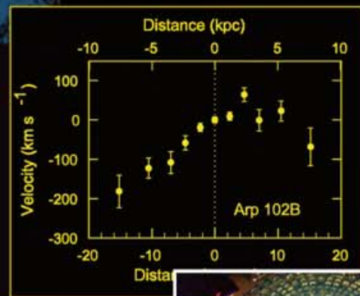

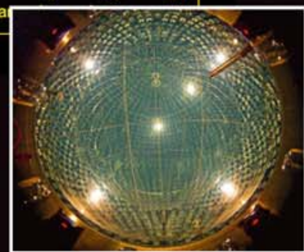

DARK ENERGY AND DARK MATTER IN THE UNIVERSE

VOLUME 3

NATIONAL ACADEMY OF SCIENCES OF UKRAINE
BOGOLYUBOV INSTITUTE FOR THEORETICAL PHYSICS
INSTITUTE FOR NUCLEAR RESEARCH
MAIN ASTRONOMICAL OBSERVATORY
NATIONAL SCIENCE CENTER
"KHARKIV INSTITUTE OF PHYSICS AND TECHNOLOGY"

MINISTRY FOR EDUCATION AND SCIENCE OF UKRAINE
TARAS SHEVCHENKO NATIONAL UNIVERSITY OF KYIV

НАЦІОНАЛЬНА АКАДЕМІЯ НАУК УКРАЇНИ
ІНСТИТУТ ТЕОРЕТИЧНОЇ ФІЗИКИ імені М.М. БОГОЛЮБОВА
ІНСТИТУТ ЯДЕРНИХ ДОСЛІДЖЕНЬ
ГОЛОВНА АСТРОНОМІЧНА ОБСЕРВАТОРІЯ
НАЦІОНАЛЬНИЙ НАУКОВИЙ ЦЕНТР
"ХАРКІВСЬКИЙ ФІЗИКО-ТЕХНІЧНИЙ ІНСТИТУТ"

МІНІСТЕРСТВО ОСВІТИ І НАУКИ УКРАЇНИ
КИЇВСЬКИЙ НАЦІОНАЛЬНИЙ УНІВЕРСИТЕТ
імені ТАРАСА ШЕВЧЕНКА

UDK 524.7+529; 539.123.17,
539.12, 539.16, 539.143, 539.1.08
BBK 22.3, 22.6
D20

Reviewers:

V.A. ZAKHOZHAJ, Dr. Sci., Prof., Professor of the Department of Astronomy and Space Informatics of the Physical Faculty of the V.N. Karazin National University of Kharkiv

I.M. KADENKO, Dr. Sci., Prof., Head of the Department of Nuclear Physics of the Taras Shevchenko National University of Kyiv

Approved for publication by:
Bogolyubov Institute for Theoretical Physics (03.07.2014, protocol No. 6)
Institute for Nuclear Research (26.06.2014, protocol No. 7)
Main Astronomical Observatory (10.07.2014, protocol No. 8)
the National Science Center
"Kharkiv Institute of Physics and Technology"
(27.08.2014, protocol No. 8)
of the National Academy of Sciences of Ukraine as well as
the Astronomical Observatory of the Taras Shevchenko National University of Kyiv
(05.06.2014, protocol No. 7)

Publication was made by a State contract promoting the production of scientific printed material

D20 **Dark** energy and dark matter in the Universe: in three volumes / Editor V. Shulga. — Vol. 3. Dark matter: Observational manifestation and experimental searches / Vavilova I.B., Bolotin Yu.L., Boyarsky A.M., Danevich F.A., Kobychev V.V., Tretyak V.I., Babyk Iu.V., Iakubovskyi D.A., Hnatyk B.I., Sergeev S.G. — K.: Akademperiodyka, 2015. — 375 p.

ISBN 978-966-360-239-4
ISBN 978-966-360-000-0 (vol. 3)

This monograph is the third issue of a three volume edition under the general title "Dark Energy and Dark Matter in the Universe". The authors discuss the observational evidence of the dark matter in the large-scale structures of the Universe as well as the dark matter particle candidates. The monograph is intended for scientists and graduate students specializing in extragalaxy astronomy, theoretical physics, nuclear physics, and high-energy astrophysics. It will be useful also for those advanced readers, who are interested in the problem of nature of the dark energy and dark matter.

UDC 524.7+529; 539.123.17, 539.12, 539.16, 539.143, 539.1.08
BBK 22.3, 22.6

ISBN 978-966-360-239-4
ISBN 978-966-360-000-0 (vol. 3)

CONTENTS

6 CHAPTER

Sterile neutrino dark matter
Boyarsky A.M., Iakubovskyi D.A.

7 CHAPTER

Search for effects beyond the Standard Model of particles in low counting experiments
Danevich F.A., Kobychev V.V., Tretyak V.I.

FOREWORD OF THE EDITOR

This monograph is the third issue of a three volume edition under the general title "Dark Energy and Dark Matter in the Universe". The authors discuss the observational evidence of the dark matter in the large-scale structures of the Universe as well as the dark matter particle candidates.

The first Chapter of this volume has a special meaning for all the authors of the "Dark Energy and Dark Matter in the Universe" monograph because it includes the last papers and notes by Prof. P.I. Fomin, the leading scientist in the "CosmoMicroPhysics" scientific field in Ukraine. In these latter issues, which have been written altogether with A.P. Fomina, they have shown that the self-gravity and gravitational interaction of quantum vacuum fluctuations radically reduces the energy density of the physical vacuum relative to the predictions of local quantum field theory. In this case, the vacuum space becomes discrete and crystal-like on the Planck length scales. The development of vacuum condensates connected with breaking continuous symmetries produces additional reduction of the vacuum energy and makes it an acceptable candidate for dark energy manifesting itself as the acceleration of the cosmological expansion of space. The condition of spatial closeness allows one to give an upper bound on the vacuum energy density. Stationary radial flows of vacuum condensates are further used to explain the nature of dark matter.

As regards the term "CosmoMicroPhysics", it might be interesting to point out several facts related to the foundation of this research field in the former USSR. Dr. Yuri Shtanov, one of the authors of Volume 1 of this monograph related to the Dark Energy problem, recalls the story told him by late Prof. P.I. Fomin that it was him who first coined this term and proposed it to the Russian colleagues who were looking for a good Russian equivalent of the term "astroparticle physics".

The astrophysical direct and indirect evidence of the presence of dark matter in galaxy clusters and groups is discussed in Chapter 2, prepared by I. Vavilova and Iu. Babyk. The authors give a brief summary of the discovery of dark matter and dark matter models. While considering the galaxy groups, the problem of a common halo of groups and halo of individual galaxies in groups is discussed under the evaluation of the "mass-to-luminosity" ratio for sparse galaxy groups in the Local Supercluster and for samples detached from the SDSS spectroscopy survey (this Chapter is prepared by A. Elyiv, O. Melnyk, and I. Vavilova). The next Chapter, written by S. Sergeev and N. Pulatova, is related to consideration of the galaxies with active nuclei, including methods and results of evaluation of the masses of supermassive black holes in their centres as well as properties of host galaxies. The great attention is paid to the dark matter evaluation in the X-ray galaxy clusters, where the DM conception is widely applied to describe the density profiles at the wide scale of cluster's radii.

In the Chapter 5 "Interaction In The Dark Sector" prepared by Yu. Bolotin, A. Kostenko, D. Yerokhin, and O. Lemets, the authors consider in detail different topics associated with interaction in the dark sector. Although the Standard Cosmological Model postulates an absence of interaction between the dark components, there is no fundamental reason for this assumption in the absence of an underlying symmetry which would suppress the coupling. Furthermore, the latest observations (such as the PLANCK collaboration) at the very least do not eliminate this possibility. For these reasons, the study of dark sector interaction is an important field of study, and holds many possibilities. The greatest amount of attention is given to the mechanisms of energy exchange between dark energy and dark matter. We do not only introduce the reader to a large amount of interaction models used in literature (both linear and nonlinear), but also demonstrate how these models affect the dynamics of the Universe. It is shown that the inclusion of dark sector interaction on the one hand greatly expands the capabilities of the Standard Cosmological Model. On the other hand, it allows for a simple return to the fundamental results of the Standard Cosmological Model when the interaction is taken to be weak. The presence of interaction in the dark sector also simplifies the solution of a series of "classical" cosmological problems, such as the cosmic coincidence problem.

Right-handed (sterile) neutrinos are one of the most popular dark matter particle candidates. In the Chapter 6, which is written by A. Boyarsky and D. Iakubovsky, the authors quantify the properties of 'sterile neutrino Universe' depending on two basic parameters — the mass of sterile neutrino dark matter particle and its interaction strength with ordinary particles. In addition to model-independent analysis, throughout this Chapter, they rely on the baseline model — minimal extension of the Standard Model with three right-handed neutrinos. This popular model, dubbed νMSM, provides viable and unified description of three major "beyond the Standard Model" phenomena — dark matter, matter-antimatter asymmetry and neutrino oscillations. It is among a very few models that provide testable resolution of these "beyond the Standard Model" puzzles in the situation when no new physics is found at the LHC (the so-called "nightmare scenario") and suggests how the nature of dark matter and other "beyond the Standard Model" phenomena may nevertheless be checked experimentally using existing experimental technologies and major infrastructure.

Particle properties play a key role in cosmology and astrophysics. Experimental investigations of neutrinoless double beta decay (an unique way to study neutrino and weak interactions) and solar axions (promising candidates for dark matter), measurements of neutrino fluxes from the Sun and the Earth, search for effects beyond the Standard Model (electric charge nonconservation, disappearance of nucleons, electromagnetic properties of neutrino), development of low counting experiments to search for dark matter are presented in this volume in the Chapter 7 prepared by F. Danevich, V. Kobychev, and V. Tretyak. The experiments call for extremely low counting rate and typically are carried out deep underground to minimize background caused by cosmic rays, and use low radioactive nuclear spectroscopy technique. Extremely low background conditions of the frontier astroparticle physics experiments provide also possibility to study very rare beta and alpha decays.

Among the numerous DM candidates ones of the most popular are weakly-interacting massive particles (WIMPs) due to the "WIMP miracle": thermally produced in hot early Universe particles with weak-scale mass and weak interaction velocity averaged cross-section automatically provide close to observed DM abundance. In the supersymmetry (SUSY) as the most promising theory for the extension of SM the lightest neutralino is a leading WIMP candidate. WIMPs can annihilate (or decay if they are metastable) into SM particles (protons-antiprotons, electrons-positrons, deuterons-antideuterons, neutrinos and photons) with energies of order of DM masses, i.e., into cosmic ray particles and photons in subGeV-TeV range. Annihilation or decay of more massive DM particles (superheavy dark matter (SHDM), WIMPZILLAS with masses up to GUT scale) could produce ultra high energy cosmic rays. These properties of DM particles open the possibility for indirect DM detection in cosmic ray window. The state-of-the-art in the search of the signatures of DM annihilation/decay in the observed spectrum of cosmic rays is discussed by B. Hnatyk in the Chapter 8.

This volume was prepared by the authors in 2012-2013 years and revised additionally in 2014.

V. SHULGA

ACKNOWLEDGMENTS

We are grateful to the National Academy of Sciences of Ukraine for the financial support of the Target Scientific Research Programs “Structure and Composition of the Universe: hidden mass and dark energy” (2007—2009) and “Astrophysical and cosmological problems of hidden mass and dark energy of the Universe” (2010—2012) [“CosmoMicroPhysics”] as well as the Target Program of the Space Scientific Research (2012—2016), within which this monograph was originated. We are thankful to academician Valery Shulga, the scientific manager of the “CosmoMicroPhysics” programs and editor of this monograph, for suggestion of its writing, participation in the formation of its content, and organization of its publication. We thank academician Yaroslav Yatskiv for his generous support of these Programs, interest in our research results, and organization of the publication of this monograph. We are also appreciating helpful and highly professional assistance from the staff of the publisher “Akademperiodyka”.

AUTHORS

Bologna—Dublin—Kharkiv—Kyiv—Leiden—Nauchnyj,

October, 2013

7 CHAPTER

SEARCH FOR EFFECTS BEYOND THE STANDARD MODEL OF PARTICLES IN LOW COUNTING EXPERIMENTS

F.A. Danevich, V.V. Kobychev, V.I. Tretyak

In fundamental physics,
if something can be tested, it should be tested.

L.B. Okun [355]

7.1. Introduction

Properties of particles and interactions — and, in particular, properties of neutrino and weak interactions — play a key role not only in particle physics, but also in cosmology and astrophysics. Measurements of neutrino fluxes from the Sun, from cosmic rays in atmosphere, from reactors and accelerators give strong evidence of neutrino oscillations, an effect which cannot be explained in framework of the Standard Model of particles. Search for neutrinoless double beta decay is considered now as an unique tool to study properties of neutrino. Study of this extremely rare nuclear decay with the help of nuclear spectrometry methods, without building of rather expensive accelerators, allows to investigate quite wide range of interesting and important effects beyond the Standard Model: nature of neutrino (is neutrino Dirac or Majorana particle), an absolute scale and the mass scheme of neutrino, to check the lepton number conservation, examine existence of hypothetical Nambu—Goldstone bosons (majorons) and right-handed currents in weak interaction.

Experiments with neutrino detectors, in addition to fundamental investigations of neutrino oscillation parameters, provide important knowledge of electromagnetic properties of neutrino, examine possible existence and mixing with heavy neutrino. Furthermore, the experiments directed to detect solar or/and reactor neutrinos can study neutrino flux from the Earth providing an unique information on our planet structure.

Development of sensitive experimental technique to search for double beta decay, the rarest process ever observed, allow in parallel to study several hypothetical particles and processes, such as decay of electron or nucleons, violation of the Pauli principle, search for mass of photon, etc. Another direction of astroparticle (underground) physics is search for axions, hypothetical particles predicted to explain the strong CP problem in quantum chromodynamics. Axions are also considered as very promising candidates to explain dark matter in the Universe.

There is an evidence for a large amount of invisible (dark) matter in the Universe, which reveals itself only through gravitational interaction. Weakly interacting massive particles (WIMPs), in particular neutralino predicted by the Minimal Supersymmetric extensions of the Standard Model, are considered as one of the most acceptable components of the dark matter. A few current large scale projects to search for dark matter require development of massive (hundreds and thousands kg) ultra-low background detectors which contain certain elements (or variety of elements), have low energy threshold, are extremely radiopure, and are able to distinguish very weak effect from background.

Scintillation detectors possess range of unique properties for the low counting experiments: low radioactive contamination, presence of different elements, stability over tens of years of operation, reasonable price. Moreover, development, during the last decade, of the technique of low temperature scintillating bolometers give a "second wind" for the scintillation method allowing to reach very high energy resolution and low energy threshold, excellent particle discrimination ability, which are especially important features for the next generation double beta and dark matter experiments.

Double β decay and dark matter experiments demand super-low radioactive background which can be reached only in deep underground laboratories and with detectors constructed with super-pure materials. Development of experimental methods to search for the rare events gives possibility to search for other rare processes in nuclear and particle physics, such as transition of nuclei to super-dense state, nuclear decays with cluster emission, rare β and α decays.

We present here brief reviews of current status and describe several recent results obtained in the field over last few years.

7.2. Double beta decay

7.2.1. Basic theory and experimental status

Double beta (2β) decay of atomic nuclei was considered by Maria Goeppert—Mayer in 1935 as nuclear process changing a nuclear charge by two units [257]. As an example, scheme of decay of ^{116}Cd is shown in Fig. 7.1.

Two neutrino (2ν) double beta decay, a process of transformation of nuclei with simultaneous emission of two electrons (positrons) and two antineutrinos (neutrinos):

$$(A, Z) \rightarrow (A, Z+2) + 2e^- + 2\bar{\nu}_e,$$
$$(A, Z) \rightarrow (A, Z-2) + 2e^+ + 2\nu_e$$

is allowed in the Standard Model (SM). In addition to decay with emission of two positrons, capture of electron with positron emission, and double electron capture are possible:

$$e^- + (A, Z) \rightarrow (A, Z-2) + e^+ + 2\nu_e,$$
$$2e^- + (A, Z) \rightarrow (A, Z-2) + 2\nu_e.$$

However, being the second order process in weak interaction, 2β decay is characterized by an extremely low probability: to-date it is the rarest decay observed in direct laboratory experiments. It was detected only for 11 nuclides; corresponding half lives are in the range of 10^{18}—10^{24} yr [410, 411]. The positive experiments where the two neutrino double beta decay was observed, and experiments giving the most stringent limits on two neutrino channel are listed in Table 7.1 (more detailed information, especially on geochemical experiments

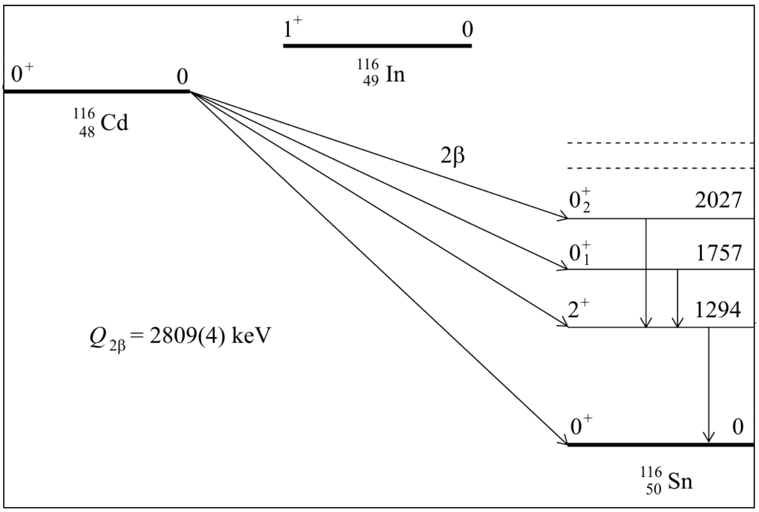

Fig. 7.1. Decay scheme of ^{116}Cd. Energies of excited levels and emitted γ quanta are in keV. $Q_{2\beta}$ is the double beta decay energy [57]

Table 7.1. **Half lives relatively to $2\nu2\beta^-$ decay. The data are presented for transitions to the ground states of the daughter nuclei. Transitions to the first 0^+_1 excited levels of the daughter nuclei ($0^+ \rightarrow 0^+_1$) are observed for ^{100}Mo and ^{150}Nd. If two uncertainties are given, the first one is statistical, and the second one is systematic**

Isotope	$T_{1/2}$, years	Experimental method	Ref.
^{48}Ca	$(4.3^{+2.4}_{-1.1} \pm 1.4) \times 10^{19}$	Enriched ^{48}Ca in time-projection chamber	[65]
	$(4.2^{+3.3}_{-1.3}) \times 10^{19}$	Enriched ^{48}Ca between planar Ge detectors	[168]
	$(4.4^{+0.5}_{-0.4} \pm 0.4) \times 10^{19}$	Tracking calorimeter NEMO-3	[413]
^{76}Ge	$(9.0 \pm 1.0) \times 10^{20}$	HPGe detectors with enriched ^{76}Ge	[418]
	$(1.1^{+0.6}_{-0.3}) \times 10^{21}$	Same	[332]
	$(8.4^{+1.0}_{-0.8}) \times 10^{20}$	"	[167]
	$(1.1 \pm 0.2) \times 10^{21}$	"	[4]
	$(1.77 \pm 0.01^{+0.13}_{-0.11}) \times 10^{21}$	"	[261]
	$(1.55 \pm 0.01^{+0.19}_{-0.15}) \times 10^{21}$	"	[291]
	$(1.74 \pm 0.01^{+0.18}_{-0.16}) \times 10^{21}$	"	[215]
^{82}Se	$(1.2 \pm 0.1 \pm 0.4) \times 10^{19}$	Geochemical	[318]
	$(1.08^{+0.26}_{-0.06}) \times 10^{20}$	Enriched ^{82}Se in time-projection chamber	[228]
	$(8.3 \pm 1.0 \pm 0.7) \times 10^{19}$	Tracking calorimeter NEMO-2	[45]
	$(9.6 \pm 0.3 \pm 1.0) \times 10^{19}$	Tracking calorimeter NEMO-3	[46]
^{96}Zr	$(3.9 \pm 0.9) \times 10^{19}$	Geochemical	[280]
	$(2.1^{+0.8}_{-0.4}) \times 10^{19}$	Tracking calorimeter NEMO-2	[44]
	$(9.4 \pm 3.2) \times 10^{18}$	Geochemical	[429]
	$(2.35 \pm 0.14 \pm 0.16) \times 10^{19}$	Tracking calorimeter NEMO-3	[36]
^{100}Mo	$(3.3^{+2.0}_{-1.0}) \times 10^{18}$	Enriched ^{100}Mo between plastic scintillators and proportional chambers	[419]
	$(1.2^{+0.5}_{-0.3}) \times 10^{19}$	Enriched ^{100}Mo between plastic scintillators in a proportional chamber (ELEGANT V)	[221]
	$(9.5 \pm 0.4 \pm 0.9) \times 10^{18}$	Tracking calorimeter NEMO-2	[202]
	$(7.6^{+2.2}_{-1.4}) \times 10^{18}$	^{100}Mo foil between Si(Li) detectors	[22]
	$(6.82^{+0.38}_{-0.53} \pm 0.68) \times 10^{18}$	^{100}Mo foil in time-projection chamber	[387]
	$(7.2 \pm 0.9 \pm 1.8) \times 10^{18}$	^{100}Mo in ionization chamber with liquid argon	[50]
	$(2.1 \pm 0.3) \times 10^{18}$	Geochemical	[265]
	$(7.11 \pm 0.02 \pm 0.54) \times 10^{18}$	Tracking calorimeter NEMO-3	[46]
^{100}Mo $0^+ \rightarrow 0^+_1$	$(6.1^{+1.8}_{-1.1}) \times 10^{20}$	HPGe γ spectrometry of ^{100}Mo sample	[71]
	$(9.3^{+2.8}_{-1.7}) \times 10^{20}$	HPGe γ spectrometry of ^{100}Mo samples	[78]
	$(5.9^{+1.7}_{-1.1} \pm 0.6) \times 10^{20}$	HPGe γ spectrometry of ^{100}Mo sample	[166]
	$(5.7^{+1.3}_{-0.9} \pm 0.8) \times 10^{20}$	Tracking calorimeter NEMO-3	[48]
	$(5.5^{+1.2}_{-0.8} \pm 0.3) \times 10^{20}$	HPGe γ spectrometry of ^{100}Mo sample	[281]
	$(6.9^{+1.0}_{-0.8} \pm 0.7) \times 10^{20}$	HPGe γ spectrometry of ^{100}Mo sample	[91]
^{114}Cd	$>1.3 \times 10^{18}$ at 90 % CL	$CdWO_4$ crystal scintillator	[92]
^{116}Cd	$(2.6^{+0.9}_{-0.5}) \times 10^{19}$	^{116}Cd foil between plastic scintillators in a proportional chamber (ELEGANT IV)	[222]
	$(2.9^{+0.4}_{-0.3}) \times 10^{19}$	$^{116}CdWO_4$ crystal scintillators	[200]

Table 7.1. **Continued**

Isotope	$T_{1/2}$, years	Experimental method	Ref.
	$(3.75 \pm 0.35 \pm 0.21) \times 10^{19}$	Tracking calorimeter NEMO-2	[47]
	$(2.88 \pm 0.04 \pm 0.16) \times 10^{19}$	Tracking calorimeter NEMO-3	[413]
^{128}Te	$(1.8 \pm 0.7) \times 10^{24}$	Geochemical	[317]
	$(7.7 \pm 0.4) \times 10^{24}$	Geochemical	[150]
	$(2.4 \pm 0.4) \times 10^{24}$	Geochemical	[329]
^{130}Te	$(2.60 \pm 0.28) \times 10^{21}$	Geochemical	[287]
	$(7.5 \pm 0.3 \pm 2.3) \times 10^{20}$	Geochemical	[317]
	$(2.7 \pm 0.1) \times 10^{21}$	Geochemical	[150]
	$(7.9 \pm 1.0) \times 10^{20}$	Geochemical	[404]
	$(6.1 \pm 1.4^{+2.9}_{-3.5}) \times 10^{20}$	Cryogenic bolometer with TeO_2 crystals	[42]
	$(9.0 \pm 1.4) \times 10^{20}$	Geochemical	[329]
	$(7.0 \pm 0.9 \pm 1.1) \times 10^{20}$	Tracking calorimeter NEMO-3	[43]
^{136}Xe	$>1.0 \times 10^{22}$ at 90 % CL	Scintillation detector with liquid xenon enriched in ^{136}Xe	[148]
	$>8.5 \times 10^{21}$ at 90 % CL	High-pressure proportional counter filled by enriched ^{136}Xe	[245]
	$(2.11 \pm 0.04 \pm 0.21) \times 10^{21}$	EXO time projection chamber filled by liquid enriched ^{136}Xe	[8]
	$(2.38 \pm 0.02 \pm 0.11) \times 10^{21}$	KamLAND-Zen liquid scintillator loaded by enriched ^{136}Xe	[243]
^{150}Nd	$(1.88^{+0.66}_{-0.39} \pm 0.19) \times 10^{19}$	^{150}Nd sample in time-projection chamber	[39]
	$(6.75^{+0.37}_{-0.42} \pm 0.68) \times 10^{18}$	^{150}Nd sample in time-projection chamber	[387]
	$(9.11^{+0.25}_{-0.22} \pm 0.63) \times 10^{18}$	Tracking calorimeter NEMO-3	[35]
^{150}Nd $0^+ \to 0^+_1$	$(1.33^{+0.36+0.27}_{-0.23-0.13}) \times 10^{20}$	HPGe γ spectrometry of ^{150}Nd sample	[79]
^{160}Gd	$>1.9 \times 10^{19}$ at 90 % CL	Gd_2SiO_5(Ce) crystal scintillator	[201]
^{186}W	$>2.3 \times 10^{19}$ at 90 % CL	$ZnWO_4$ crystal scintillators	[93]
^{238}U	$(2.0 \pm 0.6) \times 10^{21}$	Radiochemical	[415]

with ^{82}Se, ^{128}Te, ^{130}Te can be found in [410, 411]). Estimation of average half lives of the nuclides is proposed in [70]. It should be stressed, that comparison of the measured half lives of different isotopes relatively to the two neutrino mode allows to tune theoretical calculations for the neutrinoless mode (see below), important to derive values of the effective neutrino mass from experimental data.

In 1937 Ettore Majorana has introduced a true neutral neutrino equivalent to its antiparticle (Majorana neutrino, $\nu \equiv \bar{\nu}$) [323]. In 1939 W.H. Furry [240] considered at the first time possibility of neutrinoless double beta ($0\nu 2\beta$) decay, a process of transformation of (A, Z) to $(A, Z \pm 2)$ through exchange of virtual Majorana neutrinos and accompanied by emission of only electrons or positrons:

$$(A, Z) \rightarrow (A, Z \pm 2) + 2e^{\mp}.$$

Neutrinoless 2β decay of atomic nuclei is forbidden in the SM because this process violates the lepton number by two units [52, 53, 75, 225, 227, 229, 253, 259, 347, 374, 420, 421, 435]. However, this decay is predicted in many SM extensions which expect in a natural way that the neutrino is a Majorana particle with non-zero mass. While experiments on neutrino oscillations already gave evidence that the neutrino is massive [216, 341], these experiments are sensitive only to neutrino mass differences. Double beta decay experiments are considered to-date as the best instrument to determine an absolute scale of neutrino mass, establish the neutrino mass hierarchy, probe the nature of the neutrino (is it a Majorana or a Dirac particle?), test conservation of the lepton number.

The half life of $0\nu2\beta$ decay is inversely proportional to the square of the effective Majorana mass of neutrino $\langle m_\nu \rangle$:

$$(T_{1/2}^{0\nu2\beta})^{-1} = G^{0\nu}(Q_{\beta\beta}, Z) \times |M^{0\nu}|^2 \times \langle m_\nu \rangle^2 \text{ with } \langle m_\nu \rangle = |\Sigma U_{ej}^2 m_{\nu_i}|, \quad (7.1)$$

where $G^{0\nu}(Q_{\beta\beta}, Z)$ is the phase space integral, $M^{0\nu}$ is the nuclear matrix element, m_{ν_i} are the mass eigenstates of neutrino, U_{ej} — matrix elements of mixing between the mass eigenstates and flavor states of neutrino.

Experimental investigations of double β decay are carried out by different approaches: geochemical (measurements of daughter isotopes in old minerals containing element of interest), radiochemical (detection of alpha activity of daughter nuclei in a sample of uranium), direct counting methods by using nuclear detectors. According to Yu.G. Zdesenko [435], the last approach can be divided in two different classes: (a) experiments using a "passive" source placed near detectors; and (b) experiments involving an "active" source, in which a detector contains 2β decay candidate nuclei and thus serves as both source and detector simultaneously.

Developments in the experimental techniques during the last two decades lead to an impressive improvement of sensitivity to the neutrinoless mode of $2\beta^-$ decay up to 10^{23}—10^{25} yr. Readers can find an interesting historical review of double beta decay studies in [76]. History of false discoveries of this rare process is presented in [409]. Results of the most sensitive experiments to search for $0\nu2\beta^-$ decay are given in Table 7.2.

In more general terms the half life relatively to the $0\nu2\beta$ decay should include also admixtures of hypothetical right-handed currents in weak interactions:

$$(T_{1/2}^{0\nu})^{-1} = C_{mm}^{0\nu}(\frac{\langle m_\nu \rangle}{m_e})^2 + C_{m\lambda}^{0\nu}\langle \lambda \rangle \frac{\langle m_\nu \rangle}{m_e} + C_{m\eta}^{0\nu}\langle \eta \rangle \frac{\langle m_\nu \rangle}{m_e} +$$
$$+ C_{\lambda\lambda}^{0\nu}\langle \lambda \rangle^2 + C_{\eta\eta}^{0\nu}\langle \eta \rangle^2 + C_{\lambda\eta}^{0\nu}\langle \lambda \rangle \langle \eta \rangle,$$

Table 7.2. **Results of the most sensitive experiments to search for $0\nu 2\beta^-$ decay. If not specified explicitly, the limits are given for the transition to the ground state of the daughter nuclei. The values of the effective Majorana neutrino mass $\langle m_\nu \rangle$ and coupling constants $\langle \lambda \rangle$, $\langle \eta \rangle$ derived from high sensitivity $0\nu 2\beta$ decay experiments are also presented. The limits on $\langle m_\nu \rangle$ and $\langle \eta \rangle$ from the observation of 2β decay of ^{128}Te were derived under assumption that the 2β decay of this isotope is due to the neutrinoless decay [150]**

Isotope	$T_{1/2}$, years	CL	m_ν, eV	$\eta(10^{-6})$	$\lambda(10^{-8})$	Experimental method	Ref.
^{48}Ca	$>1.4 \times 10^{22}$	90 %				CaF_2 crystal scintillators	[353]
	$>5.8 \times 10^{22}$						[416]
^{76}Ge	$>7.4 \times 10^{24}$	90 %		<1.1	<0.64	HPGe detectors from	[261]
	$>1.9 \times 10^{25}$	90 %	<0.35			enriched ^{76}Ge	[291]
	$>1.57 \times 10^{25}$	90 %	$<(0.33—1.35)$				[5]
	$(2.23^{+0.44}_{-0.31}) \times 10^{25}$	68 %	0.32 ± 0.03	$0.692^{+0.058}_{-0.056}$	$0.305^{+0.026}_{-0.025}$		[290]
^{82}Se	$>2.7 \times 10^{22}$	68 %				^{82}Se foil in time-projection chamber	[228]
	$>2.7 \times 10^{22}$	90 %	$<(1.7—4.9)$	<3.8		NEMO-3	[46]
^{96}Zr	$>9.1 \times 10^{21}$	90 %				NEMO-3	[36]
^{100}Mo	$>5.5 \times 10^{22}$	90 %	$<(2.1)—4.8$			^{100}Mo foil between plastic	[220]
	$>4.2 \times 10^{22}$			$<(3.2—4.7)$		scintillators in proportional	
	$>4.9 \times 10^{22}$				$<(2.4—2.7)$	chamber (ELEGANT V)	
	$>4.6 \times 10^{23}$	90 %	$<(0.7—2.8)$	<2.5		NEMO-3	[46]
	$>8.9 \times 10^{22}$	90 %				NEMO-3	[48]
^{114}Cd	$>1.1 \times 10^{21}$	90 %				$CdWO_4$ crystal scintillator	[92]
^{116}Cd	$>1.7 \times 10^{23}$	90 %	$<(1.5—1.7)$	<2.2	<2.5	$^{116}CdWO_4$ crystal scintillators	[200]
	$>1.4 \times 10^{22}$						
	$>1.4 \times 10^{22}$ (0_1^+)						
	$>2.9 \times 10^{22}$ (2_1^+)						
^{128}Te	$>1.1 \times 10^{23}$	90 %				TeO_2 cryogenic bolometers	[42]
	$(7.2 \pm 0.4) \times 10^{24}$		$<(1.1—1.5)$		<5.3	Geochemical	[150]
^{130}Te	$>2.1 \times 10^{23}$	90 %	$<(1.6—2.4)$		$<(0.9—5.3)$	TeO_2 cryogenic bolometers	[42]
	$>3.0 \times 10^{24}$		$<(0.19—0.68)$				[41]
	$>3.1 \times 10^{22}$ (2_1^+)						[42]
^{134}Xe	$>5.8 \times 10^{22}$	90 %				Liquid xenon scintillation detector	[148]
^{136}Xe	$>3.4 \times 10^{23}$	90 %	$<(1.8)—5.2$			Time projection chamber with ^{136}Xe	[424]
	$>2.6 \times 10^{23}$			<4.4	<2.3		
	$>1.2 \times 10^{24}$		<2.9			Liquid xenon scintillation detector	[148]
^{150}Nd	$>1.2 \times 10^{21}$	90 %				Time projection chamber with ^{150}Nd foil	[387]
	$>1.8 \times 10^{22}$	90 %	$<(4.0—6.8)$			NEMO-3	[35]
^{160}Gd	$>1.3 \times 10^{21}$	90 %				$Gd_2SiO_5(Ce)$ crystal scintillator	[201]
^{186}W	$>1.1 \times 10^{21}$	90 %				$CdWO_4$ crystal scintillators	[200]

Table 7.3. **The most sensitive experiments to search for double β decay with majoron emission. All the limits are given at 90 % CL**

Isotope	$T_{1/2}$, years	Experimental method	Ref.
^{76}Ge	$>1.7 \times 10^{22}$	HPGe detectors with enriched ^{76}Ge	[87]
^{82}Se	$>1.5 \times 10^{22}$	NEMO-3	[49]
^{100}Mo	$>2.7 \times 10^{22}$	NEMO-3	[49]
^{116}Cd	$>8.0 \times 10^{21}$	$^{116}CdWO_4$ crystal scintillators	[200]
^{128}Te	$>7.2 \times 10^{24}$	Geochemical	[150]
^{130}Te	$>2.2 \times 10^{21}$	TeO_2 cryogenic bolometers	[42]
^{136}Xe	$>5.0 \times 10^{23}$	Liquid xenon scintillation detector	[148]
^{150}Nd	$>1.5 \times 10^{21}$	NEMO-3	[35]

where $\langle\lambda\rangle$ describes the coupling between the right-handed lepton current and right-handed quark current, and $\langle\eta\rangle$ describes the coupling between the right-handed lepton current and left-handed quark current. The effective Majorana neutrino mass and the right-handed current coupling constants derived from the most sensitive $0\nu2\beta$ decay experiments are presented in Table 7.2.

Neutrinoless 2β decay may also occur due to existence of majorons, hypothetical neutral pseudoscalar zero mass (or very light) Nambu—Goldstone bosons, which couple to Majorana neutrinos and may be emitted in the neutrinoless 2β decay [180, 181, 246]). The most sensitive experiments to search for majorons are presented in Table 7.3.

According to the Schechter—Valle theorem [383], observation of neutrinoless double β decay implies the Majorana nature of neutrinos with non-vanishing mass. Generally speaking, the neutrinoless double beta decay can be mediated by different hypothetical processes beyond the SM.

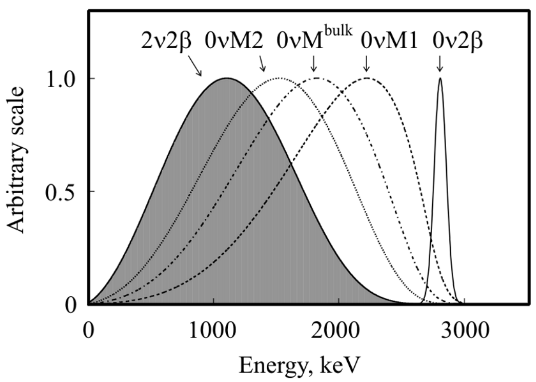

Fig. 7.2. Response functions of a detector with the energy resolution 4 % (full width at the half of peak maximum, FWHM) for the 2ν and 0ν modes of the 2β decay of ^{116}Cd

Broad energy spectra of two electrons are expected in case of two neutrino 2β decay and neutrinoless double β decay with emission of one, two and bulk [342] majorons. A sharp peak with the energy equal to $Q_{\beta\beta}$ and the width determined by the energy resolution of a detector is expected in a case of $0\nu2\beta$ decay (see Fig. 7.2).

Several high sensitivity double beta decay projects are in preparation or in R&D stage: CANDLES (search for 2β decay

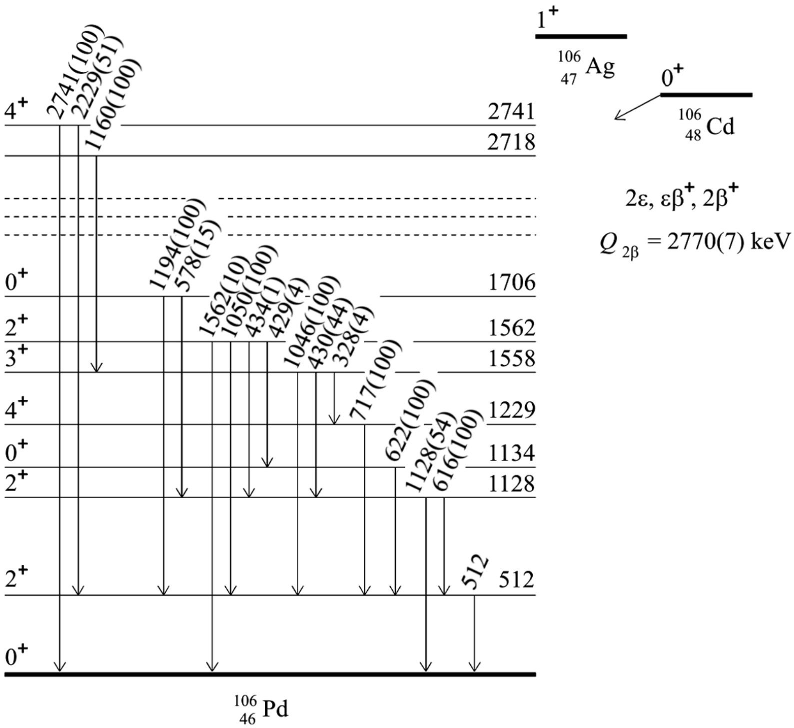

Fig. 7.3. Decay scheme of ^{106}Cd. Energies of excited levels and emitted γ quanta are in keV (relative intensities of γ quanta are given in parentheses). $Q_{2\beta}$ is the double beta decay energy

of ^{48}Ca with the help of CaF_2 scintillators [433]), CUORE (^{130}Te, low temperature TeO_2 bolometers [40, 234]), GERDA [385] and MAJORANA [3] (^{76}Ge, semiconductor high-purity germanium detectors), LUICFER (^{82}Se, ZnSe scintillating bolometers operated at 20 mK [254]) and SuperNEMO (track detector based on NEMO-3 technology [72]), AMoRE (^{100}Mo, $CaMoO_4$ crystal scintillators [314]), EXO (^{136}Xe, time-projection chamber filled by liquid xenon with detection of scintillation [23]) and KamLAND-Zen (^{136}Xe dissolved in large volume liquid scintillator [405]), SNO+ (^{150}Nd, neodymuim loaded liquid scintillator [178]). All the experiments (except the CANDLES and CUORE projects in their first stages) intend to use hundred kilograms of enriched isotopes.

Experimental investigations are concentrated mostly on $2\beta^-$ decays, processes with emission of two electrons. Results for double positron decay ($2\beta^+$), electron capture with positron emission ($\varepsilon\beta^+$), and capture of two electrons from atomic shells (2ε) are much more modest (as an example, the decay scheme of ^{106}Cd is presented in Fig. 7.3). The most sensitive experiments give limits on the 2ε, $\varepsilon\beta^+$ and $2\beta^+$ processes on the level of 10^{16}—10^{21} yr (see Table 7.4).

Table 7.4. **Results of the most sensitive experiments to search for double electron capture (2ε), electron capture with emission of positron ($\varepsilon\beta^+$), and double positron emission ($2\beta^+$). In those cases where it is not specified, the limits are given for the transitions to the ground state of the daughter nuclei. Results correspond to 90 % CL, except of [98, 145, 328] which correspond to 68 % CL**

Isotope	Modes and channels of decay	$T_{1/2}$, years	Experimental method	Ref.
^{40}Ca	$2\nu 2\varepsilon$	$>5.9 \times 10^{21}$	CaF_2(Eu) crystal scintillators	[94]
^{64}Zn	$2\nu 2K$	$>1.1 \times 10^{19}$	$ZnWO_4$ crystal scintillators	[95]
	$0\nu 2\varepsilon$	$>3.2 \times 10^{20}$	Same	
	$2\nu \varepsilon\beta^+$	$>1.0 \times 10^{21}$	”	
	$0\nu \varepsilon\beta^+$	$>8.7 \times 10^{20}$	”	
^{74}Se	$0\nu 2\varepsilon(2_2^+, 1204.2$ keV$)$	$>5.5 \times 10^{18}$	HPGe γ spectrometry of enriched ^{74}Se	[73]
^{78}Kr	$2\nu 2K$	$>1.5 \times 10^{21}$	Proportional counter with enriched ^{78}Kr	[244]
^{96}Ru	$0\nu 2K$	$>1.2 \times 10^{19}$	HPGe γ spectroscopy of Ru sample	[96]
	$2\nu \varepsilon\beta^+$	$>2.5 \times 10^{18}$	Same	
	$2\nu 2\beta^+$	$>3.9 \times 10^{18}$	”	
^{106}Cd	$2\nu 2\varepsilon$	$>3.6 \times 10^{20}$	^{106}Cd foil between HPGe (TGV)	[378]
	$2\nu \varepsilon\beta^+$	$>4.1 \times 10^{20}$	^{106}Cd sample between NaI(Tl) detectors	[98]
	$0\nu \varepsilon\beta^+$	$>3.7 \times 10^{20}$	Same	
	$(2\nu + 0\nu)\ 2\beta^+$	$>1.6 \times 10^{20}$	”	
	$0\nu 2\varepsilon$	$>1.3 \times 10^{21}$	$^{106}CdWO_4$ crystal scintillator	[99]
	$0\nu \varepsilon\beta^+$	$>2.6 \times 10^{21}$	Same	
	$2\nu 2\beta^+$	$>6.0 \times 10^{20}$	”	
	$0\nu 2\beta^+$	$>1.3 \times 10^{21}$	”	
^{108}Cd	$2\nu 2K$	$>1.1 \times 10^{18}$	$CdWO_4$ crystal scintillator	[92]
	$0\nu 2\varepsilon$	$>1.0 \times 10^{18}$	Same	
^{120}Te	$2\nu \varepsilon\beta^+$	$>7.6 \times 10^{19}$	TeO_2 cryogenic bolometers	[26]
	$0\nu \varepsilon\beta^+$	$>1.9 \times 10^{21}$	Same	
^{130}Ba	$2\varepsilon + \varepsilon\beta^+ + 2\beta^+$	$(2.2 \pm 0.5) \times 10^{21}$	Geochemical	[328]
^{132}Ba	2ε	$>2.2 \times 10^{21}$	Geochemical	[328]
^{136}Ce	$2\nu 2K$	$>3.2 \times 10^{16}$	$CeCl_3$ crystal scintillator	[100]
	$0\nu 2K$	$>3.0 \times 10^{16}$	Same	
	$2\nu \varepsilon\beta^+$	$>2.4 \times 10^{16}$	”	
	$0\nu \varepsilon\beta^+$	$>9.0 \times 10^{16}$	”	
	$2\nu 2\beta^+$	$>1.8 \times 10^{16}$	Gd_2SO_5(Ce) crystal scintillator	[201]
	$0\nu 2\beta^+$	$>6.9 \times 10^{17}$	CeF_3 crystal scintillator	[145]
^{156}Dy	$2\nu 2K$	$>6.1 \times 10^{14}$	HPGe γ spectrometry	[101]
	$0\nu 2K$	$>1.7 \times 10^{16}$	Same	
	$(2\nu + 0\nu)\ \varepsilon\beta^+$	$>1.9 \times 10^{16}$	”	
^{180}W	$2\nu 2K$	$>1.0 \times 10^{18}$	$ZnWO_4$ crystal scintillators	[95]
	$0\nu 2\varepsilon$	$>1.3 \times 10^{18}$	Same	
^{190}Pt	$2\nu 2K$	$>8.4 \times 10^{14}$	HPGe γ spectrometry	[102]
	$0\nu 2K$	$>5.7 \times 10^{15}$	Same	
	$2\nu \varepsilon\beta^+$	$>9.2 \times 10^{15}$	”	

Reasons for this situation are: (1) lower energy releases in 2ε, $\varepsilon\beta^+$ and $2\beta^+$ processes in comparison with those in $2\beta^-$ decay, that result in lower probabilities of the processes, as well as making background supp ression difficult; (2) usually lower natural abundances of $2\beta^+$ isotopes (which are typically lower- than 1 % with only few exceptions). Nevertheless, studies of neutrinoless 2ε and $\varepsilon\beta^+$ decays are important to explain the mechanism of neutrinoless $2\beta^-$ decay: is it due to non-zero neutrino mass or to the right-handed admixtures in weak interactions [266].

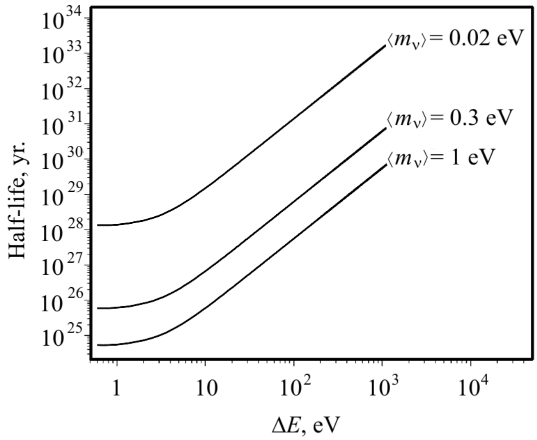

Fig. 7.4. Calculated dependence of the half life of ^{106}Cd relatively to the resonant $0\nu2\varepsilon$ capture to excited levels of ^{106}Pd on parameter ΔE (see text) for different values of the effective neutrino mass [99]

Another important motivation to search for double electron capture appears from a possibility of a resonant process due to energy degeneracy between initial and final state of mother and daughter nuclei. Such a coincidence could give a resonant enhancement of the neutrinoless double electron capture. The possibility of the resonant neutrinoless double electron capture was discussed time ago in [149, 398, 422, 432], where an enhancement of the rate by some orders of magnitude was predicted. Such a resonant process could occur if the energy of transition ($Q_{\beta\beta}$) minus two binding energies of electrons on atomic shells of daughter nucleus is near to the energy of the ground or an excited level ($E_{\rm exc}$) of a daughter isotope. Fig. 7.4 shows results of calculations [99] for one of the most promising isotopes ^{106}Cd.

The half life relatively to $0\nu2\varepsilon$ decay is expected to become shorter with decrease of the difference between the initial and the final state of mother anddaughter nuclei:

$$\Delta E = Q_{\beta\beta} - E_{\rm exc} - (E_{b_i} + E_{b_j}),$$

where E_{b_i} and E_{b_j} are the energies of binding electrons on i and j shells of daughter atoms (a combination $i = j$ is also possible). The potentially 2ε active nuclei having excited levels with energies satisfying such a condition are listed in Table 7.5.

It should be stressed that the present accuracy of the data on the energy of 2β decay (which come from the accuracy of atomic mass measurements) in most of the cases is on the level of a few keV. Therefore, precise measurements

Table 7.5. **Double electron capture processes with possibility of resonant enhancement due to energy degeneracy between initial and final state of mother and daughter nuclei**

Transition, isotopic abundance [147], energy of decay (keV) [57]	Energy (E_b) of binding electrons	Double electron capture from level(s)	ΔE, keV	Experimental limits on $T_{1/2}$	Theoretical estimations of $T_{1/2}$
^{74}Se→^{74}Ge, 0.89(4) %, 1209.7(0.6)	E_b(L$_1$) = 1.4	2L$_1$, 2$^+$, 1204.2	2.7 ± 0.6	$>5.5 \times 10^{18}$ [73]	
^{78}Kr→^{78}Se, 0.355(3) %, 2846.4(2.0)	E_b(L$_1$) = 1.7	2L$_1$, (2$^+$), 2838.5	4.5 ± 2		
^{96}Ru→^{96}Mo, 5.54(14) %, 2718(8)	E_b(K)= 20.0 E_b(L$_1$) = 2.9	KL$_1$, 2$^+$, 2700.2 2L$_1$, 2712.7	-5.1 ± 8 -0.5 ± 8	$>2.2 \times 10^{19}$ [96, 97] $>5.1 \times 10^{19}$ [96, 97]	
^{106}Cd→^{106}Pd, 1.25(6) %, 2770(7)	E_b(K)= 24.4	2K, 2717.6	3.6 ± 7	$>1.4 \times 10^{20}$ [99]	
^{112}Sn→^{112}Cd , 0.97(1) %, 1919(4)	E_b(K)= 26.4	2K, 0$^+$, 1871.0	-5.4 ± 4	$>1.4 \times 10^{18}$ [203] $>9.2 \times 10^{19}$ [74]	$\sim 10^{29}$ [149], 1.4×10^{29} [398]
^{124}Xe→^{124}Te, 0.0952(3) %, 2864.4(2.2)	E_b(L$_1$) = 4.9	2L$_1$, 2853.2 2L$_1$, 2,3, 2858.9	1.4 ± 2.2 -4.3 ± 2.2		9×10^{24}—2×10^{33} [307]
^{130}Ba→^{130}Xe, 0.106(1) %, 2630.1(2.9)	E_b(K)= 34.6 E_b(L$_1$) = 5.5	2K, 2544.4 2L$_1$, 2608.4	6.5 ± 2.9 0.7 ± 2.9	$>4.0 \times 10^{21}$ [80] $(2.2 \pm 0.5) \times 10^{21}$ [328] $>4.0 \times 10^{21}$ [80] $(2.2 \pm 0.5) \times 10^{21}$ [328]	
^{136}Ce→^{136}Ba, 0.185(2) %, 2419(13)	E_b(K) = 37.4 E_b(L$_1$) = 6.0	2K, 0$^+$, 2315.3 2K, 2349.5 2L$_1$, (1$^+$, 2$^+$), 2392.1 2L$_1$, (1$^+$, 2$^+$), 2399.9	28.8 ± 13 -5.3 ± 13 14.9 ± 13 7.1 ± 13	 $>2.4 \times 10^{15}$ [90] $>4.1 \times 10^{15}$ [90]	5×10^{29} [398], 1×10^{23}—7×10^{29} [307] 1×10^{23}—2×10^{33} [307] 8×10^{22}—3×10^{31} [307] 8×10^{22}—5×10^{31} [307]
^{152}Gd→^{152}Sm, 0.20(1) %, 55.70(18)	E_b(K) = 46.8	KL$_1$, g.s. 0$^+$	1.2 ± 0.2		5×10^{24} [398], 10^{26} [226], 2×10^{23}—2×10^{31} [307]
^{156}Dy→^{156}Gd, 0.056(3) %, 2010(6)	E_b(K) = 50.2 E_b(L$_1$) = 8.4	2K, 2$^+$, 1914.8 KL$_1$, 1$^-$, 1946.4 KL$_1$, 0$^-$, 1952.4 2L$_1$, 0$^+$, 1988.5 2L$_1$, 2$^+$, 2003.8	-3 ± 6 7 ± 6 1 ± 6 7 ± 6 -6 ± 6	$>1.1 \times 10^{16}$ [101] $>9.6 \times 10^{15}$ [101] $>2.6 \times 10^{16}$ [101] $>1.9 \times 10^{16}$ [101] $>3.0 \times 10^{14}$ [101]	 8×10^{23}—8×10^{30} [307]
^{162}Er→^{162}Dy, 0.139(5) %, 1844.2(2.7)	E_b(K) = 53.8 E_b(L$_1$) = 9.0	KL$_1$, 2$^+$, 1782.7	-1.3 ± 2.7		

^{164}Er→^{164}Dy, 1.601(3) %, 23.7(2.1)	$E_b(L_1) = 9.0$	2L$_1$, g.s. 0^+	5.7±2.1		4×10^{23}—5×10^{32} [307]
^{168}Yb→^{168}Er, 0.123(3) %, 1422(4)	$E_b(K) = 57.5$ $E_b(N_1) = 0.45$	KL$_1$, 1^-, 1358.9 2N, 0^+, 1422.1	−4.2±4 −1.0±4		4×10^{23}—5×10^{29} [307] 1×10^{24}—8×10^{32} [307]
^{180}W→^{180}Hf, 0.12(1) %, 144(4)	$E_b(K)=65.4$	2K, g.s. 0^+	13.2 ± 4	$>1.3\times10^{18}$ [95]	3×10^{27}—5×10^{30} [398], 3×10^{22}—4×10^{27} [307]
^{184}Os→^{184}W, 0.02(1) %, 1451.2(1.0)	$E_b(K) = 69.5$	2K, 0^+, 1322.1	−9.9±1		3×10^{22}—2×10^{27} [307]
^{190}Pt→^{190}Os, 0.014(1),%, 1383(6)	$E_b(N_1) = 0.65$	2N, $(0,1,2)^+$, 1382.4	−0.7±6	$>2.9\times10^{16}$ [102]	3×10^{23}—6×10^{31} [307]

of atomic mass difference for the potentially interesting isotopes and accurate determination of the excited levels characteristics (spin, parity, decay channels) are requested. Meanwhile, development of experimental technique to search for double electron capture in different nuclei is important. The resonant double electron capture experiments can be realized both by the "passive" and "active" source techniques. One should keep in mind that nuclei with high nuclear charge Z are favorable from the point of view of the decay probability.

Recently several experiments were performed to search for resonant double electron capture. Scintillation technique was applied to investigate ^{106}Cd [99] and ^{180}W [95], while ultra-low background HPGe γ spectrometry was used to search for resonant processes in ^{74}Se [73], ^{96}Ru [96,97], ^{156}Dy, ^{158}Dy [101] and ^{190}Pt [102]. According to estimations [226, 389], in case of ^{152}Gd and ^{164}Er the sensitivity can be comparable to the favored $0\nu2\beta^-$ decays of nuclei. However, the energy release in double electron capture of these nuclei is expected to be very low (several keV) which makes certain difficulties to carry out high sensitivity experiments.

7.2.2. Search for 2β processes with the help of low background γ spectrometry

Search for 2β processes in ^{96}Ru, ^{104}Ru, ^{156}Dy, ^{158}Dy, ^{190}Pt and ^{198}Pt. A search for 2β decay of ^{96}Ru and ^{104}Ru was carried out by using a ruthenium sample with mass of 473 g with the HPGe detector GeCris (468 cm^3) over 986 h, and in the GeMulti setup (four HPGe detectors, ≈225 cm^3 volume each one) over 1176 h in the Gran Sasso underground laboratory of INFN (Italy). The measurements allowed to establish limits on 2β processes in ruthenium on the level of $T_{1/2} \sim 10^{18}$—10^{19} yr [96,97]. In 2010 the ruthenium (the total mass of the initial material was increased to ≈900 g) was purified by electron beam melting to remove potassium (the activity of ^{40}K in the ruthenium before the purification was 3.3 ± 0.6 Bq/kg, while after the purification the activity was reduced by one order of magnitude). Now measurements are in progress in the GeMulti set-up. We estimate a sensitivity of the experiment to search for 2β processes in ^{96}Ru and ^{104}Ru at the level of 10^{20}—10^{21} yr depending on the decay channel.

A search for 2β decay of dysprosium was realized for the first time with the help of an ultra-low background HPGe γ detector of 244 cm^3 volume. After 2512 h of data taking with a 322 g sample of Dy_2O_3 limits on 2β processes in ^{156}Dy and ^{158}Dy have been established at the level of $T_{1/2} \sim 10^{14}$—10^{16} yr [101].

The measurements performed over 1815 h with a 42.5 g sample of platinum with the GeCrys HPGe γ spectrometer were used to set limits on double β processes in ^{190}Pt in the range of $T_{1/2} \sim 10^{14}$—10^{16} yr [102]. The search for the possible resonant $0\nu2\varepsilon$ capture to the 1382.4 keV level was realized for the first time.

Main results of investigations of possible resonant neutrinoless double electron capture in ^{96}Ru, ^{156}Dy, ^{158}Dy and ^{190}Pt are summarized in Table 7.5.

7.2.3. Two neutrino 2β decay of ^{100}Mo to the first 0^+ excited level of ^{100}Ru

A 1199 g sample of molybdenum oxide with molybdenum enriched in ^{100}Mo to 99.5 % was measured over 18120 h in the GeMulti set-up. Two γ quanta of 540 keV and of 591 keV emitted in the deexcitation process after $2\nu2\beta$ decay of ^{100}Mo to the 0^+_1 excited level of ^{100}Ru ($E_{\mathrm{exc}} = 1131$ keV) were observed both in coincidence and in the sum spectra (the sum spectrum is shown in Fig. 7.5 together with the background data). The measured half life $T_{1/2} = 6.9^{+1.0}_{-0.8}(\mathrm{stat.}) \pm 0.7(\mathrm{syst.}) \times 10^{20}$ yr [91] is in agreement with positive results obtained in previous experiments [48, 71, 281].

7.2.4. Double β experiments with the help of scintillation detectors

Search for 2β processes in ^{64}Zn, ^{70}Zn, ^{180}W and ^{186}W with low background $ZnWO_4$ crystal scintillators. A search for 2β processes in ^{64}Zn, ^{70}Zn, ^{180}W and ^{186}W has been performed in the low background DAMA/R&D set-up at the Gran Sasso underground laboratory by using $ZnWO_4$ crystal scintillators. First results of the experiment were reported in [93, 103]. New improved half life limits on double beta decay of Zn and W isotopes were set on the level of 10^{18}—10^{21} yr by analysis of the total 0.3487 kg × yr exposure [95]. In particular, limits on 2β decay in ^{64}Zn were set as: $T^{2\nu2K}_{1/2} \geq 1.1\times10^{19}$ yr, $T^{0\nu2\varepsilon}_{1/2} \geq 3.2\times10^{20}$ yr, $T^{2\nu\varepsilon\beta^+}_{1/2} \geq 9.4\times10^{20}$ yr, and $T^{0\nu\varepsilon\beta^+}_{1/2} \geq 8.5\times10^{20}$ yr (all the limits at 90 % confidence level). The energy

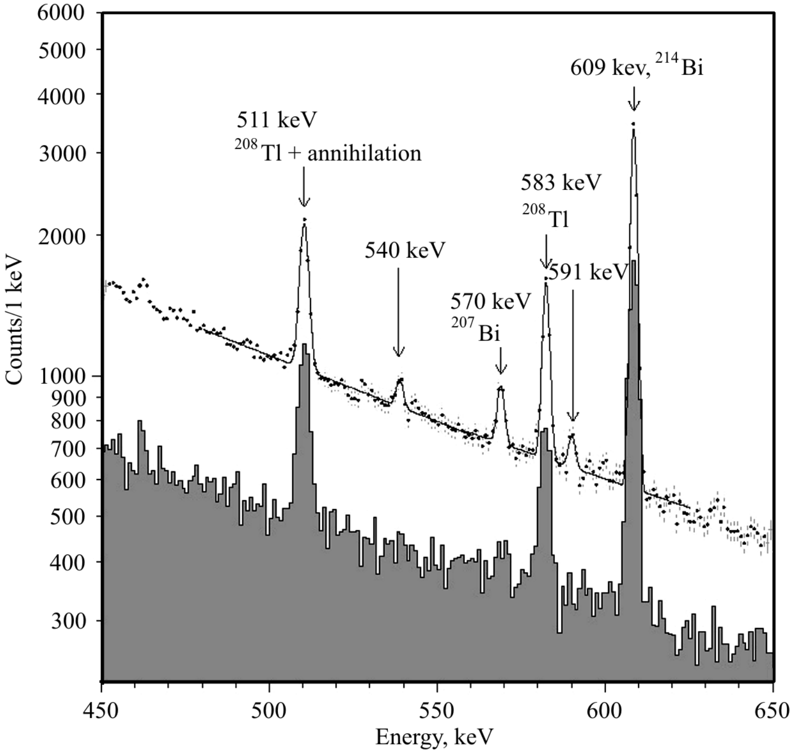

Fig. 7.5. The energy spectrum collected for 18120 h with the 1199 g $^{100}MoO_3$ sample (top) and the background spectrum collected for 7711 h (bottom; normalized to 18120 h)

spectrum of the $ZnWO_4$ crystal scintillator $\oslash 41\times 27$ mm measured over 2798 h, corrected for the energy dependence of detection efficiency, together with the $2\nu 2K$ peak of ^{64}Zn with $T_{1/2}^{2\nu 2K} = 1.1 \times 10^{19}$ yr excluded at 90 % C.L. is presented in Fig. 7.6. The measured energy spectrum of the $ZnWO_4$ scintillation crystals (the total exposure is 0.349 kg × yr) together with the GEANT4 simulated response functions for $\varepsilon\beta^+$ process in ^{64}Zn excluded at 90 % C.L. is shown in Fig. 7.7 together with the most important components of the background.

The $0\nu 2\varepsilon$ decay in ^{180}W was restricted to the level of $T_{1/2} \geq 1.3 \times 10^{18}$ yr (possibility of this decay can be increased through the resonant enhancement).

Search for 2β decay of cerium with CeCl₃ crystal scintillators. A search for 2β processes in ^{136}Ce, ^{138}Ce and ^{142}Ce has been performed over 1638 h by using a 6.9 g $CeCl_3$ crystal scintillator. New improved half life limits have been obtained, in particular for ^{136}Ce: $T_{1/2}^{2\nu 2K} \geq 3.2 \times 10^{16}$ yr, $T_{1/2}^{0\nu 2K} \geq 3.0 \times 10^{16}$ yr, $T_{1/2}^{2\nu\varepsilon\beta^+} \geq 2.4 \times 10^{16}$ yr, $T_{1/2}^{0\nu\varepsilon\beta^+} \geq 0.9 \times 10^{17}$ yr [100].

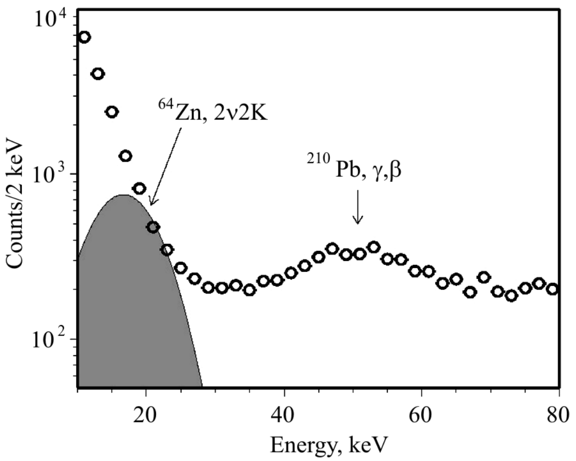

Fig. 7.6. The energy spectrum of the $ZnWO_4$ crystal scintillator ⌀41 × 27 mm measured over 2798 h, corrected for the energy dependence of detection efficiency, together with the $2\nu 2K$ peak of ^{64}Zn with $T_{1/2}^{2\nu 2K} = 1.1 \times 10^{19}$ yr excluded at 90 % C.L.

The development of radiopure $CeCl_3$ scintillators is of particular interest: a resonant 0ν double electron capture in ^{136}Ce is possible to a few excited levels of ^{136}Ba.

Search for double β processes in ^{106}Cd, ^{108}Cd, ^{114}Cd and ^{116}Cd with the help of cadmium tungstate crystal scintillators. Search for double beta processes in ^{108}Cd and ^{114}Cd was realized by using data of the low background experiment with $CdWO_4$ crystal scintillator at the the Gran Sasso underground laboratory. The $CdWO_4$ detector, experimental set-up, measurements and data analysis are described in detail in [104]. Fits of the measured spectra in different energy regions give the limits on double β processes in ^{108}Cd and ^{114}Cd (at 90 % CL): $T_{1/2}^{2\nu 2K}(^{108}\text{Cd}) \geq 1.1 \times 10^{18}$ yr, $T_{1/2}^{0\nu 2\varepsilon}(^{108}\text{Cd}) \geq 1.0 \times 10^{18}$ yr, $T_{1/2}^{2\nu 2\beta}(^{114}\text{Cd}) \geq 1.3 \times 10^{18}$ yr, $T_{1/2}^{0\nu 2\beta}(^{114}\text{Cd}) \geq$ $\geq 1.1 \times 10^{21}$ yr [92].

Cadmium tungstate crystals enriched in ^{106}Cd (231 g, isotopic abundance of ^{106}Cd 66%) [105] and in ^{116}Cd (1868 g, 82%) [77] were developed (see section 7.9.2) to search for 2β decay of ^{106}Cd and ^{116}Cd. The scintillators show excellent optical and scintillation properties thanks to a careful purification of initial materials and to the use of the low-thermal-gradient Czochralski technique to grow the crystals. Limits on different channels of 2β decay of ^{106}Cd: $T_{1/2}^{0\nu 2\varepsilon} \geq 3.6 \times 10^{20}$ yr, $T_{1/2}^{2\nu\varepsilon\beta^+} \geq 7.2 \times 10^{19}$ yr, $T_{1/2}^{0\nu\varepsilon\beta^+} \geq 2.1 \times 10^{20}$ yr, $T_{1/2}^{2\nu 2\beta^+} \geq 2.5 \times 10^{20}$ yr, $T_{1/2}^{0\nu 2\beta^+} \geq 2.1 \times 10^{20}$ yr were derived from the 1320 h experiment [106]. The resonant $0\nu 2\varepsilon$ processes were restricted as $T_{1/2}^{0\nu 2K} \geq$ $\geq 1.4 \times 10^{20}$ yr and $T_{1/2}^{0\nu KL} \geq 3.2 \times 10^{20}$ yr. An analysis of 6591 h data is in progress. A new phase of the experiment with the enriched $^{106}CdWO_4$ crystal in coincidence with the GeMulti set-up is in preparation.

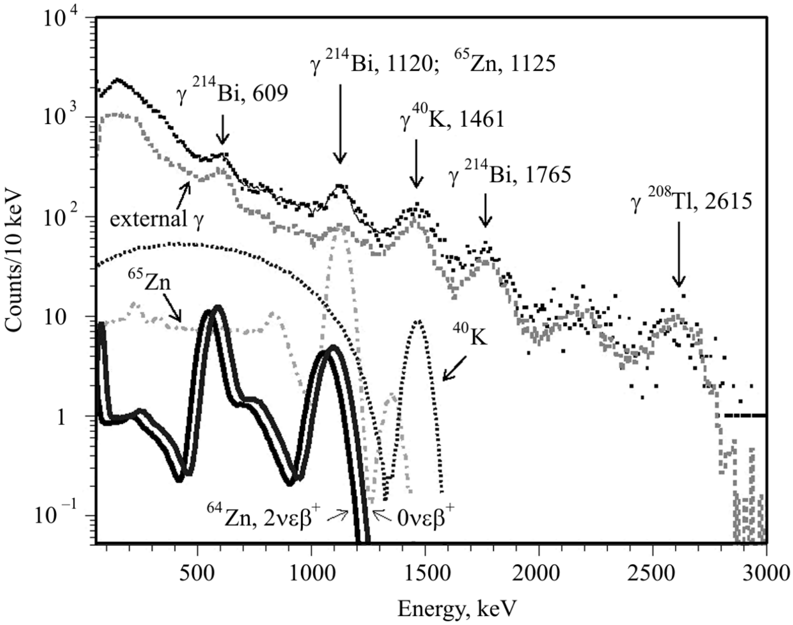

Fig. 7.7. The measured energy spectrum of the $ZnWO_4$ scintillation crystals (the total exposure is 0.349 kg × yr) together with the GEANT4 simulated response functions for $\varepsilon\beta^+$ process in ^{64}Zn excluded at 90 % C.L. The most important components of the background are shown. The energies of γ lines are in keV

A low background experiment to search for double β decay of ^{116}Cd with the help of the enriched $^{116}CdWO_4$ crystal scintillators is in progress. We estimate a sensitivity of a 5 yr experiment (depending on a level of background) as $T_{1/2} \sim (0.5\text{—}1.5) \times 10^{24}$ yr. It corresponds, taking into account the recent calculations of matrix elements [270, 298, 388], to the effective neutrino mass $\langle m_\nu \rangle \approx 0.4\text{—}1.4$ eV.

Development of crystal scintillators, rather promising technique to search for double beta decay, will be discussed in section 7.9.2.

7.3. Search for solar axions

7.3.1. Introduction of axions

The general form of the Hamiltonian of quantum chromodynamics (QCD) contains a term that violates the CP symmetry in the strong interaction [179, 282]. However, this violation is not observed experimentally. For example, only upper (and very strict) limit is measured for the neutron electric dipole moment, which is related with the CP violating term: $d < 2.9 \times 10^{-26}\ e \times$ cm [347]. This contradiction is known as the strong CP problem of QCD. One of the most simple and elegant solutions of this contradiction was proposed by Peccei and Quinn in 1977 [359, 360] by introducing a new global symmetry. The spontaneous violation of the PQ symmetry at the energy scale f_a totally suppresses the CP violating term in the QCD Hamiltonian. Weinberg [426] and Wilczek [431] have independently shown that this model leads to existence of axion — a new pseudo-scalar neutral particle. The mass of axion is connected with the scale of the PQ symmetry violation: $m_a(\text{eV}) \approx 6 \times 10^6/f_a(\text{GeV})$.

The interaction of axion with different components of usual matter is described by different effective coupling constants: $g_{a\gamma}$ (interaction with photons), g_{ae} (electrons), g_{aN} (nucleons), which are also inversely proportional to f_a and those values are unknown (additionally, one should note that relations of $g_{a\gamma}$, g_{ae}, g_{aN} with f_a are model dependent).

In the first works, the energy of the PQ symmetry violation was considered to be close to the scale of the electro-weak symmetry violation and, therefore, the axion mass is $\approx$ 100 keV. But this value of the axion mass was soon excluded by experiments with radioactive sources, reactors and accelerators (see reviews [51, 179, 282, 283, 319, 347, 368, 369] and references therein). Then the standard axion (known as PQWW by names of authors) was substituted by other models which allow much bigger values of f_a up to the Planck mass of 10^{19} GeV: the hadronic axion model (KSZV) [284, 384] and the model of the GUT axion (DFSZ) [212, 441]. The axion mass and the coupling constants $g_{a\gamma}$, g_{ae}, g_{aN}, which are inversely proportional to f_a, can have very small values (m_a down to 10^{-12} eV) in these models, and these axions are sometimes named as "invisible". It should be noted that, besides the solution of the strong CP problem, axion is one of the best candidates on the role of the dark matter particles [51, 146, 283, 319, 368, 369, 393].

If axions exist, the Sun can be an intensive source of these particles. They can be born: (1) in the interaction of thermal γ quanta with fluctuating electromagnetic fields within the Sun due to the Primakoff effect and (2) in nuclear magnetic transitions in nuclides present in the Sun.

The first effect generates the continuous spectrum of axions with energy up to ~20 keV and the mean value of 4.2 keV [152]. The total thermal axion flux on Earth depends on the coupling constant $g_{a\gamma}$ as $\varphi = (g_{a\gamma} \times 10^{10}\ \text{GeV})^2\ 3.5 \times \times 10^{11}\ \text{cm}^{-2}\ \text{s}^{-1}$. The relation of the axion mass m_a with $g_{a\gamma}$ is model dependent; for example, this flux is equal (in terms of m_a) to $\varphi = (m_a/1\ \text{eV})^2\ 7.4 \times\ 10^{11}\ \text{cm}^{-2}\ \text{s}^{-1}$ in the model with GUT axion, whereas other models can possess a deeply suppressed axion-photon coupling constant [152].

In the second effect, de-excitation of excited nuclear levels in magnetic (M1) transitions can produce quasi-monoenergetic axions instead of gamma quanta, due to axion-nucleon coupling g_{aN}. The total energy of axions is equal to the energy of gamma quanta. These levels can be excited by thermal movement of nuclei (the temperature of the solar core is equal to $\approx$1.3 keV, and, therefore, only low-lying levels, like 14.4 keV level of ^{57}Fe or 9.4 keV level of ^{83}Kr, are excited effectively). Other possibility of populating the excited levels is the nuclear reactions in the Sun (for example, the 477.6 keV level of ^{7}Li is populated in the main *pp* cycle).

In spite of the theoretical attractivity of axions, any direct experimental evidences of their existence are still absent. Indirect astrophysical and cosmological arguments give advantage to the axion mass in the range 10^{-6}—10^{-2} eV or about 10 eV [51, 284, 319, 347, 368, 369]. The laboratory searches for axion are based on several possible mechanisms of axion interactions with the ordinary matter [51, 283, 319, 368, 369]: (1) the inverse Primakoff effect, i.e. conversion of axion to photon in laboratory magnetic field (an example of such the experiment is CAST [443]) or in a crystal detector (for example, NaI(Tl) [144]); (2) the Compton conversion of axion to photon (analogue of the Compton effect) $a + e \to \gamma + e$ [122]; (3) the decay of axion to two photons $a \to \gamma\gamma$ [122]; (4) the axioelectric effect of interaction with an atom $a + (A, Z) \to e + (A, Z)^{+}$ (analogue of photoeffect) [122]; (5) the resonant absorption of axions emitted in nuclear M1 transitions in a radioactive source, a nuclear reactor or the Sun by the analogue nuclei in a target (see details below). It should be noted that these mechanisms are based on different kinds of interactions of axion with matter, they are sensitive to different coupling constants ($g_{a\gamma}$, g_{ae}, g_{aN}), and the limits on the values of the constants and on the axion mass are model dependent. Thus, diverse experiments are mutually complementary. While the most of experiments concern the axion-photon coupling constant $g_{a\gamma}$, only the mechanism (5) is related to the axion-nucleon constant g_{aN} both in emission and in absorption of axion. This allows to exclude uncertainty related to the values of $g_{a\gamma}$ and g_{ae}.

Coming to the Earth, such quasi-monoenergetic axions could resonantly excite corresponding levels of the same nuclei (^{7}Li, ^{57}Fe, ^{83}Kr, ...). In the subsequent deexcitation process, γ quanta are emitted; they can be observed with the help of some detectors located near a sample with ^{7}Li, ^{57}Fe, ^{83}Kr, ... nuclei (or incorporating these nuclei). Experiments searching for these γ's have the following advantages: (1) probability of emission of such axions at birth and at capture is related only with coupling constant of axions with nucleons g_{aN}; uncertainties related with $g_{a\gamma}$, g_{ae} dissapear; (2) flux of ^{7}Li axions is directly related with the main *pp* cycle, which determines luminosity of the Sun (in contrast to axions, connected with thermal excitation of ^{57}Fe and ^{83}Kr which have some uncertainties in their solar abundances and distribution of temperature inside the Sun). Summary of all experiments searched for resonant excitation of nuclei by solar axions is given in Table 7.6.

As one can see from Table 7.6, the best limits on axion mass in the resonant excitation experiments were obtained in measurements with ^{57}Fe. However, it should be noted that, because energy of ^{57}Fe excited level is 14.4 keV, axions

Table 7.6. **Summary of searches for quasi-monoenergetic solar axions coupled to nucleons through resonant excitation of nuclei**

Axion source, E_γ (keV)	Short description	$\lim m_a$ (keV)	Year [Ref.]
^{7}Li, $E_\gamma = 477.6$	HP Ge 78 cm^3, Li 61.4 g, 2667 h	32.0^a	2001 [305]
	HP Ge 160 cm^3, LiOH 3.9 kg, 3028 h	16.0^b	2005 [204]
	HP Ge 408 cm^3, LiF powder 243 g, 722 h	13.9^b	2008 [107]
	HP Ge 244 cm^3, LiF crystal 553 g, 4044 h	8.6^b	2012 [108]
^{57}Fe, $E_\gamma = 14.4$	Si(Li), Fe 33 mg (^{57}Fe 95 %), 1472 h	0.745^a	1998 [306]
	Si(Li), Fe 16 mg (^{57}Fe 80 %), 712 h	0.360^b	2007 [207]
	Si PIN, Fe 206 mg (^{57}Fe 96 %), 334 h	0.216^a	2007 [348]
	Si(Li), Fe 290 mg (^{57}Fe 91 %), 2028 h	0.159^a	2009 [205]
	Total Earth heat flux	1.6	2009 [185]
	Si(Li), Fe 1.26 g (^{57}Fe 91 %), 1075 h	0.145^a	2010 [206]
^{83}Kr, $E_\gamma = 9.4$	PC^c 243 cm^3, Kr gas 1.7 g, 564 h	5.5^a	2004 [274]

^{a} At 95 % C.L. ^{b} At 90 % C.L. ^{c} Proportional counter.

with mass greater than 14.4 keV (if they exist) just cannot be emitted instead of γ quanta in ^{57}Fe deexcitation. What is why experiments with ^{7}Li, which has greater excitation energy of 477.6 keV, are also valuable: it is important to set in ^{7}Li measurements m$_a$ limit lower than 14.4 keV widening a window in excluded axion masses to [477.6, 0.145] keV limits. This was done at the first time in [107]; improved results were reached in [108].

7.3.2. Limit on axion mass from measurements with different samples containing lithium

In previous experiments searching for solar ^{7}Li axions, peak at energy of 477.6 keV was not observed, and only limits on the peak amplitude and the corresponding mass of the axions m_a were set: (1) in [305], Li sample with mass of 61 g was measured with HPGe detector 78 cm^3 during 2667 h that gave $m_a < 32$ keV; (2) in [204], LiOH target of 3.9 kg was measured with HPGe 160 cm^3 during 3036 h resulting in $m_a < 16$ keV. Both these experiments were performed at the Earth level.

Recently, the following samples were measured in the Gran Sasso underground laboratory of the INFN (Italy) with low background HPGe detectors to search for solar ^{7}Li axions:

• LiF powder 243 g, HPGe 408 cm^3, 722 h; it was found that the sample is polluted by U/Th at ~0.5 Bq/kg, see Fig. 7.8;

• LiF powder 47 g (of different producer), HPGe 408 cm^3, 914 h; polluted by U/Th at 0.2 Bq/kg;

• LiF(W) crystal 224 g, HPGe 244 cm^3, 633 h; radiopure, U/Th < < 0.02 Bq/kg, see Fig. 7.9.

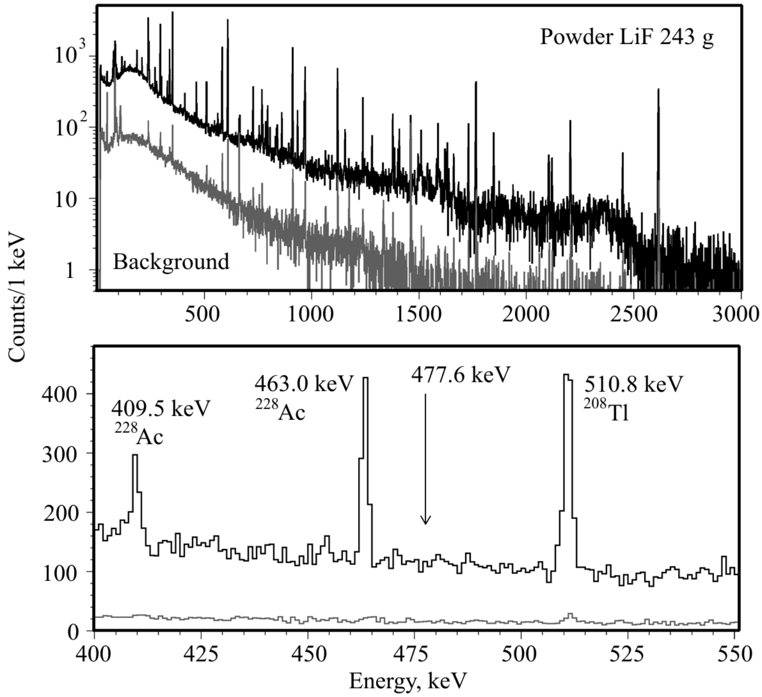

Fig. 7.8. Energy spectrum of LiF powder 243 g measured with HPGe detector 408 cm^3 during 722 h at LNGS in comparison with background

The 477.6 keV peak was not observed in any measurements; only limit on the peak area and corresponding axion mass can be derived as:

$$m_a = 1.55 \times 10^{11} \times (S/\varepsilon N_7 t)^{1/4} \text{ eV},$$

where m_a is in eV, S is the area of the peak, ε is the efficiency of registration of the 477.6 keV γ quanta by the detector, N_7 is the number of ^{7}Li nuclei in the target, t is the time of measurement in seconds. While the LiF powder shown in Fig. 7.8 was polluted, nevertheless it gave slightly better limit on axion mass of $m_a < 13.9$ keV at 90 % C.L. than other two samples, due to better efficiency reached with greater HPGe detector [107].

However, it was clear that in the following measurements a LiF(W) crystal should be used because of its radiopurity. Bigger sample was prepared with mass of 553 g. It was measured in the underground conditions of the Gran Sasso underground laboratory with HPGe detector 244 cm^3 during 4044 h. Only limits on U/Th pollutions were set as < 0.01 Bq/kg, see Fig. 7.10 (left). With the values of: $S < 37$, $\varepsilon = 2.3 \times 10^{-2}$, $N_7 = 1.2 \times 10^{25}$, the following limit was obtained: $m_a < 8.6$ keV at 90 % C.L. This is the best limit for the ^{7}Li axion mass to-date.

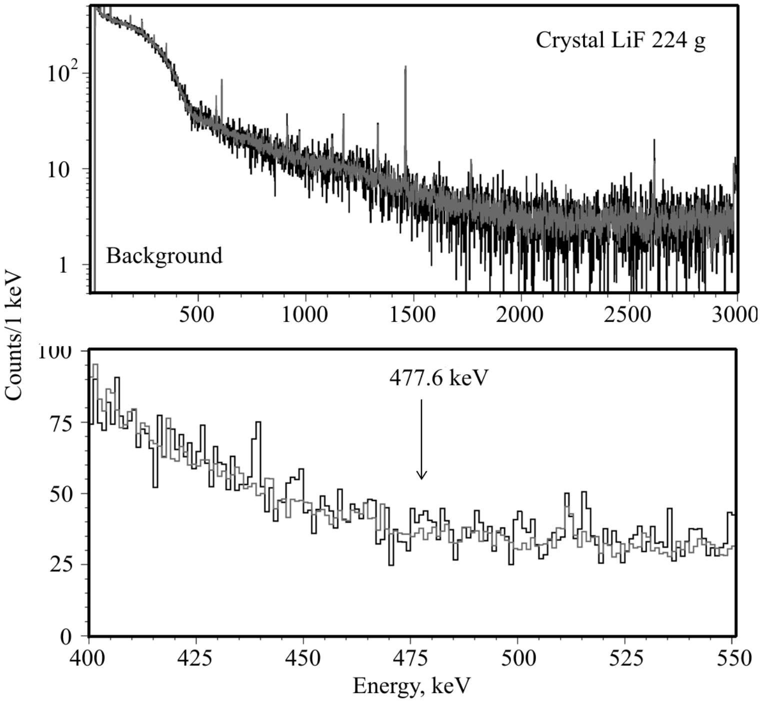

Fig. 7.9. Spectrum measured with LiF(W) crystal 224 g with HPGe 244 cm^3 during 633 h. In lower panel, region around the expected energy of 477.6 keV is shown in more detail

The best limit on axion mass related only with the g_{aN} coupling constant was determined in a similar search with ^{57}Fe nuclei: $m_a < 145$ eV [206]. However, as we already noted, possible masses of axions which could be born in ^{57}Fe deexcitation cannot be greater than 14.4 keV. Thus, a window of 14.4—16.0 keV in axion masses was not closed in previous experiments (14.4 keV — maximum axion mass emitted in ^{57}Fe; 16.0 keV — limit on sensitivity in previous experiments with ^{7}Li). Now this window is closed. Current situation with limits on axion masses from resonant excitation experiments is shown in Fig. 7.10 (right).

7.3.3. Resonance capture of solar ^{57}Fe axions and heat flow of the Earth

It is possible to obtain upper limit on the axion mass if — very conservatively — to suppose that the total heat flow of the Earth is caused exclusively by resonance capture of solar axions inside the Earth [185]. According to the contemporary conceptions [25], the Earth mantle (which gives ~68 % of the Earth's mass) contains 6.26 % of Fe; core (~32 % of the Earth's

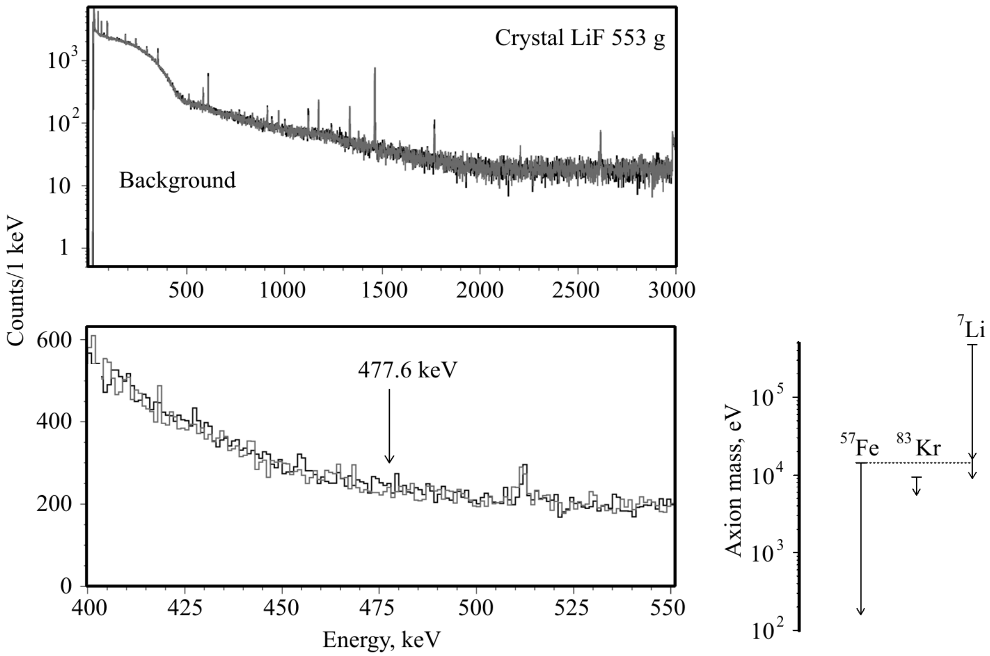

Fig. 7.10. Left: Energy spectrum of LiF(W) crystal measured during 4044 h with HPGe 244 cm^3. Right: Current situation with limits on axion masses from resonant excitation experiments. Empty arrow shows improvement reached in measurements with LiF targets

mass) contains 78.0—87.5 % of Fe. Altogether, the Earth in total consists of 29.6—32.6 % of Fe; isotopic natural abundance of ^{57}Fe is 2.119 %; this gives the number of ^{57}Fe nuclei in the Earth as: $N_{57} = (4.0—4.4) \times 10^{47}$.

Flux of ^{57}Fe axions from the Sun is estimated as the greatest one [263] because of small excitation energy of ^{57}Fe (14.4 keV) and big occurrance of Fe in the Sun. Number of resonance captures per 1 sec in a target at the Earth with N_{57} nuclei of ^{57}Fe is equal [207]:

$$R = 4.5 \times 10^{-33} N_{57} (m_a/1 \text{ eV})^4.$$

In each capture, energy of 14.4 keV is released; it is totally absorbed in the Earth. Equalizing this energy release to the Earth's heat flux (which is equal (31—46) $\times 10^{12}$ W in different estimations, see details in [185]; here we will take maximal value of 46×10^{12} W and minimal value of $N_{57} = 4.0 \times 10^{47}$), one can get:

$$m_a = 1.8 \text{ keV}.$$

The mass of axion m_a cannot be greater than this value. If to subtract energy release from radioactive decays of U/Th chains and ^{40}K in the Earth (conservative estimation is 20×10^{12} W [233]), this limit can be slightly improved:

$$m_a < 1.6 \text{ keV}.$$

Both these values are better than that obtained here earlier for ^{7}Li ($m_a < 8.6$ keV) and for ^{83}Kr ($m_a < 5.5$ keV [274], but worse than limits from specialized experiments with ^{57}Fe (145—745 eV, see Table 7.6). It should be also noted that this estimation has evident drawback: such a limit depends on our knowledge of the Earth structure.

7.3.4. Possible experiment with the TGV detector: sensitivity to the mass of solar ^{57}Fe axions

Limit on the solar ^{57}Fe axion mass could be further improved in measurements with the TGV detector (Telescope Germanium Vertical, created by JINR, Dubna, Russia in collaboration with France, Czech Republic, Slovakia). The TGV set-up [379] consists of 32 HPGe detectors $\oslash 60 \times 6$ mm with total sensitive volume ~400 cm^3; it is installed in the Modane underground laboratory (France, 4800 m w.e.). Currently it is used for search for 2β decays of ^{106}Cd (with thin ~50 μm ^{106}Cd foils located between HPGe detectors). Energy threshold of the detector allows to detect X-rays/γ quanta with energy more than 5—6 keV.

After finish of the experiment with ^{106}Cd, the TGV set-up could be used for search for the solar ^{57}Fe axions with energy of 14.4 keV. For their effective registration, thin foils, as in case of ^{106}Cd, should be used; and it is important that low enough energy threshold is already achieved with the set-up.

Sensitivity of possible experiment is estimated: it is related with the maximal value of the product εN_{57}. Calculations for Fe foils' thickness from 10 to 100 μm show that after 50—70 μm, value of εN_{57} is increased only slightly due to self-absorption in the sample ($\varepsilon N_{57} \approx 7 \times 10^{20}$ for a foil with 100 % enrichment in ^{57}Fe).

For measurements with ^{57}Fe, $m_a = 2.15 \times 10^8 \times [S/\varepsilon N_{57} t]^{1/4}$ eV. In measurements during $t = 1$ year and 0 events in the peak of 14.4 keV, maximal sensitivity to m_a can be reached with 16 samples of ^{57}Fe of 100 % enrichment and thickness $d = 50$ μm (total mass of ^{57}Fe — 12.8 g): $m_a < 9.2$ eV. More real estimation (8 samples of ^{57}Fe, 80 % enrichment, $d = 70$ μm, total mass of ^{57}Fe — 9.0 g) is the following: $m_a < 33$ eV. It is ~5 times better than the most stringent limit known today ($m_a < 145$ eV [206]).

7.3.5. Search for solar axions emitted in the M1-transition of ^{7}Li* with Borexino CTF

The described above searches for ^{7}Li solar axion ($E =$ $= 478$ keV) were performed with resonant absorption on ^{7}Li target. Non-resonant interactions of mono-energetic axions have much lower cross-sections, but it can be compensated by using larger targets. Other possible reactions for detections of ^{7}Li solar axions are interactions with electrons by Compton axion to photon conversion $a + e \to e + \gamma$ and the axioelectric effect $a + e + Z \to e + Z$ (cross-sections of these reactions are defined by axion-electron g_{ae} coupling constant), as well as the Primakoff conversion on nuclei $a + Z \to \gamma + Z$ and the decay of the axion into two γ quanta (amplitudes of these processes depend on axion-photon coupling $g_{a\gamma}$); Z is the charge of the nucleus. All these reactions would lead to appearance of 478 keV peak in the energy spectrum of a calorimeter. In this chapter we describe an experimental search for ^{7}Li solar axions performed with the prototype of the Borexino detector [1], Counting Test Facility (CTF).

CTF is a large liquid scintillation detector constructed in order to test the key concepts of Borexino, namely the possibility to purify a large mass of liquid scintillator down to the level of contamination for U and Th of 10^{-16} g/g. The detector is placed in the Hall C of the Gran Sasso underground laboratory. The active volume of CTF is 4 tons of liquid scintillator contained in a transparent spherical nylon vessel, 2 m diameter and 0.5 mm thick, which is viewed by 100 PMTs with light concentrators mounted on a support structure. The construction is immersed in 1000 m^3 of high purity shielding water, contained in an external cylindrical tank 10 m diameter and 11 m high. The water shielding covers the scintillator against gamma quanta emitted by radioactive contaminants in the PMTs and their support structure and by nuclei capturing neutrons generated within the walls of the experimental hall. On the bottom of the tank, 16 upward-looking PMTs of the muon-veto system are mounted, for detection of the Cherenkov light of muons that cross the water. One can find a detailed description of the CTF in [157].

The extremely low background level and the large mass of the CTF allowed to set limits on many processes including hypothetical particles and interactions. The data taken during 548 days of live-time in the CTF-3 campaign, when the detector was filled by 3.75 t of pseudo-cumene (1,2,4-trimethylbenzene) with PPO (2,5-diphenyloxazole, 1.5 g/L), have been used by the Borexino collaboration to set limits on the properties of axion.

The response functions of the detector for the above listed reactions of axions were obtained by Monte-Carlo simulation. No statistically significant indications on axion interactions were found. Using the experimental data one can set new, model independent, upper limits on constants of interaction of axion with electrons, photons and nucleons: $g_{ae}g_{aN} \leq (1.0–2.4) \times 10^{-10}$ at $m_a \leq 450$ keV and $g_{a\gamma}g_{aN} \leq 5 \times 10^{-9}$ GeV^{-1} at $m_a \leq 10$ keV. For heavy axions the limits $g_{ae} < (0.7–2.0) \times 10^{-8}$ and $g_{a\gamma} < 10^{-9}–10^{-8}$ at $100\,\text{keV} < m_a < 400\,\text{keV}$ are obtained in assumption that g_{aN} depends on m_a as for KSVZ axion model [122]. All the limits were set at 90 % CL.

[1] The detector Borexino is described in the next chapter.

7.4. Study of neutrino properties in underground experiments

7.4.1. The Borexino detector at the Laboratori Nazionali del Gran Sasso

The detector CTF (Counting Test Facility) described in the end of the previous chapter is a prototype of the Borexino, a large liquid scintillation detector, which was designed for real-time detection of low-energy solar neutrinos. The primary aim of Borexino is detection of monoenergetic ^{7}Be neutrino with energy of 862 keV, emitted in solar *pp*-cycle in the electron capture reaction of $^7\mathrm{Be}(e,\nu)^7\mathrm{Li}$. The measurement of this flux provides an information on the mass and mixture matrix of neutrino. Additionally, the unique properties of the detector (large target mass and very high radiopurity) have been used in order to obtain limits on probabilities of many hypothetical processes.

The Borexino detector is placed in the Hall C of the Gran Sasso underground laboratory, on the depth of 3600 m of water equivalent. The active mass of the target scintillator in Borexino is 278 tons of pseudo-cumene (PC, 1,2,4-trimethylbenzene), doped with a fluorescent dye (1.5 g/L of PPO, 2,5-diphenyloxazole). The scintillator is contained in a thin (125 μm) transparent spherical nylon vessel (the volume is 315 m^3) which is enclosed in two concentric buffers (323 and 567 tons of PC with admixture of 5.0 g/L of dimethylphthalate, a component quenching the PC scintillation light). The two PC buffers are separated by a thin transparent nylon film to prevent diffusion of radon towards the scintillator. The scintillator and the buffers are contained in a stainless steel sphere (SSS, $\oslash$13.7 m) which is surrounded by a 18.0 m diameter, 16.9 m high domed water tank (WT), containing 2100 tons of ultrapure water as an additional shield. The scintillation light is detected via 2212 8-inch PMTs uniformly distributed on the inner surface of the SSS and directed to the center of the sphere. Additional 208 8-inch PMTs are placed on the external surface of the SSS to view the water tank, serving as a muon veto; they detect the Cherenkov light radiated by muons in the water shield. The key features of the Borexino detector are described in [158, 159].

The first physical run of the detector started on 16 May, 2007. The main achievement of the Borexino Collaboration was the first real-time direct measurement of the low energy (0.862 MeV) ^{7}Be solar neutrinos which had been performed from an analysis of data obtained during 192 live days in the period from 16 May, 2007 to 12 April, 2008, totaling a 41.3 ton$\times$yr fiducial exposure to solar neutrinos [160].

7.4.2. The first direct real-time measurement of ^{7}Be solar neutrino flux

Before the observations performed by Borexino, the real-time measurements were available only for high-energy solar neutrinos (more than 4.5 MeV) with water Cherenkov detectors SuperKamiokande [181—183] and SNO [390,391]. The flux of lower (sub-MeV) energy solar neutrinos was measured by the chlorine-argon [182] and gallium-germanium [242,256,380] radiochemical detectors which integrate the neutrino flux over periods of ~1 month and cannot provide spectral information. The preferred explanation of the observed lack of electron neutrinos in the flux was the mechanism of neutrino flavour oscillations. The oscillations were observed also for atmospheric neutrinos [401], for reactor anti-neutrinos [276] and for accelerator neutrinos [278, 334].

Solar neutrinos are detected in Borexino through their elastic scattering on electrons in the scintillator. Electron neutrinos interacting through charged and neutral currents have a cross section ~5 times larger than muon neutrinos and tau neutrinos in the energy range of interest, because ν_μ and ν_τ interact only through neutral currents. The electrons scattered by neutrinos are detected by means of the scintillation light retaining the information on the energy, while information on the direction of the scattered electrons is lost. The basic signature for the monoenergetic 862 keV ^{7}Be neutrinos is the Compton-like edge of the recoil electrons at 665 keV.

The interaction rate of ^{7}Be solar neutrinos in the pseudo-cumene target is expected to be of 0.5 counts/(ton × day), so the requirements to the radioactive contamination of the target are extremely strict. The thick layers of the shield cover the internal part of the detector and screen the target from the external radioactivity. The liquids are purified during the filling of the detector. Position sensitivity of the detector (as obtained from the PMTs timing data via a time-of-flight algorithm) allows to distinguish events in the innermost spherical part of the active target, approximately 1/3 of the scintillator (78.5 tons); the external layer of the target serves as an active shield. Alpha and beta/gamma particles can be distinguished by different scintillation pulse shape for alphas and gammas [163].

In the spectrum in the Fig. 7.11, one can see ^{14}C beta-decays ($Q_\beta =$ $= 156$ keV) in the low energy part (<100 photoelectrons, p.e.); the peak around 200 p.e. due to alpha decay of ^{210}Po (5.14 MeV) is moved to the lower energies by alpha-quenching (about 13 times) of pseudo-cumene. The Compton-like edge at 300—350 p.e. is created by solar ^{7}Be neutrinos. The spectral continuum from 400 to 900 p.e. is created by β^+ decay of cosmogenic ^{11}C which is produced by neutron spallation from ^{12}C by muons *in situ*.

The Bi-Po fast chains allow to define the content of U and Th in the scintillator (assuming non-broken equilibrium in the families): $1.6(1) \times 10^{-17}$ g

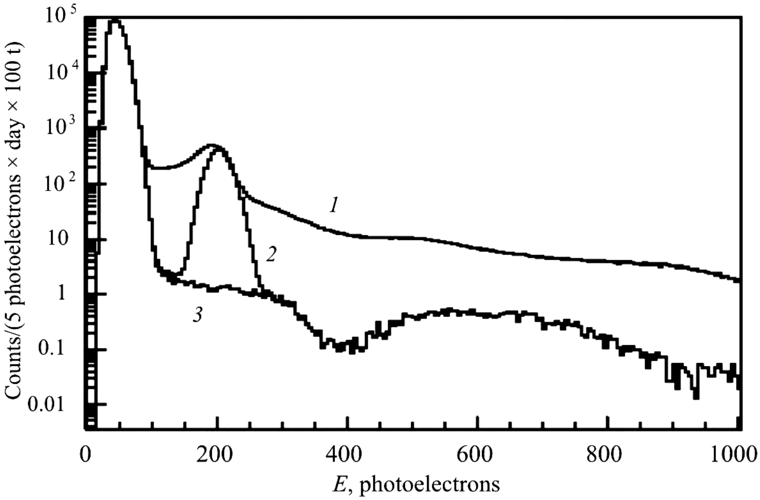

Fig. 7.11. The charge spectra of Borexino measured during 192 live days, all curves scaled to exposure of 100 days × ton: line *1* — after base cuts suppressing time-correlated events related to muons, ^{214}Bi—^{214}Po chains, and pile-ups (removing about 0.7 % of events); line *2* — after fiducial cut removing events in the external part of the target; line *3* — after the statistical subtraction of the alpha-emitting contaminants, mainly ^{210}Po

[^{238}U]/g and $6.8(15) \times 10^{-18}$ g[^{232}Th]/g. The ^{85}Kr content in the scintillator is dangerous because it overlaps with the expected spectrum of ^{7}Be solar neutrinos. The activity of ^{85}Kr in the detector was estimated via the rare decay sequence $^{85}\mathrm{Kr} \to {}^{85m}\mathrm{Rb}$ ($\tau = 1.5\,\mu$s, branching ratio 0.43 %) $\to {}^{85}$Rb that allows to apply the delayed coincidences technique; the activity is 29(14) counts/(day × 100 tons). The light yield is about 500 p.e./MeV, and the energy resolution is $\sim 5\,\% \cdot (E/1\,\mathrm{MeV})^{-1/2}$.

The spectral fit of the spectrum in the 160 – 2000 keV energy region gives the solar ^{7}Be scattering rate equal to 49 ± 3(stat.) ± 4(syst.) counts/(day·100 t) (see Fig. 7.12). The main background components have amplitudes (in the same units) of 25 ± 3(stat.) ± 2(syst.) for ^{85}Kr β^- decay (this is in a good agreement with the independent measurement of ^{85}Kr activity, see above); 25 ± 1(stat.) ± 2(syst.) for ^{11}C β^+ decay; and 23 ± 2(stat.) ± 2(syst.) for ^{210}Bi β^- decay together with scattering of CNO solar neutrinos which should produce a very similar spectrum.

The expected flux of ^{7}Be neutrinos for the Standard Solar Model with high metallicity [62] is $5.08(25) \times 10^{9}\,\mathrm{cm}^{-2} \cdot \mathrm{s}^{-1}$, which would give 74(4) counts/(day · 100 t) if no oscillations occur. The scenario of MSW-LMA (Large Mixing Angle, Mikheev—Smirnov—Wolfenstein effect of neutrino flavour oscillation in matter) would give the rate of 48 ± 4 counts/(day · 100 t), which is consistent with the measured rate. The MSW-LMA scenario predicts the dominant mode of neutrino oscillations to be the matter oscillations for

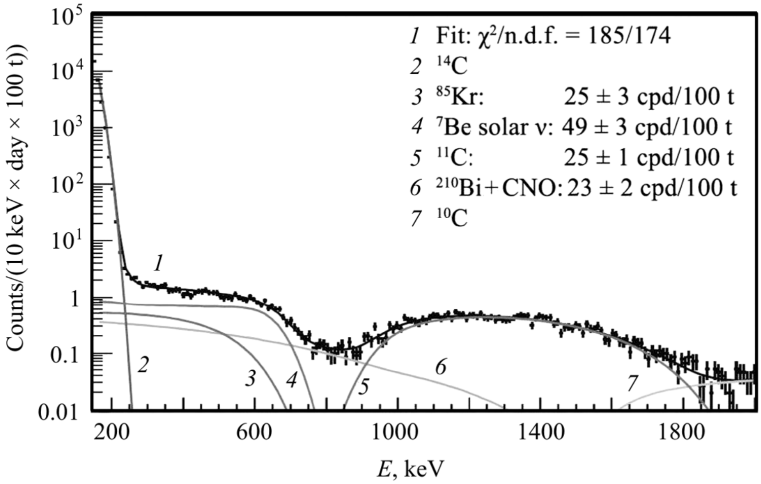

Fig. 7.12. The spectral fit in 160—2000 keV region

$E > 3$ MeV and the vacuum oscillations for $E < 0.5$ MeV. Before the Borexino result, the direct measurements of the electron neutrino survival probability P_{ee} were performed only for energies $E > 5$ MeV, in the matter-dominant region [390, 391]. The measurement of P_{ee} around the transition region is an important test of the MSW-LMA scenario.

7.4.3. The limit on electromagnetic properties of neutrino from Borexino measurements

A minimal extension of the electroweak standard model with a massive neutrino requires a non zero neutrino magnetic moment proportional to the neutrino mass [239, 315, 324]. The experimental evidence from solar and reactor neutrinos has demonstrated that neutrinos are massive, and should thus possess a non-null magnetic moment. The non-zero values of neutrino mass yields the lower limit for the magnetic moment to be $4 \times 10^{-20}\mu_\mathrm{B}$ [64] where $\mu_\mathrm{B} = e/2m_e$ is the Bohr magneton. The current experiments are not sensitive enough for such low magnetic moments, but larger values are possible in other extensions of the Standard Model [89, 248].

In case of a non-null neutrino magnetic moment, a new term

$$\left(\frac{d\sigma}{dT}\right)_\mathrm{EM} = \mu_\nu^2 \frac{\pi\alpha_\mathrm{EM}^2}{m_e^2}\left(\frac{1}{T} - \frac{1}{E_\nu}\right)$$

should be added to the standard electroweak cross section

$$\left(\frac{d\sigma}{dT}\right)_\mathrm{W} = \frac{2G_F^2 m_e}{\pi}\left(g_L^2 + g_R^2\left(1 - \frac{T}{E_\nu}\right)^2 - g_L g_R \frac{m_e T}{2E_\nu^2}\right),$$

where E_ν is the neutrino kinetic energy and T is the recoil electron kinetic energy. At the low energy, $\left(\frac{d\sigma}{dT}\right)_{\rm EM} \sim \frac{1}{T}$. The coupling of neutrinos to an electromagnetic field due to a neutrino magnetic moment is expressed by a 3×3 matrix. Dirac neutrinos can have both diagonal and off-diagonal (transition) moments, whereas the Majorana neutrino can have only transitional moments.

The analysis of Borexino data with the same statistics as for the measurements of ^{7}Be solar neutrino allowed to set the upper limit on the neutrino magnetic moment to be $5.4 \times 10^{-11}\mu_{\rm B}$ (90 % CL) which was the best experimental limit on the time of publication (currently, the best limit is set for the electron anti-neutrino in a reactor experiment [249], $3.2 \times 10^{-11}\mu_{\rm B}$). The sensitivity of Borexino to the magnetic moment, due to the larger target, is about 10 times better than it was obtained for similar search performed by the Borexino Collaboration in the CTF detector [164], $5.5 \times 10^{-10}\mu_{\rm B}$.

The searches of different electromagnetic properties of neutrino had been performed [164] with the second phase of the CTF detector (CTF-2), the pilot version of the Borexino detector described above. The liquid scintillator used at this stage was a phenylxylylethane (PXE, $C_{16}H_{18}$) with p-diphenylbenzene (para-terphenyl) as a primary wavelength shifter at a concentration of 2 g/L, along with a secondary wavelength shifter 1,4-bis-(2-methylstyrol)-benzene (bis-MSB) at 20 mg/L. The density of the scintillator is 0.99 kg/L. The total number of target electrons in CTF-2 $N_e = 1.36 \times 10^{30}$, the live time of data taking $t = 32.1$ days.

If neutrinos have mass and the flavour lepton number is not conserved, then the heavier neutrino flavours could decay to lighter ones: $\nu_H \to \nu_L + \gamma$. The above-mentioned minimal extension of the Standard Model (modified by non-zero neutrino mass and non-conservation of the flavour lepton number) predicts the lifetime for neutrino via this channel as high as $\tau/m_\nu \approx 10^{29}$ yr/eV. In the laboratory frame, the spectrum of photons emitted by decaying ultra-relativistic neutrino is described [208] as

$$\frac{dN}{dE_\gamma} = \frac{m_\nu}{\tau}\frac{1-\alpha+2\alpha E_\gamma/E_\nu}{E_\nu^2},$$

where E_γ and E_ν are energies of the gamma quantum and the decaying neutrino, respectively. The parameter α defines the angular distribution of the photon, relative to the spin of the decaying neutrino in the neutrino rest frame:

$$\frac{dN}{d(\cos\vartheta)} = \frac{1+\alpha\cos\vartheta}{2},$$

where ϑ is the angle between photon momentum and the spin of neutrino in the rest frame. This parameter relates to the space-time structure of the decay

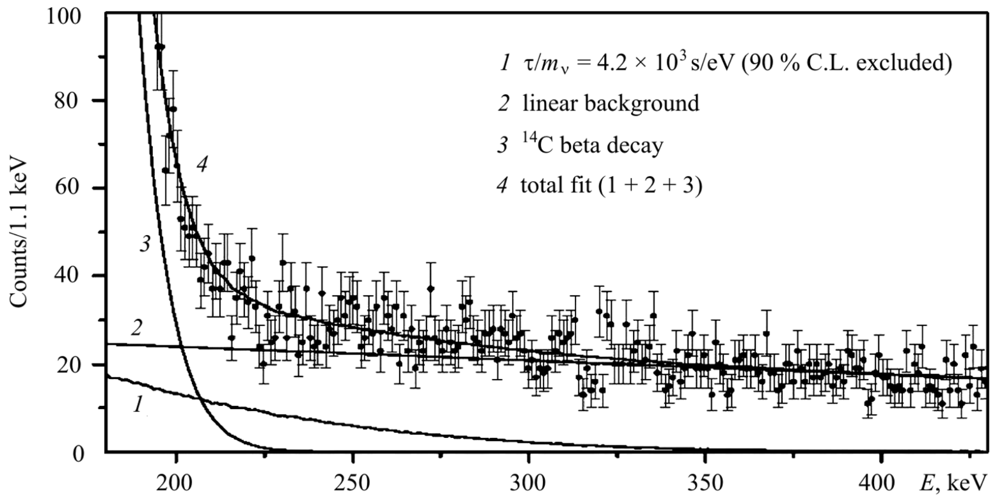

Fig. 7.13. Monte Carlo simulation of the signal in CTF-2 from radiative decay of solar neutrino for $\tau/m_\nu = 4.2\times10^3$ s/eV ($\alpha = 0$) and the experimental background data of CTF-2 for 32.1 days of live time

vertex and should be 0 for Majorana neutrino, $-1 \le \alpha \le 1$ for Dirac neutrino; for the case of total parity violation, $\alpha = \pm 1$.

The CTF detector is irradiated by the flux of solar neutrinos and can detect the gamma quanta emitted in this neutrino radiative decay. The limits on the ratio of lifetime of neutrino to their mass had been derived from a likelihood function analysis at 90 % CL (Fig. 7.13): $\tau/m_\nu > 4.2 \times 10^3$ s/eV ($\alpha = 0$), $\tau/m_\nu > 9.7 \times 10^3$ s/eV ($\alpha = +1$) and $\tau/m_\nu > 1.5 \times 10^3$ s/eV ($\alpha = -1$).

The sensitivity of the Borexino detector to this process is estimated to be two orders of magnitude better, but the results of searches of the neutrino radiative decay with this detector are still not published. The limit for radiative decay obtained in CTF-2 of Borexino is the best for laboratory searches (in reactors, accelerators, etc.) of this process, but it is much less restrictive than the astrophysical limits from the solar gamma ray flux (7×10^9 s/eV [370]) and from distortion of CMB spectrum (lifetime $< 4 \times 10^{20}$ s for $m_{\rm min} <$ < 0.14 eV [337]).

7.4.4. Limits on the heavy neutrino mixing in solar ^{8}B decay

In the previous chapter, the radiative decay of light massive neutrino $\nu_H \to \nu_L + \gamma$ had been discussed. For heavy neutrino with the mass $\ge 2m_e$, this mode of decay can be accompanied by decay into a light neutrino and electron-positron pair: $\nu_H \to \nu_L + e^+ + e^-$ (see Fig. 7.14).

This heavy neutrino due to its mass can be only a small admixture to the three neutrino flavours of the Standard Model. It cannot be coupled (or this

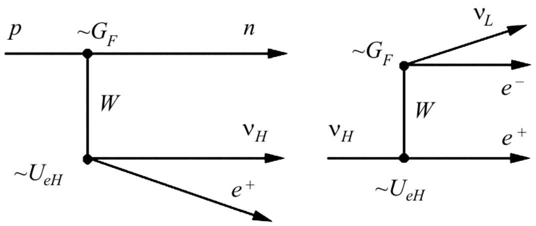

Fig. 7.14. (left) Emission of heavy neutrino in a positronic beta decay (for example, in the decay of ^{8}B $\to$ $\to {}^8\text{Be} + e^+ + \nu_H$). (right) Decay of the heavy neutrino into a light neutrino and electron-positron pair

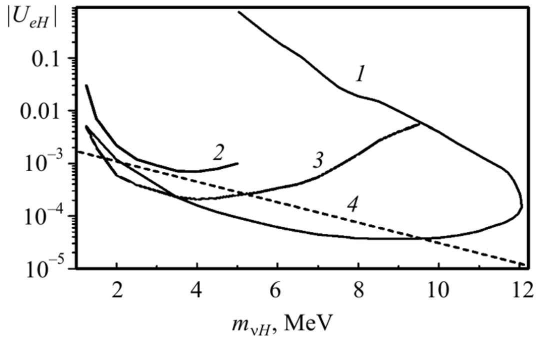

Fig. 7.15. The excluded values (90% CL) in the $m_{\nu_H} - U_{eH}$ parameters space. The experimental limits are obtained: *1* — from CTF-2 data [162]; *2*, *3* — from reactor neutrino experiments [209] and [264], respectively; *4* — from search of $\pi \to e\nu$ decay in accelerator experiment [169]. The plot is taken from [162]

coupling is very small) to Z^0 boson because only contribution of three types of neutrino to the decay width of Z^0 is observed. However, the hypothetical heavy sterile neutrino is predicted by many extensions of the Standard Model and proposed as candidate to the dark matter particles [165,214]. Possible indications of sterile neutrino existence have been obtained in accelerator experiments LSND [321] and recently in MiniBooNE [333].

The rest frame width of the decay of heavy neutrino can be described as [386]

$$\Gamma = \frac{G_F^2}{192\pi^3} m_{\nu_H}^2 |U_{eH}|^2 |U_{eL}|^2 h(m_e^2/m_{\nu_H}^2).$$

The U_{eH} (small) and U_{eL} ($\sim$1) are the mixing parameters of heavy and light neutrinos to the electron neutrinos, $h(m_e^2/m_{\nu_H}^2)$ is the phase space factor. The probability of the electron-positron pair decay mode is predicted to be, in general, much higher than that of the radiative decay. The emission of the heavy neutrino with mass <15 MeV is kinematically allowed in the beta decay of ^{8}B; thus, these neutrinos, if exist, can contribute to the solar neutrino flux and their decay to e^+e^- pair can be registered in Earth-based experiments.

The data of CTF-2 experiment described in the previous chapter had been used by the Borexino Collaboration to restrict the mass and U_{eH} parameters of the heavy neutrino [162]. The data were collected during 29.1 days in August—September 2000. The in-flight decay of a solar boron neutrino to e^+e^- pair in the sensitive volume of the detector would result in registration of event with energy equal to the full energy of the neutrino. All the observed events with energy >4.5 MeV were associated with muons. The partial suppression of non-muonic high-energy events by the muon veto had been taken into account. The non-observation of the sought decays leads to the restrictions on the mass and mixture parameter of the heavy neutrino shown in Fig. 7.15.

7.4.5. Limits on the solar electron antineutrino flux with the Borexino Counting Test Facility

A small antineutrino flux from the Sun is not completely excluded. One of possible production mechanisms is the neutrino-antineutrino conversion due to spin-flavour precession, induced by a neutrino non-diagonal magnetic moment and originally proposed as a possible solution to the observed solar neutrino deficit [383]. This could be a sub-dominant process in addition to the MSW-LMA solution of the solar neutrino problem. A random magnetic field in the convection zone of the Sun can increase the flux of $\tilde{\nu}_e$ through spin/flavour conversion [336]. Such enhancement would improve the detectability of a neutrino magnetic moment down to the level of $10^{-12}\mu_{\rm B}$.

The electron antineutrinos can be detected in CTF by the inverse beta decay of protons $\tilde{\nu}_e + p \to n + e^+$ with a threshold of 1.806 MeV. The cross section for this process is two orders of magnitude higher than that for $\tilde{\nu}_e$ elastic scattering on electron. In organic scintillators, the inverse beta decay reaction generates a prompt signal from the positron and a delayed one, following the neutron capture on protons $n + p \to d + \gamma + 2.22\,\text{MeV}$. The total energy released by the positron after annihilation is $E = T + 2m_e c^2$, where T is the positron kinetic energy. Neglecting the small neutron recoil, the visible prompt energy is $E_{\tilde{\nu}_e} - 0.78$ MeV. The capture of thermalized neutrons on protons with a mean life-time of ~200—250 μs provides a delayed tag for this reaction in a LS detector, allowing significant reduction of background. Neutron capture on ^{12}C is also possible but with a much smaller probability.

The data obtained in CTF-3 during 855.6 days of data collection (764.2 days of live time) were processed using the series of cuts for suppressing backgrounds. For example, the event pairs with the distance of >0.7 m between the prompt and delayed events were rejected, as well as the events tagged by the muon veto system.

Taking into account the 62(2) % efficiency of registration after the applied cuts, the estimated background sources for 764.2 days of CTF-3 live time were the following: 0.08 expected events of accidental coincidences; 0.37 events from reactor antineutrinos; 0.8(3) events of scattering of fast neutrons on target protons; 0.07(3) events of scattering of fast neutrons on target ^{12}C with exciting 4.4 MeV level of this nuclei. The cosmogenic activity that can simulate the inverse beta decay (mainly ^{8}He and ^{9}Li nuclei created by muons by spallation

Table 7.7. **Experimental constraints on the flux (in $cm^{-2} \cdot s^{-1}$) of solar $\tilde{\nu}_e$'s. The measured flux in the table is the limit on the flux within the experimental energy range (in MeV) at 90 % CL. The total flux is the limit scaled to the total energy range. The version BP04 of the Standard Solar Model [63] predicts a $\tilde{\nu}_e$'s flux from ^{8}B equal to $(5.79 \pm 1.33) \times 10^6$ $cm^{-2} \cdot s^{-1}$**

	LSD	SK	KamLAND	SNO	CTF
Exposure, kt · yr	0.094	92.2	0.28	0.584	0.0078
Energy range of $\tilde{\nu}_e$	7—17	8—20	8.3—14.8	4—14.8	1.8—20
Measured flux of $\tilde{\nu}_e$	$<0.46 \times 10^5$	$<1.32 \times 10^4$	$<3.7 \times 10^2$	$<3.4 \times 10^4$	$< 1.06 \times 10^5$
Total flux of $\tilde{\nu}_e$	$<1 \times 10^5$	$<4 \times 10^4$	$<1.3 \times 10^3$	$<5.2 \times 10^4$	$< 1.08 \times 10^5$
$\frac{\varphi_{\tilde{\nu}_e}}{\varphi_{\nu_e}}$ (^8B)	$\leq 1.7 \times 10^{-2}$	$\leq 0.7 \times 10^{-2}$	$\leq 2.2 \times 10^{-4}$	$\leq 1 \times 10^{-2}$	$\leq 1.9 \times 10^{-2}$
Ref., year	[320], 1996	[402], 2003	[277], 2004	[392], 2004	[161], 2006

of ^{12}C) was reduced to 10^{-4} simulating events by setting a 2 s veto time window after every muon crossing the set-up. The background from $^{13}C(\alpha, n)^{16}O$ reaction is negligible due to very low content of alpha active nuclides in the CTF scintillator (mainly ^{210}Po with activity of $\sim$20 μBq/t).

Only one candidate event had been observed. Its prompt energy was 4.37 MeV, so one cannot exclude the chance that this event is the de-excitation of the 4.4 MeV level of ^{12}C (excited by a muon-induced fast neutron) with the following thermalization and capture of the neutron. Taking into account the estimated background of 1.3 ± 0.7 events, the upper limit (with 90 % CL) on number of events that should be excluded for given condition is 3.3.

The hypothetical flux of $\tilde{\nu}_e$'s from ^{8}B, assuming no spectral distortion, can be obtained from the following equation:

$$\varphi_{\tilde{\nu}_e} = \frac{N_{\tilde{\nu}_e}}{N_p t \varepsilon \langle \sigma \rangle},$$

where $N_{\tilde{\nu}_e}$ is the number of detected events, $N_p = 2.25 \times 10^{29}$ is the number of target protons, $t = 6.60 \times 10^7$ s is the live time, $\varepsilon = 62\,\%$ is the mean detection efficiency, and $\langle \sigma \rangle = 3.4 \times 10^{-42}$ cm^2 is the mean cross-section over the ^{8}B neutrino spectrum in the energy range of interest. An upper limit for the electron antineutrino flux, assuming no distortion in the ^{8}B spectrum, is derived from the upper limit of 3.3 candidate events. The ^{8}B solar electron antineutrino flux limit (90 % CL) is $<1.1 \times 10^5$ cm^{-2} s^{-1}, or <1.9 % of the ^{8}B neutrino flux. This experiment was the first search for solar anti-neutrino flux including the low-energy range of 1.8—4 MeV. The sensitivity of the Borexino detector to the ratio $\frac{\varphi_{\tilde{\nu}_e}}{\varphi_{\nu_e}}$ (^{8}B) is estimated to be three orders of magnitude better, $\sim 10^{-5}$ in all the range $E_\nu > 1.8$ MeV. All current limits are summarized in Table 7.7.

7.5. Searches for the electric charge non-conservation

The conservation of the electric charge is one of the fundamental laws of standard quantum electrodynamics based on underlying principle of gauge invariance. In accordance with the Weinberg theorem [427], charge conservation (CC) is also related with masslessness of the photon. Nevertheless, the possibility that the electric charge conservation may be broken in future unified gauge theories and the implications of such a violation have been intensively discussed in literature [340, 355—358, 423]. We would like to note that for fundamental questions any "a priori" argument based on pure esthetic or other principles could give wrong results (as it was demonstrated, for instance, with parity conservation), and on some level we could face unexpected things. In 1992, Lev Okun wrote: "In spite of the fact that at present we have no theoretically self-consistent framework for a description of violation of charge conservation or the exclusion principle, experimentalists should not stop testing these most fundamental concepts of modern physics. In fundamental physics, if something can be tested, it should be tested" [355]. Because of its fundamental status, law of charge conservation should be verified with the best possible to-date accuracy.

Since the electron is the lightest electrically charged particle, its stability implies charge conservation. The electron's life time was estimated using the following indirect considerations:

(a) In [367], balance of electric currents in the Earth atmosphere was examined. If the disbalance current (200 A) is caused by the electron decay, with number of electrons in the Earth of 2×10^{51} one can derive limit on the electron life time $\tau_e > 5 \times 10^{22}$ yr;

(b) In [322], it was noted that expansion of the Universe could be caused by disbalance in the electric charge on the level of 2×10^{-18}; then from time of life of the Universe of 10^{10} yr follows $\tau_e > 10^{28}$ yr;

(c) In [269], a relation between the electron life time τ_e and mass of gamma quantum m_γ was obtained in framework of the SU(5) model as: $\tau_e = 10^{-25}(m_Z/m_\gamma)^2$ yr where $m_Z = 91.2$ GeV is the mass of the Z boson. Limits on the m_γ value were derived from observations of the magnetic field of Jupiter as $m_\gamma < 6 \times 10^{-16}$ eV [211] and from intergalactic magnetic field as $m_\gamma < 2 \times 10^{-27}$ eV [177]. From that follows $\tau_e > 10^{27}$ yr and $\tau_e > 10^{51}$ yr, respectively; however, these limits are model-dependent.

The following schemes were proposed to test the charge conservation in direct laboratory experiments which are continuing since 1959:

(1) to look for decay of electron to gamma quantum and electron neutrino: $e^- \to \gamma + \nu_e$, first discussed in [232] (ν_e is supposed here for conservation of the lepton number);

(2) to search for decay of electron into invisible modes, like $e^- \to \nu_e \bar{\nu}_e \nu_e$ [232] or disappearance;

(3) to search for decay of electron into *invisible* with excitation of neighboring nucleus (first proposed in [267]);

(4) to look for charge non-conserving (CNC) beta decay [232];

(5) to search for CNC decays of other charged particles (protons, or pairs of protons, etc.).

We discuss here processes (1)—(4) while more details on the process (5) will be given in the next section.

(1) Decay of electron to γ quantum and neutrino. Because both emitted particles are (almost) massless, they are kinematically equivalent and each of them has energy equal to half of energy available. In case of a free electron, energy of γ quantum is $E_\gamma = m_e c^2/2 = 255.5$ keV ($m_e c^2$ is the electron mass). If an electron is bound on atomic shell with binding energy E_b, energy of γ quantum will be $E_\gamma = (m_e c^2 - E_b)/2$. Because of non-zero velocity of an atomic shell electron, the Doppler broadening should be taken into account (as it was noted in [124] at the first time). The expected shape is the Gaussian with the width at half maximum FWHM $= 0.104 \times E_\gamma \times \sqrt{E_b}$ (all values — in keV). F.e., for K electrons in Ge detector ($E_b = 11.1$ keV), FWHM is 86.7 keV that is quite big value compared with typical Ge energy resolution of 1—2 keV at energy $\simeq$250 keV. Energy release in a detector is equal $E_d = E_\gamma = (m_e c^2 - E_b)/2$ if an electron decay occurs outside a detector's sensitive volume. However, if decay occurs in a detector itself, a vacation which is created in the atomic shell will be filled in the subsequent deexcitation process with emission of cascade of X rays and Auger electrons with total energy E_b; thus total energy release in the detector is $E_d = E_\gamma + E_b = (m_e c^2 + E_b)/2$. An expected response function of a detector will be the sum of many Gaussians with proper centers and widths which takes into account all atomic shells in atoms or molecules located in a detector itself and in surrounding materials. Further details can be found in [293].

The $e^- \to \gamma + \nu_e$ CNC decay is still not observed, and only limits on the electron life time were established. The first experimental restriction $\tau_e(e^- \to \gamma + \nu_e) > 1.0 \times 10^{18}$ yr was set in 1959 in short (6.5 h) measurements at the Earth level with NaI(Tl) scintillator of 1287 cm^3 [232]. The most restrictive to-date value was obtained with massive (near 4 tons) CTF Borexino detector installed deep underground (3600 m w.e.) in the Gran Sasso underground laboratory as $\tau_e(e^- \to \gamma + \nu_e) > 4.2 \times 10^{26}$ yr [59]. All experimental results are summarized in Table 7.8.

(2) Decay of electron into invisible modes. In result of electron decay into particles which leave detector without interaction (f.e., two neutrinos and one antineutrino [232]) or just electron disappearance (f.e., into extra dimensions [37]), an electron hole will be created in atomic shell. In the subsequent

Table 7.8. **Experimental limits on the electron life time at 68 % (90 %) C.L. for channels: $e^- \to$ *invisible* and $e^- \to \nu_e\gamma$. Best limits are in bold**

Detector	Volume, cm^3	Time of measurement, h	Limit on $\tau_e(e^- \to invisible)$, yr	Limit on $\tau_e(e^- \to \nu_e\gamma)$, yr	Year [Ref.]
NaI(Tl)	1287	6.5	1.0×10^{18}	1.0×10^{19}	1959 [232]
NaI(Tl)	348	$110^a, 362^b$	2.0×10^{21}	4.0×10^{22}	1965 [339]
Ge(Li)	66	1185	$5.3 \times 10^{21\ c}$	–	1975 [395]
NaI(Tl)	1539	515	2.0×10^{22}	3.5×10^{23}	1979 [299]
Ge(Li)	130	$3760^a, 3616^b$	2.0×10^{22}	3.0×10^{23}	1983 [124]
HP Ge	135	8850	–	$1.5(1.1) \times 10^{25}$	1986 [54]
HP Ge	3×140	1662	$2.7(1.7) \times 10^{23}$	–	1991 [373]
NaI(Tl)	17×10570	2823	1.2×10^{23}	–	1992 [223]
HP Ge	591	3199	–	$2.4(1.2) \times 10^{25}$	1993 [67]
HP Ge	$48 + 2 \times 209$	$13404^a, 7578^b$	$4.3(2.6) \times 10^{23}$	$3.7(2.1) \times 10^{25}$	1995 [9]
BaF_2	2×103	986	–	3.2×10^{21}	1996 [21]
Xe^d	2000	$2340^a, 257^b$	1.5×10^{23}	$2.0(1.0) \times 10^{25}$	1996 [109]
HP Ge	132	12600	1.3×10^{24}	–	1998 [295]
NaI(Tl)	9×2643	5354	$\mathbf{4.2(2.4) \times 10^{24}}$	–	1999 [110]
Xe^d	2000	8336	–	$3.4(2.0) \times 10^{26}$	2000 [111]
$C_{16}H_{18}{}^d$	4.2×10^6	770	–	$\mathbf{-(4.6) \times 10^{26}}$	2002 [59]
HP Ge	437	33233	–	$1.9(1.0) \times 10^{26\ e}$	2007 [293]

[a] For channel $e^- \to$ *invisible*. [b] For channel $e^- \to \nu_e\gamma$. [c] At 84% C.L. [d] Liquid scintillator. [e] This result was critisized in [210] as being overestimated at ≃5 times.

deexcitation process this hole will be filled by electrons from higher shells, and cascade of X rays and Auger electrons will be emitted; total released energy will be equal to the binding energy E_b of the disappeared electron on the atomic shell. If this decay occurs inside some detector, peak at energy E_b should be observed. For Ge, NaI(Tl) and Xe detectors, which were used in searches for $e^- \to$ *invisible* up to now, E_b values for K electrons are equal $E_b(\mathrm{Ge}) = 11.1$ keV, $E_b(\mathrm{I}) = 33.2$ keV, $E_b(\mathrm{Xe}) = 34.6$ keV. In all experiments, except of [110], decays of K electrons were searched for. In the DAMA experiment [110] with massive (around 100 kg) NaI(Tl) scintillators, low energy threshold of ≃2 keV was reached, and this allowed to investigate L electrons with $E_b(\mathrm{I})$ ≃5 keV at the first time. There are 8 electrons on L atomic shell compared with 2 electrons on K shell, and factor 4 in the electron number together with big mass of the detector, low background and big time of measurements resulted in the best to-date limit $\tau(e^- \to invisible) > 2.4 \times 10^{24}$ yr at 90 % C.L. Results of all experimental searches for CNC decay $e^- \to$ *invisible* are summarized in Table 7.8.

(3) Decay $e^- \to$ invisible with excitation of nuclear levels. In 1987 Holjevic et al. [267] proposed additional approach for testing the charge conservation: to search for processes in which electron disappears and the nei-

Table 7.9. **Experimental life time limits on the electron disappearance with nuclear levels excitation of ^{23}Na, ^{127}I and ^{129}Xe. Best values are in bold**

Nucleus, $E_{\rm exc}$	Life time limits τ, yr				
	[267] 90 % C.L.	[224] 68 % C.L.	[110] 90 % C.L.	[112] 90 % C.L.	[19] 68 % C.L.
^{23}Na					
440.0 keV			$\mathbf{1.5 \times 10^{23}}$		
^{127}I					
57.6 keV	2.1×10^{21}	5.8×10^{22}	$\mathbf{2.4 \times 10^{23}}$		
202.9 keV	1.9×10^{21}	5.6×10^{22}	$\mathbf{2.0 \times 10^{23}}$		
375.0 keV	2.4×10^{21}		$\mathbf{1.8 \times 10^{23}}$		
418.0 keV	2.4×10^{21}		1.6×10^{23}		$\mathbf{1.2 \times 10^{24}}$
^{129}Xe					
39.6 keV				$\mathbf{1.1 \times 10^{24}}$	
236.1 keV				$\mathbf{3.7 \times 10^{24}}$	
318.2 keV				$\mathbf{2.2 \times 10^{24}}$	
321.7 keV				$\mathbf{2.5 \times 10^{24}}$	
411.5 keV				$\mathbf{2.3 \times 10^{24}}$	

ghboring nucleus is left in an excited state. Such a process is analogous to the usual electron capture but does not change the nucleus' charge: $(A, Z) + e^- \to$ $\to (A, Z)^* + \nu_e$, and sometime it is named the CNC electron capture. It includes both the weak boson and photon mediating processes and gives possibility to investigate both the lepton and quark sectors [224, 267].

Levels with energies up to $m_e c^2 - E_b$ can be excited, but it is supposed that the lowest levels with difference in spin between the ground and excited state $\Delta J = 0, 1$ are fed with higher probability, and that K electrons are mostly involved being the closest to the nucleus. Deexcitation γ quanta can be observed with a proper detector located close to a sample (or containing atoms under investigation). Up to now, only 5 experiments searching for CNC electron capture were performed in which NaI(Tl) and liquid Xe scintillators were used; results are summarized in Table 7.9.

(4) CNC beta decay. CNC β decay, first considered for testing the charge conservation in [12], is a process in which the $(A, Z) \to (A, Z+1)$ transformation is not accompanied by the emission of an electron. It is supposed that instead of an e^-, a massless particle is emitted (for example, a ν_e, a γ quantum, etc.): $(A, Z) \to (A, Z + 1) + (\nu_e$ or γ, etc.$) + \bar{\nu}_e$. In this case the energy available in the (A, Z) decay is increased of 511 keV, that are normally spent for the electron rest mass. This makes possible some transitions to the ground or excited states of the daughter $(A, Z + 1)$ nucleus which are energetically forbidden for the normal, charge conserving β decay $(A, Z) \to (A, Z + 1) + e^- + \bar{\nu}_e$.

Table 7.10. **Limits on life time established in direct experiments to search for charge non-conserving β decay. Best limit is in bold**

CNC β decay	Target, weight	Technique, detector	$\tau_{\rm CNC}$, yr (C.L.)	Year [Ref.]
^{87}Rb → ^{87m}Sr	RbF, 30 g	CS [a], NaI(Tl)	1.8×10^{16}	1960 [399]
^{87}Rb → ^{87m}Sr	Rb_2CO_3, 400 g	CS, Ge(Li)	1.9×10^{18} (90 %)	1979 [352]
^{71}Ga → ^{71}Ge	Ga, 300 kg	CS, prop. counter	2.3×10^{23} (90 %)	1980 [69]
^{87}Rb → ^{87m}Sr	Rb_2CO_3, 800 g	CS, Si(Li)	7.5×10^{19} (90 %)	1983 [417]
^{113}Cd → ^{113m}In	$CdCl_2$, 1.5 kg	CS, Si(Li), NaI(Tl)	1.4×10^{18} (90 %)	1983 [376]
^{71}Ga → ^{71}Ge	$GaCl_3$—HCl, 101 t + Ga, 57 t	CS, prop. counter	$\mathbf{3.5 \times 10^{26}}$ (68 %)	1996 [351] [b]
^{73}Ge → ^{73}As	Ge, 952 g	RT [c], HP Ge	2.6×10^{23} (90 %)	2002 [296]
^{136}Xe → ^{136}Cs	Xe, 6.5 kg [d]	RT, LXe	1.3×10^{23} (90 %)	2004 [140]
^{115}In → ^{115m}Sn	In, 928 g	RT, HP Ge	4.1×10^{20} (90 %)	2005 [174]
^{139}La → ^{139}Ce	$LaCl_3$, 50 g	RT, $LaCl_3$(Ce)	1.0×10^{18} (90 %)	2006 [141]
^{100}Mo → ^{100}Tc	$^{100}MoO_3$, 1199 g	RT, 4 HP Ge	4.5×10^{19} (90 %)	2010 [91]

[a] CS means chemical separation of the daughter product. [b] Accounting for contribution from the solar neutrinos, the limit for ^{71}Ga was improved to $\tau_{\rm CNC} > 1.4 \times 10^{27}$ yr in [406]. [c] RT means real-time experiment. [d] 68.8 % ^{136}Xe.

The CNC β decay was searched for in several experiments since 1960. Only lower limits on the corresponding life times were established in the range of 10^{16}—10^{26} yr (see Table 7.10). We note here that capture of solar neutrinos $(A, Z) + \nu_e \to (A, Z+1) + e^-$ results in the same daughter nucleus $(A, Z+1)$ as in the CNC β decay, and these processes cannot be distinguished if daughter nuclei are extracted by chemical separation which was traditional techniques for experiments investigating solar neutrinos. The same techniques was used in searches for CNC β decay up to 2002 when the real-time approach was proposed and applied at the first time [296]. The best to-date limit was derived from the data of the SAGE and GALLEX solar neutrino experiments which used near 100 t of Ga [351].

7.6. Searches for invisible decays of nucleons and disappearance of matter

The baryon (B) and lepton (L) numbers are considered in the Standard Model (SM) as conserved values [2]. However, any underlying symmetry principle behind this fact is unknown, unlike f.e. the gauge invariance in electrodynamics which guarantees the masslessness of the photon and absolute conservation of the electric charge. Many extensions of the SM, in particular, grand unified theories consider conservation of B and L charges as approximate

[2] At non-perturbative level, B and L are not conserved even in the SM; however these effects are important at high energies ($\simeq$100 GeV) in the early Universe but are non-observable at current low temperatures [268].

law; they incorporate B and L violating interactions and predict decays of protons and neutrons bounded in nuclei. The processes with $\Delta B = 1$, $\Delta B = 2$, $\Delta(B - L) = 0$, $\Delta(B - L) = 2$ have been discussed in literature [309, 349].

Stimulated by theoretical predictions, nucleon instability has been searched for in many underground experiments with the help of massive detectors such as IMB, Fréjus, Kamiokande, SuperKamiokande and others (for experimental activity see [83, 292, 361] and references therein). About 90 decay modes have been investigated; however, no evidence for the nucleons (N) decay has been found. A complete summary of the experimental results is given in the Review of Particle Physics [347]. For the modes in which the nucleon decays to particles strongly or electromagnetically interacting in the detector's sensitive volume, the obtained life time limits are in the range of 10^{30}—10^{34} yr, while for decays to only weakly interacting products (neutrinos) the bounds were up to 10 orders of magnitude lower and only during the last decade they were significantly improved.

Interest to invisible decays of nucleons (and/or di- and tri-nucleons) and their disappearance is related with recently developed theories in which our world is described as a brane inside higher-dimensional space [37, 217, 218]. Particles, initially confined to the brane, may escape to extra dimensions (ED), thus disappearing for a normal observer. While energy, momentum, electric charge, etc. are conserved in full space, their balance could be broken in our 3-dimensional world. Tunneling of particles to EDs is predicted to be a generic property of massive matter [377]. Arkani-Hamed, Dimopoulos, and Dvali wrote in [38]: "The presence and properties of the extra dimensions will be investigated by looking for any loss of energy from our 3-brane into the bulk".

Theoretical estimations of the corresponding life times are quite uncertain because even the number of extra dimensions is unknown. Dubovsky [219] gives τ values for electron as $\tau(e \to nothing) = 9.0 \times 10^{25}$ yr in case of three EDs, and for proton $\tau(p \to nothing) = 9.2 \times 10^{34}$ yr for four EDs [3]. Recently a novel baryon number violating process, in which two neutrons in a nucleus disappear, emitting a bulk majoron $nn \to \chi$, was discussed by Mohapatra et al. [342]; the expected life time was estimated as $\sim 10^{32-39}$ yr. Also mechanisms for the tri-nucleon decay have been discussed; in recent theory by Babu et al. [58] processes with $\Delta B = 1, \Delta B = 2$ are forbidden but tri-nucleon decays with $\Delta B = 3$ are allowed.

Up to now we do not know which mode of nucleon decay is realized in the nature; different theories give different values for the nucleon's life time and

[3] We are using the following classification of decay channels: decay to *nothing* means disappearance (tunneling to EDs); decay to *invisible* means disappearance or decay to weakly interacting particles (one or few neutrinos of any flavors, majorons, etc.). Channel to *anything* means any possible mode of decay.

disagree which mode of decay is the most probable. In this relation experimental limits on the nucleons life time independent on the decay mode are also interesting and important. We will concentrate below on experiments where τ limits for nucleons (also di- and tri-nucleons) independent on mode or on their decays into *invisible* were established. The following approaches were used to set the τ limits:

(1) Spontaneous fission of ^{232}Th. In 1958, Flerov et al. derived limit on nucleon life time from an experiment searching for the spontaneous fission of ^{232}Th [237]. It was assumed (following idea [372]) that decay or disappearance of p or n in ^{232}Th will blow up the nucleus: it can be destroyed in the initial N decay or in the subsequent deexcitation of the nucleus. From the limit on ^{232}Th spontaneous fission [237] $T_{1/2} > 1.0 \times 10^{21}$ yr and taking into account that ^{232}Th contains 90 protons and 142 neutrons, the following limits were derived (see Table 7.11 for summary): $\tau(p \to \mathit{anything}) > 1.2 \times 10^{23}$ yr, $\tau(n \to \mathit{anything}) > 1.8 \times 10^{23}$ yr. These limits are considered as independent on mode [347] but, in fact, the τ values depend (inside a factor of few) on type of decay, see f.e. [272] [4].

(2) Geochemical search. In [231] the bounds on N decay to *invisible* were determined on the basis of mass-spectrometric measurements with Te ore samples (2.5×10^9 yr old) by looking for the possible daughter nuclide ^{129}Xe (^{130}Te $\to ... \to$ ^{129}Xe).

(3) Radiochemical method. In the experiment [235] the target of 1710 kg of potassium acetate $KC_2H_3O_2$, which contained 9.7×10^{27} atoms of ^{39}K, was exposed deep underground (4400 m w.e.) for about one year. Then, the candidate daughter ^{37}Ar, which could be created in result of nucleon disappearance in ^{39}K and subsequent evaporation of additional nucleon (^{39}K $\to ... \to$ ^{37}Ar), was extracted and its activity was measured as 0.3 ± 0.6 decays per day, which leads to the nucleon's life time limit $\tau(N \to \mathit{invisible}) > 1.1 \times 10^{26}$ yr. Reanalysis of these data in [407] allowed to set limits also for the nn and pn invisible decays.

(4) Study of the neutron production rate in deuterium. The decay or disappearance of proton bounded in deuterium nucleus, which consists only of proton and neutron, will result in the appearance of free neutron: $d \to n + ?$. Appearance of free neutrons was investigated in a shielded liquid scintillator enriched in deuterium [213], as well as in D_2O target with mass of 267 kg, installed at Reactor 5 of the Centrale Nucleaire de Bugey (France) and well shielded against cosmic rays and natural radioactivity; this allowed to set the best current limit for the p decay to *anything* as $\tau > 4.0 \times 10^{23}$ yr [408]. Analysis of the data collected with massive (1000 t) D_2O detector in the Sudbury Neutrino

[4] Spontaneous fission of ^{232}Th was observed in 1995; measured half life is $T_{1/2} = (1.2 \pm \pm 0.4) \times 10^{21}$ yr [155].

Observatory (SNO) located on the depth of 6000 m w.e. (Canada) lead to limit $\tau(p \to invisible)$ around 10^{28} yr [10, 434].

(5) Search for prompt γ quanta emitted by a nucleus in a de-excitation process after N decays within the inner nuclear shell (valid for invisible channels). Energies of the emitted γ quanta in the range of 19—50 MeV were investigated with the Kamiokande detector [403]. In search for the 6—7 MeV γ quanta with the SNO detector [11], the best limit for the p decay to *invisible* was set as $\tau(p \to invisible) > 2.1 \times 10^{29}$ yr.

(6) Search for bremsstrahlung γ quanta emitted because of a sudden disappearance of the neutron magnetic moment (limits depend on the number of emitted neutrinos) [255].

(7) Considering the Earth as a target with nucleons which decay by emitting electron or muon neutrinos; these neutrinos can be detected by a large underground detector [127, 310] (valid for decay into neutrinos with specific flavors).

(8) Very often daughter nuclei created after N disappearance in mothers are unstable. Search for their radioactive decay (time-resolved from prompt products) can be performed with a proper low background detector (especially effective if mother nuclei are incorporated in a detector itself). Such investigations were done with liquid Xe scintillators (enriched by ^{129}Xe [142] or ^{136}Xe [143]) and with the BOREXINO Counting Test Facility (CTF), a 4 t liquid scintillation detector [60].

(9) Search for radioactive decay of daughter nuclei (with character half lives in the range of seconds or minutes) can be combined with registration of prompt energy release after N decay or disappearance. Such a combined approach was used with the massive (currently the world's largest low background liquid scintillator, 1000 t) KamLAND detector [33] that allowed to establish the best τ limits (near 10^{30} yr) for n and nn decays to *invisible*.

All experimental results on searches for invisible decays of nucleons are summarized in Table 7.11.

Concluding this section, we would like to note that decays to *invisible* or disappearance were searched for not only for nucleons but also for other constituents of matter. Experiments on disappearance of electrons were described in the previous section; best limits on life time τ are on the level of $\simeq 10^{24}$ yr [110, 113]. Upper limits on the branching ratio λ for decay of positronium into *invisible* were obtained in [61]; in particular, for the direct annihilation $e^+e^- \to invisible$ $\lambda < 2.1 \times 10^{-8}$. Decay of unstable particles into *invisible* was looked for with the BABAR detector that gives $\lambda < 2.2 \times 10^{-4}$ for B^0 mesons [55] and $\lambda < 3.0 \times 10^{-4}$ for $Y(1S)$ [56], and with the BES detector λ limits are $\simeq 10^{-2}$ for η, η' [6] and J/ψ [7]. Astrophysical bounds for tunneling of γ quanta into EDs – that leads to additional cooling of stars – were discussed in [238].

Table 7.11. **Lower limits on the life time for N, NN and NNN decays into invisible channels established in various approaches. The best limits for specific channels are in bold**

Nucleon(s) decay	τ limit, yr and C.L.	Year [Ref.]	Short explanation
$p \to anything$	1.2×10^{23}	1958 [237]	Limit on ^{232}Th spontaneous fission
	3.0×10^{23}	1970 [213]	Search for free n in liquid scintillator enriched in deuterium ($d \to n+?$)
	$\mathbf{4.0 \times 10^{23}}$ 95 %	2001 [408]	Free n in reactor experiment with D_2O
$\to invisible$	7.4×10^{24}	1977 [231]	Geochemical search for $^{130}Te \to ... \to {}^{129}Xe$
	1.1×10^{26}	1978 [235]	Radiochemical search for $^{39}K \to ... \to {}^{37}Ar$
	1.9×10^{24} 90 %	2000 [142]	Search for ^{128}I decay in ^{129}Xe detector
	$\simeq 10^{28}$	2002 [10]	Free n in the SNO D_2O volume
	1.1×10^{26} 90 %	2003 [60]	Search for ^{12}B decay in CTF detector
	3.5×10^{28} 90 %	2003 [434]	Free n in the SNO D_2O volume
	$\mathbf{2.1 \times 10^{29}}$ 90 %	2004 [11]	Search for γ with $E_\gamma = 6$—7 MeV emitted in ^{15}N deexcitation in SNO detector
$n \to anything$	$\mathbf{1.8 \times 10^{23}}$	1958 [237]	Limit on ^{232}Th spontaneous fission
$\to \nu_\mu \overline{\nu}_\mu \nu_\mu$	5.0×10^{26} 90 %	1979 [310]	Massive liquid scint. detector fired by ν_μ in result of n decays in the whole Earth ^{a,b}
	1.2×10^{26} 90 %	1991 [127]	Fréjus iron detector fired by ν_μ ^{b}
$\to \nu_e \overline{\nu}_e \nu_e$	3.0×10^{25} 90 %	1991 [127]	Fréjus iron detector fired by ν_e ^{c}
$\to \nu_i \overline{\nu}_i \nu_i$	2.3×10^{27} 90 %	1997 [255]	Search for bremsstrahlung γ with $E_\gamma > 100$ MeV emitted due to sudden disappearance of n magnetic moment (from Kamiokande data) ^{d}
$\to \nu_i \overline{\nu}_i \nu_i \overline{\nu}_i \nu_i$	1.7×10^{27} 90 %	1997 [255]	The same approach ^{d}
$\to invisible$	8.6×10^{24}	1977 [231]	Geochemical search for $^{130}Te \to ... \to {}^{129}Xe$
	1.1×10^{26}	1978 [235]	Radiochemical search for $^{39}K \to ... \to {}^{37}Ar$
	4.9×10^{26} 90 %	1993 [403]	Search for γ with $E_\gamma = 19$—50 MeV emitted in ^{15}O deexcitation in Kamiokande detector
	1.8×10^{25} 90 %	2003 [60]	Search for ^{11}C decay in CTF detector
	1.9×10^{29} 90 %	2004 [11]	Search for γ with $E_\gamma = 6$—7 MeV emitted in ^{15}O deexcitation in SNO detector
	$\mathbf{5.8 \times 10^{29}}$ 90 %	2006 [33]	Search for correlated decays in KamLAND detector
$nn \to \nu_\mu \overline{\nu}_\mu$	6.0×10^{24} 90 %	1991 [127]	Fréjus iron detector fired by ν_μ ^{e}
$\to \nu_e \overline{\nu}_e$	1.2×10^{25} 90 %	1991 [127]	Fréjus iron detector fired by ν_e ^{f}
$\to invisible$	1.2×10^{25} 90 %	2000 [142]	Search for ^{127}Xe decay in ^{129}Xe detector
	4.9×10^{25} 90 %	2003 [60]	Search for ^{10}C and ^{14}O decay in CTF
	4.2×10^{25} 90 %	2004 [407]	Radiochemical search for $^{39}K \to ... \to {}^{37}Ar$ ^{g}
	$\mathbf{1.4 \times 10^{30}}$ 90 %	2006 [33]	Search for correlated decays in KamLAND detector
$pp \to invisible$	5.5×10^{23} 90 %	2000 [142]	Search for ^{127}Te decay in ^{129}Xe detector
	$\mathbf{5.0 \times 10^{25}}$ 90 %	2003 [60]	Search for ^{11}Be decay in CTF detector
	1.9×10^{24} 90 %	2006 [143]	Search for decays $^{134}Te \to ... \to {}^{134}Xe$ in ^{136}Xe detector

Table 7.11. **Continued**

Nucleon(s) decay	τ limit, yr and C.L.	Year [Ref.]	Short explanation
$pn \to invisible$	$\mathbf{2.1 \times 10^{25}}$ 90 %	2004 [407]	Radiochemical search for $^{39}K \to ... \to ^{37}Ar$ [g]
	3.2×10^{23} 90 %	2006 [143]	Search for decays $^{134}I \to ^{134}Xe$ in ^{136}Xe detector
$ppp \to invisible$	$\mathbf{3.6 \times 10^{22}}$ 90 %	2006 [143]	Search for decays $^{133}Sb \to ... \to ^{133}Cs$ in ^{136}Xe detector
$ppn \to invisible$	$\mathbf{2.7 \times 10^{22}}$ 90 %	2006 [143]	Search for decays $^{133}Te \to ... \to ^{133}Cs$ in ^{136}Xe detector
$pnn \to invisible$	$\mathbf{1.4 \times 10^{22}}$ 90 %	2006 [143]	Search for decays $^{133}I \to ... \to ^{133}Cs$ in ^{136}Xe detector

[a] The result of [310] was reestimated in [127] to be more than one order of magnitude lower. [b] The limit is also valid for $p \to \nu_\mu \overline{\nu}_\mu \nu_\mu$ decay. [c] The limit is also valid for $p \to \nu_e \overline{\nu}_e \nu_e$ decay. [d] $i = e, \mu, \tau$. [e] The limit is also valid for pn and pp decays into $\nu_\mu \overline{\nu}_\mu$. [f] The limit is also valid for pn and pp decays into $\nu_e \overline{\nu}_e$. [g] On the basis of the data of [235].

7.7. Search for spontaneous emission of heavy clusters

The spontaneous emission of nuclear fragments heavier than α particles and lighter than the most probable fission fragments, named cluster decay, was theoretically predicted in 1980 [381] and experimentally observed at the first time in 1984 [14, 241, 375]. Up to date, spontaneous emission of clusters ranging from ^{14}C to ^{34}Si from near twenty trans-lead nuclei (from ^{221}Fr to ^{242}Cm) have been observed with branching ratios relative to α decay from 10^{-9} down to 10^{-16} and partial half lives from 3.2×10^3 yr up to 1.2×10^{20} yr [156, 414]. In all these decays double magic nucleus ^{208}Pb, or nuclei close to ^{208}Pb, are produced that even allows to consider this domain of cluster decays as “lead radioactivity” [414], analogously to ”α radioactivity”. For about ten cases, only the half life limits are known with the highest value of $T_{1/2} > 5.0 \times \times 10^{21}$ yr for decay $^{232}Th \to ^{24-26}Ne + ^{208-206}Hg$ [155, 156].

A new region of parent nuclei, for which cluster radioactivity can be observed experimentally, was predicted recently [366]: these are the nuclei with $Z = 56$—64 and $N = 58$—72; daughter nuclei are close to double magic $^{100}_{50}Sn$. First searches in this domain were performed resulting only in limit $T_{1/2} > 3.5$ h for $^{114}Ba \to ^{12}C + ^{102}Sn$ [262].

The most widely used technique in experiments on cluster radioactivity is based on solid state nuclear track detectors which are able to register track of heavy cluster emitted from thin sample while rejecting much more numerous low energy α particles with great efficiency [156]. In few first measurements also Si detector telescopes were applied [375]. Ge detectors were used in two experiments looking for γ rays from created in cluster decay nuclear residuals: ^{24}Na in decay of ^{233}U (where the limit $T_{1/2} > 1.7\times10^{17}$ yr was established) [66], and various clusters in decays of Hg isotopes (with $T_{1/2}$ limits up to few by 10^{21} yr) [170].

Very interesting approach — search for the initial energy release and subsequent decay (or chains of decays) of created clusters (which usually are radioactive) — was used in experiment [138] to look for possible cluster decays of ^{127}I. In this research mother ^{127}I nuclei were incorporated in the NaI(Tl) detector (natural abundance of ^{127}I is 100 % [147]) that ensured high efficiency of detection of the decays. The data used were collected deep underground (about 3600 m w.e.) at the Gran Sasso underground laboratory by using the highly radiopure $\simeq$100 kg NaI(Tl) set-up of the DAMA experiment (DAMA/NaI) devoted mainly for investigation of Dark Matter particles [146]. The set-up consisted of 9 NaI(Tl) scintillators with mass of $\simeq$9.7 kg each; the analyzed statistics was 33834 kg $\cdot$ days.

Using table of atomic masses [57], one can find that 215 different decay modes are possible for ^{127}I nucleus with positive energy release Q. However, the most interesting are those with emission of double magic nucleus $^{48}_{20}$Ca and its neighbor $^{49}_{21}$Sc: they have the highest Q values of 28.9 and 29.4 MeV, respectively [57]. Nucleus ^{48}Ca created in decay $^{127}_{53}\mathrm{I} \to {}^{48}_{20}\mathrm{Ca} + {}^{79}_{33}\mathrm{As}$ is practically stable, $T_{1/2}(2\beta) \simeq 4\times10^{19}$ yr, but supplementary nucleus ^{79}As has quite short half life of 9.01 m, and in its decay emits γ quanta with energy of 0.432 MeV (probability 1.49 %) and 0.365 MeV (1.86 %) [236]. The sequence of events searched for was the following: (1) first event with energy >5 MeV (from initial cluster decay with $Q = 28.9$ MeV; here the NaI(Tl) quenching factor for ions with high stopping power was taken into account); (2) $\Delta t < 270$ s between the first and the second events; (3) energy release in one of NaI(Tl) between 1.00 and 1.85 MeV (from electron emitted in β decay); (4) coincident energy release in other NaI(Tl) between 0.365 and 0.432 MeV ($\pm2\sigma$ energy resolution) from emitted γ quanta. Efficiency to detect such a sequence of events was calculated with Monte Carlo program as 3.6×10^{-4} [138]. Number of registered events in the experimental data, which satisfy the selection criteria, was found as 348, in full agreement with the expected number of random coincidences (361 ± 5). This gives the following limit for the life time:

$$\tau({}^{127}_{53}\mathrm{I} \to {}^{48}_{20}\mathrm{Ca} + {}^{79}_{33}\mathrm{As}) > 6.8\times10^{21}\ \mathrm{yr\ at\ 90\%\ C.L.}$$

For other possible modes of ^{127}I cluster decay, investigated in this work (^{24}Ne + ^{103}Tc, ^{28}Mg + ^{99}Nb, ^{30}Mg + ^{97}Nb, ^{32}Si + ^{95}Y, ^{34}Si + ^{93}Y, ^{49}Sc + + ^{78}Ge) also only τ limits were found; they were in the range of 2.8×10^{21} yr to 2.1×10^{24} yr, up to 3 orders of magnitude higher than the best τ limits established for other perspective nuclides in other works.

7.8. Rare α and β decays

While α decay is well known nuclear phenomenon with more than 100 years history, interest to its investigation even increased during last years. At present days researches are concentrated mainly on studies of short-living exotic isotopes close to the proton drip line, decays of superheavy elements, and on search for α activity of naturally occurring isotopes. Despite alpha decay is energetically allowed for several primordial natural elements from cerium to uranium, during the 20th century α activity was observed (apart from uranium and thorium families) only for neodymium, samarium, gadolinium, hafnium, osmium and platinum. Recently two extremely rare α decays were discovered. Alpha activity of bismuth, being considered the heaviest stable element, was observed with the half life $T_{1/2} = 1.9 \times 10^{19}$ yr (the longest measured $T_{1/2}$ for α decays) by using a BGO crystal (bismuth germanate, $Bi_4Ge_3O_{12}$) as a low-temperature scintillating bolometer [325]. Alpha decay of tungsten (isotope ^{180}W) with $T_{1/2} = 1.1 \times 10^{18}$ yr was detected [186] with the help of cadmium tungstate crystal scintillators.

Isotopes ^{50}V, ^{115}In and ^{113}Cd are only three nuclei which enable study of four-fold forbidden β decays in a practical way, when rare β decay is not masked by much more rapid β decays. The high order of forbiddeness leads to high half lives, in the range of 10^{14}—10^{17} yr. It should be noted an interesting possibility of an independent estimation of neutrino mass in case of a very low energy of β decay of ^{115}In to the first excited level of daughter nucleus.

Usually investigations of rare α and β decays are by-products of experiments aimed to search for double beta decay and dark matter, measure neutrino fluxes, screening of materials for development of ultra-low background nuclear spectrometry.

7.8.1. Beta decay of ^{113}Cd

Isotope ^{113}Cd is present in the natural composition of cadmium with abundance of 12.22 %, however, it is β unstable with $Q_\beta = 320(3)$ keV [57]. Radioactivity of ^{113}Cd was observed for the first time only in 1970 [260], after a number of unsuccessful attempts since 1940 (see references in [260]). Then this decay was investigated in works [15, 199, 258, 338].

The most precise study of β decay of ^{113}Cd (measurement of $T_{1/2}$ and spectrum shape) was realized in [104] by using a low background $CdWO_4$ crystal scintillator to investigate the β decay of ^{113}Cd with precision better than those of the previous studies. The $CdWO_4$ crystal with mass of 434 g, used in the experiment [199] and then stored during last 10 years in the Solotvina Underground Laboratory on a depth of 1000 m w.e., was transported in a lead container by surface and immediately placed underground in the Gran Sasso underground laboratory to avoid its cosmogenic activation. It was installed in a

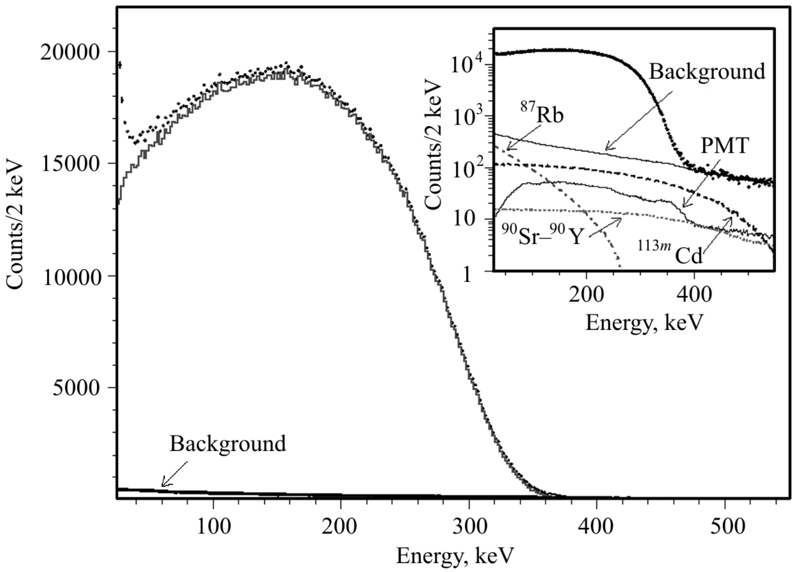

Fig. 7.16. The raw energy spectrum of the $CdWO_4$ scintillator measured over 2758 h in the low background set-up is shown by dots. The energy spectrum, obtained after the PMT noise rejection and the correction for related efficiency and the subtraction of the background, is shown by histogram. (Inset) The raw spectrum is shown together with the model of the background and its main components: β spectra of ^{87}Rb, ^{113m}Cd and ^{90}Sr—^{90}Y, and the contribution from the external γ quanta from PMTs in these experimental conditions

low background DAMA/R&D set-up (see e.g. [136]) surrounded by low radioactive shield of high purity Cu, Pb, Cd and polyethylene/paraffin to reduce the external background. The whole shield has been closed inside a Plexiglas box, continuously flushed by high purity N_2 gas. An event-by-event data acquisition system records amplitude, arrival time of event, and shape of scintillation signal with a 20 MS/s transient digitizer. Data were accumulated during 2758 h. The abundance of ^{113}Cd in the $CdWO_4$ crystal was determined with precise mass spectrometric measurements. Contribution of radioactive contamination in the crystal in the region of the ^{113}Cd β spectrum was estimated by the time-amplitude and pulse-shape analyzes of the collected data, and with the help of GEANT4 software package [13]. Mass spectrometry was also used to check presence of radioactive elements. Pulse-shape analysis allowed to reject α events and PMT noise, and to reach quite low energy threshold of 28 keV.

The signal to background ratio was equal 56/1, which is the best value among all to-date experiments. More than 2.4×10^6 events were collected, and half life of ^{113}Cd was determined as:

$$T_{1/2} = (8.04 \pm 0.05) \times 10^{15} \text{ yr.}$$

Accumulated during 2758 h spectrum with its fit by a model function and components of background are shown in Fig. 7.16.

7.8.2. First observation of β decay of ^{115}In to the first excited level of ^{115}Sn

In accordance with the last tables of atomic masses [57], mass difference between ^{115}In and ^{115}Sn is equal to 499 ± 4 keV. It is enough to populate in β decay of ^{115}In not only the ground state but also the first excited level of ^{115}Sn with $E_{\text{exc}} = 497.4$ keV. However, because of extremely low energy release of 1.6 ± 4 keV and related with this low probability, decay to ^{115}Sn* was observed only very recently [173].

In the experiment carried out in the underground conditions of the Gran Sasso underground laboratory, a high purity indium metal sample with natural composition (95.71 % of ^{115}In) and mass of 928 g was measured during 2762 h in the ultra-low background set-up with four HPGe γ detectors of 225 cm^3

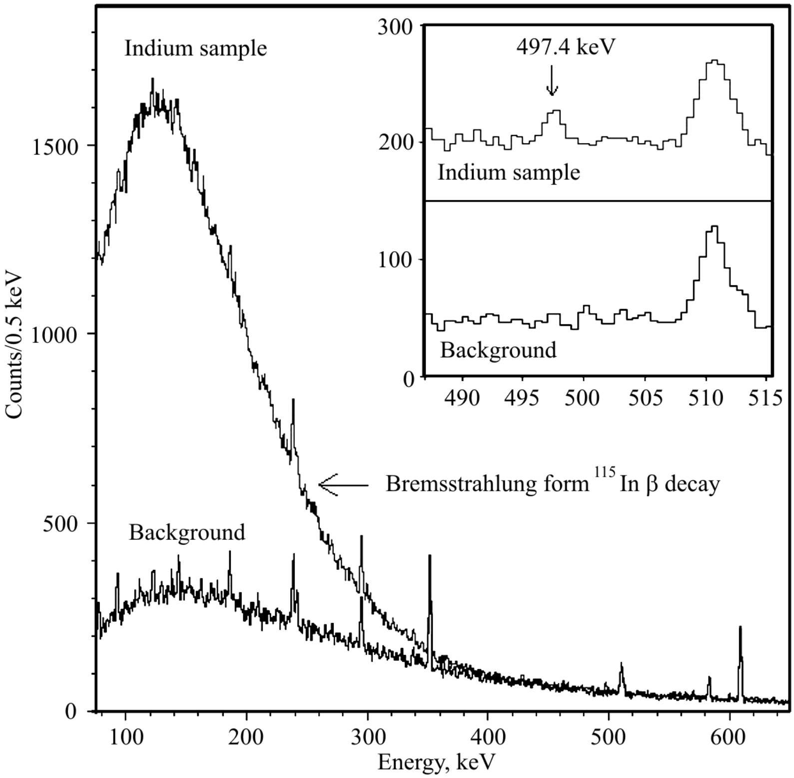

Fig. 7.17. Experimental spectrum of the In sample (accumulated for 2762 h) and background spectrum (1601 h) measured with four HPGe detectors in the energy interval 70—600 keV. The region of 600—2800 keV, where the spectra are practically indistinguishable, is not shown. Background is normalized to the same counting time. In the inset, the region of the 497.4 keV peak is shown in more detail; here, the In spectrum is shifted upward by 150 counts

volume each. A γ spectrum of the In sample in comparison with background is shown in Fig. 7.17. All lines (except of line at 497.4 keV) were related with natural, cosmogenic or man-made nuclides; their rates in background and the In sample were equal inside the statistical uncertainties. The line at 497.48 ± 0.21 keV was present only in the In spectrum, with area of 90 ± 22 counts. The energy of the peak is in agreement with the expected energy of γ quantum (497.358 ± 0.024 keV) emitted in deexcitation of the first excited level of ^{115}Sn. Counting rate in the peak corresponds to probability of 1.2×10^{-6} (relatively to decay to the ground state), and to half life of 3.7×10^{20} yr (see Fig. 7.18).

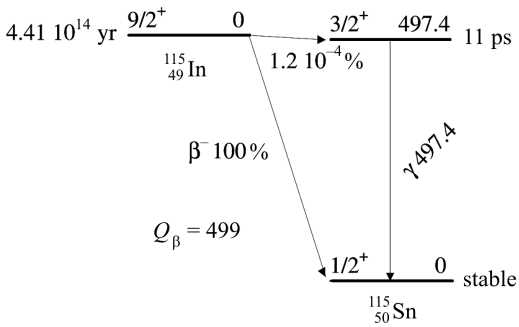

Fig. 7.18. New scheme of ^{115}In→^{115}Sn decay

The observation of ^{115}In →^{115}Sn* decay was recently confirmed also in measurements [27, 430]. In accordance with the atomic mass tables [57], the value of $Q_\beta = 1.6 \pm 4.0$ keV was considered as possibly the lowest energy release in β decays (to be compared with 2.555 keV for ^{163}Ho, and 2.469 keV for ^{187}Re). To resolve this puzzling situation, the masses of ^{115}In and ^{115}Sn atoms were measured with unprecedent accuracy of ≃10 eV in [345]. This gives for decay to the ground ^{115}Sn state Q_β value of 497.489 ± 0.010 keV. Taking into account energy of the first ^{115}Sn excited level $E_{\rm exc}$ = 497.334 ± 0.022 keV, the Q_β value for decay to this level is 155 ± 24 eV, i.e. this decay really has the lowest known value of Q_β.

We have here a paradoxical situation: we know masses of ^{115}In and ^{115}Sn (near 115 GeV each) with accuracy of 10 eV, while the energy of the first ^{115}Sn excited level (which has energy 497 keV, i.e. 5 orders of magnitude lower) is known with worse accuracy of 22 eV giving the biggest contribution to the overall error bar of 24 eV. Measurements of $E_{\rm exc}$ with much better accuracy of ≃5 eV is currently realized at the INR, Kyiv.

7.8.3. Alpha decay of natural europium

Two naturally occurring europium isotopes (^{151}Eu and ^{153}Eu) are potentially α active. A CaF_2(Eu) crystal scintillator with mass of 370 g was used to search for α decay of ^{151}Eu (Q_α = 1.964 MeV). While Eu is present in the crystal as a dopant with mass fraction of only ∼0.4 %, theoretical estimations (on the basis of work [365]) of the expected half life gave the value of $T_{1/2} \approx 4 \times 10^{18}$ yr, which is reachable with current experimental techniques.

Measurements were performed over 7426 h by using the DAMA/R&D set-up at the Gran Sasso underground laboratory. An event-by-event data acquisi-

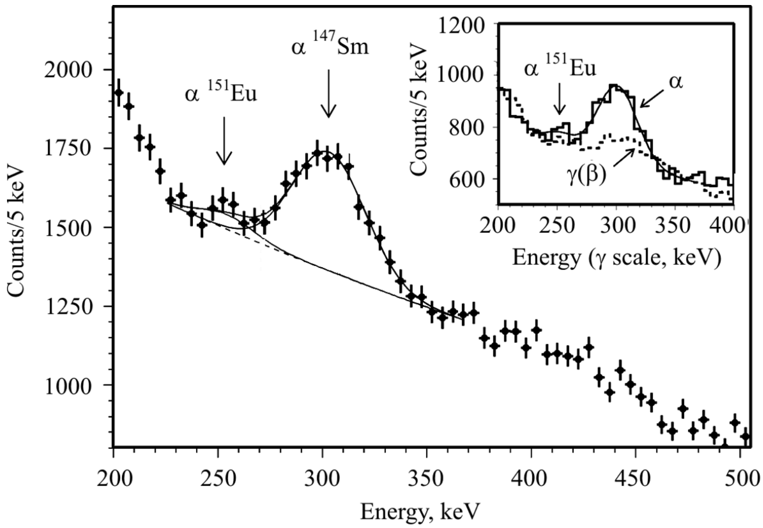

Fig. 7.19. Low energy part of the spectrum measured during 7426 h in the low background set-up with the CaF_2(Eu) scintillator. The peculiarity on the left of the ^{147}Sm peak can be attributed to the decay of ^{151}Eu with $T_{1/2} = 5 \times 10^{18}$ yr. (Inset) Spectra obtained by applying the pulse-shape discrimination technique shown by dashed ($\gamma(\beta)$ component) and solid (α component) lines

tion system has been recording amplitude, arrival time of event, and shape of scintillation signal with a 160 MS/s transient digitizer over a window of 3125 ns. Response of the detector to γ quanta and α particles was measured with a set of external radioactive sources and by using the trace internal pollution of the crystal by α decaying nuclides. In accordance with measured α/β ratio [5], the expected energy of ^{151}Eu peak in γ scale of the CaF_2(Eu) scintillator is 245(36) keV. The concentration of Eu in the crystal was checked with the help of the Inductively Coupled Plasma Mass Spectrometry analysis as 0.4 %, which is in agreement with the data provided by producer of the scintillator.

Internal radioactive contamination of the crystal by ^{40}K, U/Th chains and other nuclides was determined — on the level of mBq/kg — by the time-amplitude analysis and simulation of radioactive decays with the GEANT4 package. Peaks of alpha particles were identified in the data as being caused by α particles despite rather modest pulse shape discrimination between $\gamma(\beta)$ and α events in the CaF_2(Eu) scintillator.

Measured spectrum of the CaF_2(Eu) scintillator is shown in Fig 7.19. Peculiarity on the left of the ^{147}Sm peak has energy of 255(7) keV, in agreement with the expected energy of ^{151}Eu α decay. Pulse shapes of events in this peculi-

[5] The detector energy scale is measured with γ sources, thus the notation "α/γ ratio" could be more adequate. However, because γ rays interact with matter by means of the energy transfer to electrons, we are using the traditional notation "α/β ratio".

arity correspond to shapes caused by α particles. Determined experimentally half life $T_{1/2} = (5^{+11}_{-3}) \times 10^{18}$ yr [116] is in accordance with theoretical predictions.

This first indication should be confirmed in other experiments. One of the possibilities could be the use of $Li_6Eu(BO_3)_3$ crystals as a cryogenic bolometer with energy resolution for alpha particles at the level of several keV [117, 326].

7.8.4. α activity of natural tungsten

A first indication of the alpha decay of ^{180}W (the expected energy of alpha particles is 2460(5) keV [57], isotopic abundance of ^{180}W is $\delta = 0.12(1)\,\%$ [147]), with a half life $T_{1/2} \sim 10^{18}$ yr was obtained in the measurements with low background $CdWO_4$ crystal scintillators [186], and then was confirmed with $CaWO_4$ crystals as scintillators [436] and scintillating bolometers [184]. Recently the observation was also confirmed in measurements with low background $ZnWO_4$ crystals scintillators in the DAMA/R&D at the Gran Sasso underground laboratory [118]. There is a peculiarity in the α spectrum of a few $ZnWO_4$ detectors accumulated over 3197 kg · h of exposure at the energy of 325(11) keV. This energy in the γ scale corresponds to the α particle energy of 2358(80) keV. These alpha events can be ascribed to the α decay of ^{180}W with the half life $T_{1/2} = (1.3^{+0.6}_{-0.5}) \times 10^{18}$ yr. This result is in agreement with the data published earlier. It should be stressed that the isotope ^{180}W has the lowest ever measured specific α activity ($\simeq$2 decays per year per gram of the natural tungsten to be compared with the value of $\simeq$100 for natural bismuth).

7.8.5. First detection of α decay of ^{190}Pt to excited level of ^{186}Os

All six naturally occurring isotopes of platinum are potentially α unstable. However, only for one of them, ^{190}Pt (with the biggest energy release of $Q_\alpha = 3251(6)$ keV), α decay to the ground state of ^{186}Os was experimentally observed. The currently recommended half life value is $T_{1/2} = (6.5 \pm 0.3) \times 10^{11}$ yr. However, the first excited level of ^{186}Os ($J^\pi = 2^+$) has quite low energy: $E_{\text{exc}} = 137.2$ keV, and energy available to α particle in decay to this level, $Q^*_\alpha = 3114(6)$ keV, is high enough to make the decay to be observed (theoretical estimations are in the range of $T_{1/2} = 10^{13}$—10^{14} yr). This allowed to detect the $^{190}\text{Pt} \to {}^{186}\text{Os}(2^+_1)$ decay through detection of the 137.2 keV γ quantum with the help of an ultra-low background HPGe detector even using a platinum sample with natural isotopic composition with very low percentage of ^{190}Pt (0.012(2) % [147]).

The measurements were performed deep underground in the Gran Sasso underground laboratory. Two platinum crucibles with the total mass of 42.6 g

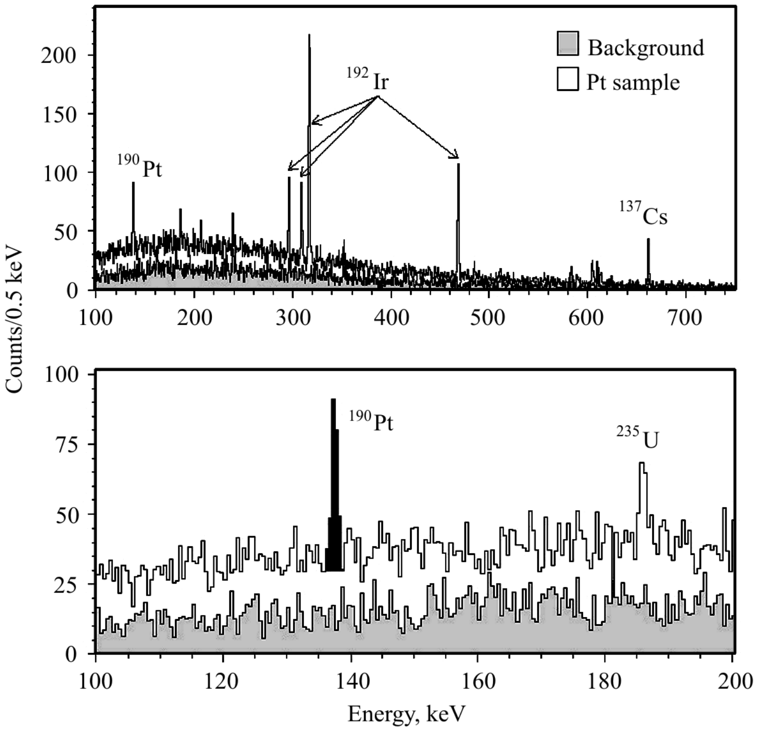

Fig. 7.20. Energy spectrum of the Pt sample with mass of 42.6 g measured over 1815 h (upper part), and in more detail around the 137 keV region (lower part). The background spectrum (measured without the Pt sample during 1046 h but normalized here to 1815 h) is also shown (filled histogram)

were used as a Pt sample. Data with the Pt were collected with HPGe detector of 468 cm^3 volume during 1815.4 h, while background spectrum of the detector was measured over 1045.6 h. The energy resolution of the detector is FWHM = = 2.0 keV for the 1332 keV γ line of ^{60}Co. To reduce external background, the detector was shielded by layers of low-radioactive copper ($\sim$10 cm) and lead ($\sim$20 cm); the set-up has been continuously flushed by high purity nitrogen (stored deep underground for a long time) to avoid presence of residual environmental radon. Part of the spectrum accumulated with the Pt sample in comparison with the background in the energy range of 100—700 keV is shown in Fig. 7.20.

The peak at energy of 137.1 ± 0.1 keV after α decay of ^{190}Pt to the 2^+_1 excited level of ^{186}Os is clearly visible in the Pt spectrum being absent in the background. Its area of 132 ± 17 counts corresponds to $T_{1/2} = 2.6^{+0.4}_{-0.3}(\text{stat.}) \pm$ $\pm\, 0.6(\text{syst.}) \times 10^{14}$ yr. An updated scheme of the ^{190}Pt decay is shown in Fig. 7.21. Half life limits for α decays of other platinum isotopes with emission of γ quanta were also obtained for the first time on the level of 10^{16}–10^{18} yr [119].

7.9. Development of experimental technique to search for rare nuclear and sub-nuclear processes

Searches for double beta decay, dark matter, hypothetical decays and processes, investigations of rare α and β decay require development of particle detectors with very low radioactive contamination, high energy resolution, very low energy threshold (especially important to search for the two neutrino electron capture and direct interaction of dark matter particles), containing certain elements (to study α, β and 2β decays) or variety of elements (for dark matter detectors). Most of scintillation materials possess unique properties required for high-sensitivity rare decay experiments: presence of certain elements, low level of intrinsic radioactivity, reasonable spectrometric characteristics, pulse-shape discrimination ability. Most of the crystal scintillators can be applied as cryogenic scintillating bolometers, which are extremely promising detectors thanks to high energy resolution and excellent particle discrimination. Here we briefly discuss development of low background scintillation detectors for low counting experiments.

7.9.1. Radioactive contamination of scintillators

Double beta decay and dark matter projects require low as much as possible — in ideal case zero — background of a detector in a region of interest. Radioactive contamination of scintillation material is the major cause of background as far as appropriate shielding against external irradiation is provided. A summary of radioactive contamination of scintillators is given in Table 7.12 [191]. The most dangerous radionuclides for 2β experiments are ^{226}Ra and ^{228}Th with daughters (^{214}Bi and ^{208}Tl) with energies of β decay of 3270 keV and 4999 keV, respectively. Naturally occurring ^{40}K usually provides

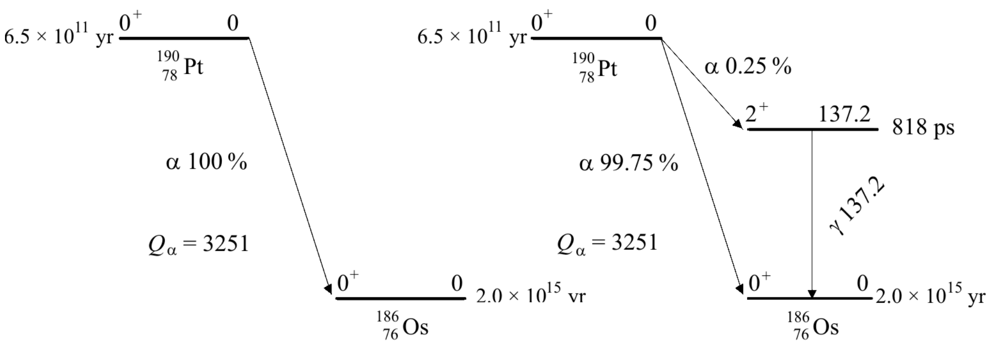

Fig. 7.21. Old (left) and new (right) schemes of α decay of ^{190}Pt

Table 7.12. **Radioactive contamination of scintillators (mBq/kg). Data for germanium crystals of HPGe detectors are given for comparison**

Scintillator	Total α activity (U + Th)	^{228}Th	^{226}Ra	^{40}K	Particular radioactivity	References
$MgWO_4$	5700 ± 400	<50	<50	<1600		[196]
$CaWO_4$	400—1400	<0.2—0.6	5.6—7	<12		[175, 193, 271, 436]
$ZnWO_4$	0.2	0.002	0.002	<0.4	0.5 (^{65}Zn)	[118]
$CdWO_4$	0.3—2	<0.003—0.039	<0.004	0.3—3.6	558 (^{113}Cd) <3—30 (^{113m}Cd)	[104, 189, 200, 247]
$PbWO_4$	$(53—79) \times 10^3$	<13	<10		$(53—79) \times 10^3$	[190]
$PbWO_4$ (from ancient lead)					<4 (^{210}Pb)	[18]
$PbMoO_4$					$(67—192) \times 10^3$	[437]
$CaMoO_4$	<10	0.04	0.13	<3		[31]
Li_2MoO_4	<300	<12	<21	170		[81, 82]
$ZnMoO_4$	73 ± 2	<(0.3—1.1)	<1.1—8.1			[88, 251]
YAG		70	170	3300		[271]
YAG:Nd	<20					[188]
$Li_6Eu(BO_3)_3$		<130	<70	<1500	949 (^{152}Eu) 212 (^{154}Eu)	[117]
BGO		<0.4—6	<1.2	<7	$7—3 \times 10^3$ (^{207}Bi)	[68, 183]
GSO(Ce)	40—217	2.3—100	0.3	<14	1200 (^{152}Gd)	[201, 425]
Lu_2SiO_5(Ce)					3.9×10^7 (^{176}Lu) [a]	
NaI(Tl)	0.08—2.4	0.009—0.02	0.012—0.2	0.6		[24, 84, 134]
CsI(Tl)		0.0015—0.009	0.009—0.010		6 (^{134}Cs) 14—61 (^{137}Cs)	[313, 442]
$LaCl_3$(Ce)		<0.4	<34		4.1×10^5 (^{138}La)	[135]
$LaBr_3$					3.2×10^5 [b]	
LuI_3					1.6×10^7 (^{176}Lu) [a]	
LiF(W)		<20	<20	<66		[107]
CaF_2(Eu)	8	0.1—0.13	1.1—1.3	<7	10 (^{152}Eu)	[116, 354]
CeF_3	3400	1100	<60	<330		[114]
BaF_2		400	1400			[176]
Plastic scintillator		<0.00013				[34]
Liquid scintillator	$\approx 10^{-6}$	$(0.21—1.2) \times 10^{-6}$ (^{232}Th)	$(0.043—6.3) \times 10^{-6}$ (^{238}U)	$<7 \times 10^{-5}$	0.3 (^{14}C)	[19, 126, 397]
HPGe		$<2 \times 10^{-5}$	$<2 \times 10^{-5}$			[215, 294]

[a] Calculated value based on ^{176}Lu half life, isotopic composition and chemical formulae of LuI_3 and Lu_2SiO_5 compounds. [b] Calculated value based on ^{138}La half life, isotopic composition and chemical formula of $LaBr_3$ compound.

rather high counting rate up to 1461 keV. Anthropogenic ^{90}Sr is also troublesome radionuclide because it is in equilibrium with ^{90}Y with high energy of decay $Q_\beta = 2280$ keV (in addition, both ^{90}Sr and ^{90}Y are nuclides rather hard to measure due to absence of γ rays detectable by HPGe γ spectrometers). Presence of cosmogenic radioactivity should be also controlled and decreased as much as possible. A reachable (and *measurable* with present instrumentation) level of tens μBq/kg is discussed now (see, e.g. [31, 34, 120, 190, 433, 439]. However, further progress in the searching for 2β decay and dark matter will be possible only using crystal scintillators with higher radiopurity.

7.9.2. Development of crystal scintillators for double β decay experiments

High sensitivity experiments to search for double β processes in different nuclei are strongly required both for theoretical and experimental reasons. Scintillation detectors are rather promising technique from this point of view. Indeed, there are several scintillation materials containing elements with potentially 2β active isotopes. It is worth to mention a pioneer work of der Mateosian and Goldhaber to search for neutrinoless double β decay of ^{48}Ca by using enriched in ^{48}Ca and ^{40}Ca CaF_2(Eu) crystal scintillators [327]. Several high sensitivity studies of the double β decay processes were performed using crystal scintillators, which contain candidate nuclei: ^{40}Ca [137], ^{48}Ca [353,416], ^{70}Zn and ^{64}Zn [93,95,103,192], ^{106}Cd [105,189,200], ^{108}Cd and ^{114}Cd [92,200], ^{116}Cd [200], ^{130}Ba [176], ^{136}Ce and ^{138}Ce [100,114], ^{160}Gd [171,201,297], ^{180}W and ^{186}W [93, 194, 200]. For instance in the Solotvina experiment [200] with the cadmium tungstate scintillators enriched in ^{116}Cd one of the lowest in the 2β experiments counting rate of 0.04 counts/(year keV kg) was reached in the energy window 2.5—3.2 MeV where a peak from $0\nu2\beta$ decay of ^{116}Cd is expected. The half life limit on neutrinoless double β decay of ^{116}Cd was set as $T_{1/2} \geq 1.7 \times 10^{23}$ years at 90 % C.L., which leads to one of the strongest restriction on the effective Majorana neutrino mass $\langle m_\nu \rangle \leq$ (1.5—1.7) eV. A number of large-scale scintillator-based projects to search for neutrinoless double β decay with sensitivity on the level of the inverted hierarchy of neutrino mass have been proposed [88, 120, 121, 172, 433, 439, 444]. The projects intend to use 10^2—10^3 kg of double β active isotopes. It should be also mentioned SuperNEMO double β decay project [279,362] aiming to utilize a large amount of plastic or liquid scintillators.

It should be stressed, that the energy resolution in a high sensitivity neutrinoless double β decay experiment aiming to explore inverted hierarchy of the neutrino mass (such an experiment should have a sensitivity to the effective neutrino mass on the level of 0.02—0.05 eV, which corresponds to half lives $T_{1/2} \sim 10^{26-28}$ yr) plays a crucial role due to irremovable background

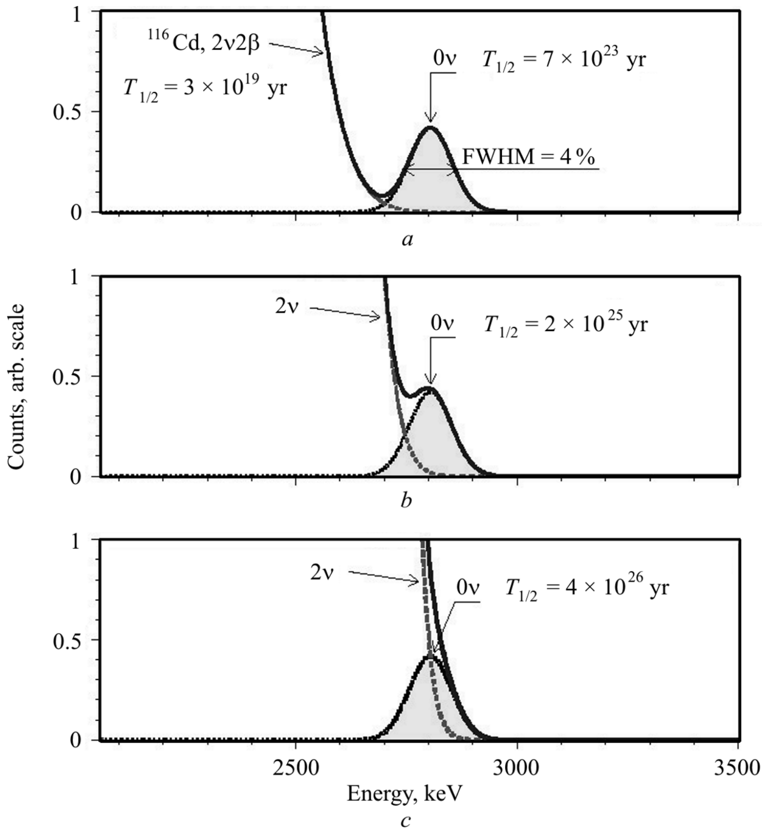

Fig. 7.22. Spectra of 0ν and $2\nu2\beta$ decays for different half life of ^{116}Cd relatively to $0\nu2\beta$ decay. Due to not perfect energy resolution, the $2\nu2\beta$ decay provides irremovable background in the region of the $0\nu2\beta$ peak

coming from two neutrino decay [438]. Importance of energy resolution for high sensitivity $0\nu2\beta$ decay experiments is demonstrated in Fig. 7.22, where the energy resolution FWHM = 4 %, a typical for scintillation experiment, is taken to show the problem of background coming from two neutrino mode. At the same time, rather modest energy resolution of scintillation detectors (typically a full width at the half of maximum is 100—150 keV for 1—3 MeV γ quanta) limits their application in high sensitivity experiments. Cryogenic scintillation bolometers (see e.g. [88, 251, 252, 363, 364]) with a typical energy resolution of a few keV looks extremely perspective technique for future neutrinoless double β decay experiments able to explore even the normal hierarchy of the neutrino mass (half life sensitivity on the level of 10^{28}—10^{30} years) [438]. At present $CdWO_4$ [252], ZnSe [187], $CaMoO_4$ [314] and recently developed $ZnMoO_4$ [88, 251, 273, 346] are considered as the most promising materials for high sensitivity cryogenic double β decay experiments.

Development of molybdates to search for neutrinoless double β decay of ^{100}Mo. ^{100}Mo is one of the most promising candidates for 2β experiments because of its high transition energy ($Q_{2\beta} = 3034.40 \pm 0.17$ keV [371]) and comparatively high isotopic abundance $\delta = 9.82 \pm 0.31\,\%$ [147]. There exist several crystal scintillators containing molybdenum: molybdate of calcium ($CaMoO_4$) [31, 123, 285], cadmium ($CdMoO_4$) [330, 364], lead ($PbMoO_4$) [197, 335, 363, 437], lithium-zinc ($Li_2Zn_2(MoO_4)_3$) [85], lithium (Li_2MoO_4) [81, 82], zinc ($ZnMoO_4$) [251, 273, 346] (the main properties of the molybdates are presented in Table 7.13). However, $CdMoO_4$ contains β active ^{113}Cd ($T_{1/2} = 8.04 \times 10^{15}$ yr [104], $\delta = 12.22\,\%$ [147]). In addition ^{113}Cd has very high cross section for capture of thermal neutrons 20600(4000) barn [236], which leads to γ background from neutron-gamma capture up to the energy of several MeV. Disadvantage of $PbMoO_4$ (even supposing that crystals would be produced from low-radioactive ancient lead [16,17,198]) is high effective Z value which causes stronger interactions with background γ quanta, and comparatively low concentration of molybdenum. $Li_2Zn_2(MoO_4)_3$ has low light yield. Besides the material is hard to grow. Here we describe recent performance of the most promising crystal scintillators containing molybdenum for cryogenic 2β experiments: $CaMoO_4$, Li_2MoO_4 and $ZnMoO_4$.

The only known molybdate crystal scintillator with reasonable light output at room temperature is calcium molybdate ($CaMoO_4$) proposed in [285] to search for the 0ν double beta decay of ^{100}Mo. The scintillation properties and the radioactive contamination of $CaMoO_4$ crystals produced by two companies in Ukraine and Russia have been studied. The best energy resolutions 10.3 % and 4.7 % for the 662 and 2615 keV γ lines were obtained with the $CaMoO_4$ sample of $\oslash 38 \times 20$ mm produced in Ukraine. Three components of the scintillation decay ($\approx$0.7 μs, 4 μs and 17 μs) and their intensities for α particles and γ quanta were observed, that allows to discriminate α particles and γ quanta. The temperature dependences of the light output and pulse shape were tested in the temperature range from -175 to $+40$ °C. The radiopurity

Table 7.13. **Main characteristics of molybdates promising for experiments to search for $0\nu2\beta$ decay of ^{100}Mo**

Crystal	Density, g/cm^3	Melting point, °C	Index of refraction	Wavelength of emission max, nm	Concentration of Mo, %
Li_2MoO_4	3.0—3.1	701		580	55.2
$Li_2Zn_2(MoO_4)_3$	4.38	890	2.0	550—610	46.1
$CaMoO_4$	4.2—4.3	1445—1480	1.98	520	48.0
$ZnMoO_4$	4.3	1003	1.9	585—625	42.6
$CdMoO_4$	4.35	1175	2.2	550	35.2
$PbMoO_4$	6.95	1060	2.4	540	26.1

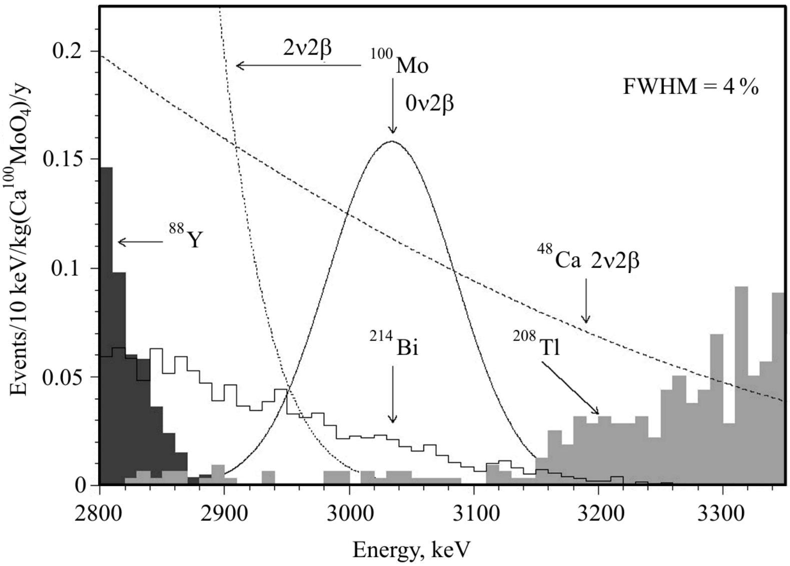

Fig. 7.23. Calculated backgrounds from the $2\nu2\beta$ decay of ^{48}Ca ($T^{2\nu}_{1/2} = 4\times10^{19}$ yr), internal pollutions by ^{208}Tl and ^{214}Bi (both with 0.1 mBq/kg), and ^{88}Y isotope from cosmogenic activity. The amplitude of the ^{88}Y distribution corresponds to 1000 decays in $CaMoO_4$, while the expected ^{88}Y cosmogenic activity is 4 events/kg/year during 5 years. Distributions for ^{100}Mo are shown for $T^{2\nu}_{1/2} = 7 \times 10^{18}$ yr and $T^{0\nu}_{1/2} = 10^{24}$ yr

of $CaMoO_4$ crystals was estimated in the low background measurements in the Solotvina underground laboratory. $CaMoO_4$ scintillators produced in Ukraine show contamination by uranium and thorium (particularly by ^{210}Po) at the level of 0.4—0.5 Bq/kg. The contamination of the $CaMoO_4$ crystal produced in Russia is one–two orders of magnitude higher.

Perspectives for high sensitivity experiments to search for the $0\nu2\beta$ decay of ^{100}Mo are discussed in [31]. The energy resolution of 4—5 % (looks realistic for ordinary scintillation detector) is enough to reach a sensitivity at the level of 10^{25} yr. The contamination of crystals by ^{226}Ra and ^{232}Th should not exceed the level of 0.1 mBq/kg. Disadvantage of $CaMoO_4$ is presence of $2\nu2\beta$ active isotope ^{48}Ca with abundance in natural calcium on the level of $\delta = 0.187\,\%$ [147], which creates background at $Q_{2\beta}$ energy of ^{100}Mo [31]. Therefore the $2\nu2\beta$ decay of ^{48}Ca restricts the sensitivity of an experiment to search for the $0\nu2\beta$ decay of ^{100}Mo by using $CaMoO_4$ crystal scintillators. Calculated background components ($2\nu2\beta$ decay of ^{48}Ca, internal pollutions by ^{208}Tl, ^{214}Bi and ^{88}Y isotopes are presented at Fig. 7.23 together with a peak of $0\nu2\beta$ decay of ^{100}Mo corresponding to the half life $T^{0\nu}_{1/2} = 10^{24}$ yr. To avoid the effect of ^{48}Ca, calcium molybdate crystals from enriched isotope ^{100}Mo and from calcium depleted in ^{48}Ca were developed [286]. A final goal

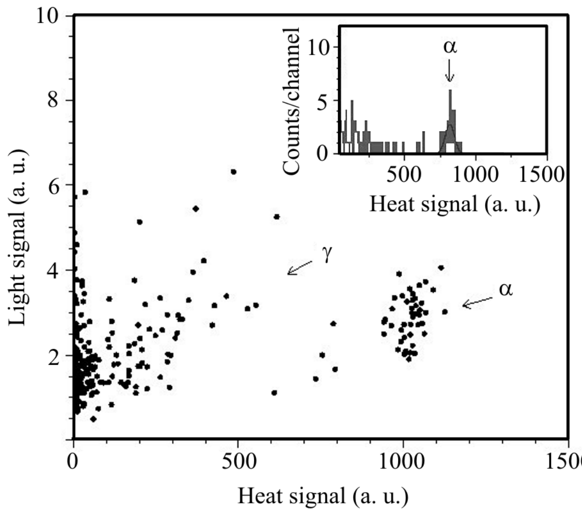

Fig. 7.24. Scatter plot of the light signal versus heat signal for 37 h background exposition with Li_2MoO_4 crystal ⌀25 × × 0.9 mm. (Inset) Distribution of heat signals. Fit of α peak by Gaussian function with the energy resolution FWHM = 9 % is shown by solid line [81]

of the AMoRE collaboration (Korea, Russia, Ukraine, China) is a large scale high sensitivity experiment to search for $0\nu2\beta$ decay of ^{100}Mo by using enriched in ^{100}Mo and depleted in ^{48}Ca calcium molybdate crystals as cryogenic scintillating bolometers [314].

A sample of Li_2MoO_4 crystal (⌀25 × 0.9 mm) was measured over 37 h as bolometer at ≈10 mK in the CUORE R&D set-up [363] in the Gran Sasso underground laboratory. In addition to the heat signal, the scintillation light was read by an additional Ge bolometer. Light output of the sample was estimated as 7 % relatively to $CdMoO_4$ crystal 10×10×2 mm. Taking into account relative light outputs of $CdMoO_4$ and $CaMoO_4$ at 9 K [330], this corresponds to ≈20 % of $CaMoO_4$. Light output for α particles is ≈30 % relatively to γ quanta, which allows to discriminate α and $\gamma(\beta)$ events (see Fig. 7.24).

The peak observed in the heat signal spectrum is probably due to contamination of the crystal by ^{210}Pb (or ^{210}Po if the equilibrium is broken). However, it could be due to contamination of the set-up. Therefore one can give only limit on activity of ^{210}Po in the sample as ≤0.3 Bq/kg. Radiopurity of a Li_2MoO_4 crystal with mass of 34 g was also measured at the Gran Sasso underground laboratory with an ultra-low background HPGe γ spectrometer [82]. Li_2MoO_4 had shown good perspectives as a possible detector to search for double beta decay of molybdenum, and resonant capture of hypothetical solar axions on ^{7}Li [81]. However, taking into account rather low purity grade of the raw materials used to produce the tested Li_2MoO_4 sample (the crystal was obtained by a solid state synthesis technique from MoO_3 and Li_2CO_3 powders both of 99.5 % purity), further R&D to improve the material would be useful.

Recently developed $ZnMoO_4$ [273, 346] is surely one of the most promising molybdates. For the first time comparatively large $ZnMoO_4$ single crystals were grown by the Czochralski and Kyropoulos methods from a melt [273]. Luminescence of the compound was measured under X ray excitation in the temperature range 85—400 K and properties of $ZnMoO_4$ crystal as cryogenic low temperature scintillator were checked for the first time [251]. Radioactive contamination of the $ZnMoO_4$ crystal was estimated as $\leq$0.3 mBq/kg (^{228}Th) and 8 mBq/kg (^{226}Ra). Thanks to the simultaneous measurement of the scintillation light and the phonon signal, the α particles can be discriminated from the γ/β interactions. The detector also shows a clear ability to discriminate the α induced background without the light measurement, thanks to a different shape of the thermal signal that characterizes γ/β and α particle interactions.

An important advantage of $ZnMoO_4$ in comparison to $CaMoO_4$ is lower melting temperature which allows to apply the so called low-thermal-gradient Czochralski technique to produce crystals from enriched ^{100}Mo. Obvious advantages of the low-thermal-gradient method in comparison to the conventional Czochralski technology are higher quality of crystals, high utilization factor of the initial charge (up to 90 %), closed platinum crucible providing a shield against evaporation from ceramic details, potentially the most radioactively contaminated part of a growing set-up. Thanks to good particle discrimination ability and high scintillation properties at low temperatures, $ZnMoO_4$ compound is extremely promising for the search of neutrinoless 2β decay of ^{100}Mo [251]. Further development of this material is in progress [88].

Development of $CdWO_4$ crystal scintillators from enriched isotopes ^{106}Cd and ^{116}Cd. The Solotvina experiment [200] has demonstrated important properties of $CdWO_4$ crystals required for a high sensitivity ^{116}Cd 2β decay experiments. Another application of $CdWO_4$ scintillating crystals is search for double β processes in ^{106}Cd. One of the highest for $2\beta^+$ nuclides value of $Q_{2\beta}$ = 2770 keV allows three modes of decay: decay with emission of two positrons ($2\beta^+$), electron capture with emission of positron ($\varepsilon\beta^+$) and double electron capture (2ε, see the decay scheme of ^{106}Cd in Fig. 7.3). ^{106}Cd looks as one of the most promising nuclei to study the $2\beta^+$ processes.

A cadmium tungstate crystal scintillator enriched in ^{106}Cd to 66 % (natural abundance is 1.25 %) was developed [105] with the aim to realize an experiment to search for double beta processes in ^{106}Cd. Sample of cadmium enriched in ^{106}Cd was purified by vacuum distillation. Cadmium tungstate compound for crystal growth was synthesized from solutions. Contamination of the enriched cadmium and synthesized compounds were controlled by mass-spectrometry and atomic absorption spectroscopy. The absolute isotopic composition of the enriched cadmium was accurately determined by thermal ionisation mass-spectrometry. In particular, the concentration of ^{106}Cd is 66 %, while abundance of β active isotope ^{113}Cd is 3.9 %. A $^{106}CdWO_4$ crystal boule, with mass of 231 g (87 % of initial mass of powder), was grown by the low-thermal-gradient Czochralski technique (see Fig. 7.25, left). The total irrecoverable loss

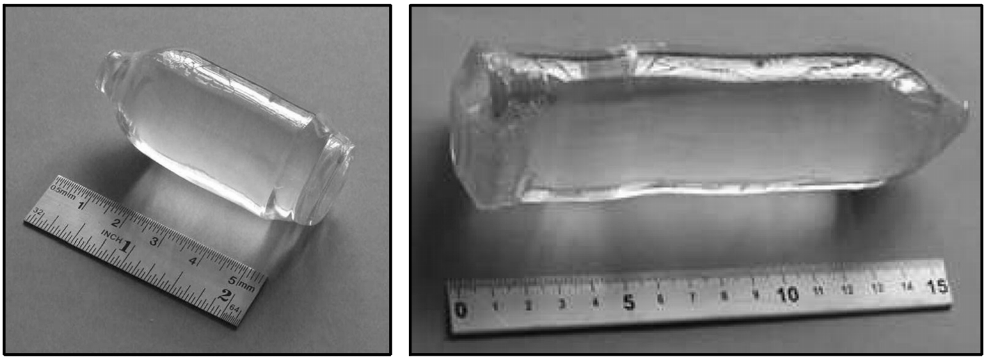

Fig. 7.25. Boules of $^{106}CdWO_4$ (left) and $^{116}CdWO_4$ (right) single crystals grown by the low-thermal-gradient Czochralski process

of enriched cadmium, on the stages of purification, raw material production, crystal growth, and scintillation element production, does not exceed 2.3 %.

A $^{106}CdWO_4$ crystal scintillator with mass of 216 g exhibits excellent optical and scintillation properties. In particular, the energy resolution FWHM $= 10\,\%$ was measured with 662 keV γ quanta of ^{137}Cs source. From the data of transmittance measurements (see Fig. 7.26) an attenuation length of the material 60 ± 7 cm at the wavelength of the emission maximum (490 nm) was derived. Such a high transmittance was newer reported for cadmium tungstate crystals. One could naturally explain this improvement by the deep purification at the stage of the enriched cadmium distillation and of the $^{106}CdWO_4$ compound synthesis, and also by the advantages of the low-thermal-gradient Czochralski technique. An experiment to search for double β processes in ^{106}Cd was performed in the Gran Sasso underground laboratory [99, 106, 115].

Cadmium tungstate crystal scintillator was also developed from cadmium enriched in ^{116}Cd. The enriched cadmium was purified by chemical methods, the most polluted part was additionally purified by vacuum distillation [300]. Cadmium tungstate compounds were synthesized from solutions. A $^{116}CdWO_4$ crystal boule with mass of 1868 g (which is 87 % of the initial charge) was grown by the low-thermal-gradient Czochralski technique (see Fig. 7.25). The ab-

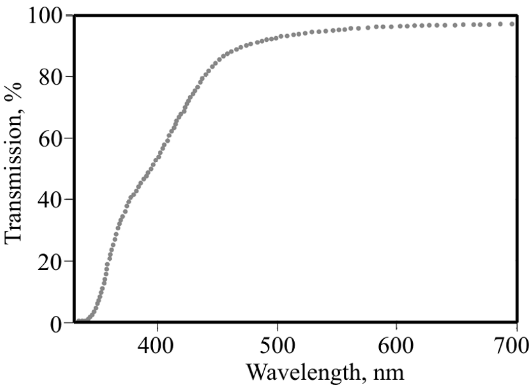

Fig. 7.26. The optical transmission curve of $^{106}CdWO_4$ crystal 50 mm long measured with a thin sample of the crystal in reference beam

solute isotopic composition of ^{116}Cd in the crystal was determined as 83 % by mass-spectrometry. Crystal scintillators produced from the boule were subjected to characterization that included measurements of transmittance and energy resolution. Low background detector with the enriched $^{116}CdWO_4$ crystal scintillators was installed in the Gran Sasso underground laboratory. Monte Carlo simulation of double β processes in ^{116}Cd was performed to estimate sensitivity of an experiment to search for double β decay of ^{116}Cd [77]. An experiment to search for double beta decay of ^{116}Cd by using the developed crystal scintillators is in progress in the Gran Sasso underground laboratory.

7.9.3. Crystal scintillators for cryogenic experiments to search for dark matter

There is an evidence for a large amount of invisible (dark) matter in the Universe, which reveals itself only through gravitational interaction. Weakly interacting massive particles (WIMPs), in particular neutralino, predicted by the Minimal Supersymmetric extensions of the Standard Model, are considered as one of the most acceptable components of the dark matter [128, 129, 151, 394]. WIMPs can be detected due to their scattering on nuclei producing low energy nuclear recoils. Extremely low counting rate and small energy of recoil nuclei are expected in experiments to search for the WIMPs. Another experimental difficulty is absence of a clear signature of the effect. In fact, near to exponential distributions of the recoils are expected, while background of a nuclear detector has also typically a behavior near to exponential. There are three signatures of the dark matter interaction with matter: dependence of the effect on nuclei (mass and spin), annual and diurnal modulations of counting rate of the recoil events. Direct methods of WIMPs detection are based on registration of ionization or/and excitation of recoil nucleus in the material of the detector itself. At present, the most sensitive direct experiments apply different detectors for WIMPs search: Ge semiconductor detectors [1, 2, 86, 316, 344], cryogenic bolometers [12, 29, 382], noble gases [28, 32, 125, 311] and scintillation detectors: NaI(Tl) [20, 130—132] CsI(Tl) [312, 313]. An interesting possibility to reject background caused by electrons and gamma quanta provides cryogenic technique, which uses simultaneous registration of heat and light signals from crystal scintillators applied already by the CRESST collaboration [29]. These detectors combine excellent energy resolution and low threshold with the ability to discriminate between different types of interactions (electron, alpha or neutron interactions).

A multi target detector with semiconductor and scintillation bolometers is under development by the EURECA collaboration (European Underground Rare Event Calorimeter Array). It should be stressed, the EURECA project requires a variety of scintillation targets to verify the nature of a detected

Table 7.14. **Relative light output (relative pulse amplitude) *LY* of crystal scintillators at liquid helium temperature under α particles irradiation measured with bialkali photomultiplier [154]**

Sample	*LY*,%	Sample	*LY*,%	Sample	*LY*,%
$CaWO_4$	100	$CaMoO_4$	46	$MgWO_4$	15
$ZnWO_4$	77	$PbWO_4$	24	LiF(W)	<5
ZnSe	61	$PbMoO_4$	21	$ZnMoO_4$	<5

signal. The most promising scintillators with high light output for cryogenic dark matter search are $ZnWO_4$, $CaWO_4$, and $CaMoO_4$ [304]. Collaboration carries out development of novel materials ($MgWO_4$ [196], $ZnMoO_4$ [346]) as well as further optimization and improvement of $ZnWO_4$, $CaWO_4$, $CaMoO_4$, CaF_2, BGO, Al_2O_3, LiF, ZnSe, $PbWO_4$, $PbMoO_4$.

Relative pulse amplitude of some crystal scintillators (which can be used as an estimation of relative light output) at helium temperature under α particles irradiation measured with bialkali photomultiplier is presented in Table 7.14.

Radioactive contamination of target scintillation crystals will play a key role to decrease background of a detector. Counting rate of a few counts per kg per day in the energy interval 2—20 keV is typical in the present scintillator-based dark matter experiments [20, 132, 312, 428]. However, to elaborate region of WIMP-nucleon scattering cross sections predicted by the different models, background of a detector should be further decreased by a few orders of magnitude. For instance, the EURECA dark matter project calls for background counting rate lower than a few events per keV per 100 kg per year at energies of a few keV [301, 302]. The project makes strict enough demands to scintillators: they should not contain paramagnetic elements, possess high light output (more than 1.5×10^4 photons/MeV), a very low level of radioactive impurity. Fig. 7.27 shows simulated by GEANT4 energy spectra of a scintillation detector contaminated by ^{40}K, ^{60}Co, ^{87}Rb, ^{90}Sr—^{90}Y, ^{137}Cs, ^{232}Th, ^{238}U on the level of 0.1 mBq/kg by each radionuclide [195]. Equilibrium of ^{232}Th and ^{238}U chains assumed to be broken: contributions of ^{234}Th + ^{234m}Pa, ^{210}Pb + ^{210}Bi from the ^{238}U family, and ^{228}Ra + ^{228}Ac, ^{212}Pb + ^{208}Th (^{232}Th) are considered separately. The energy resolution dependence on energy is assumed to be described by square root function with FWHM = 10 % for 662 keV γ line of ^{137}Cs. Supposing a suppression factor 10^2—10^3, which can be reached thanks to the active background rejection using a combination of phonon and scintillation signals, radioactive contamination of crystal scintillators should not exceed a level of ~0.01 mBq/kg for total activity. As one can see in Table 7.12, there is no crystal scintillator satisfying such a strong demand. Therefore, an extended R&D are necessary to reach the level of radiopurity requested by the next generation dark matter experiments.

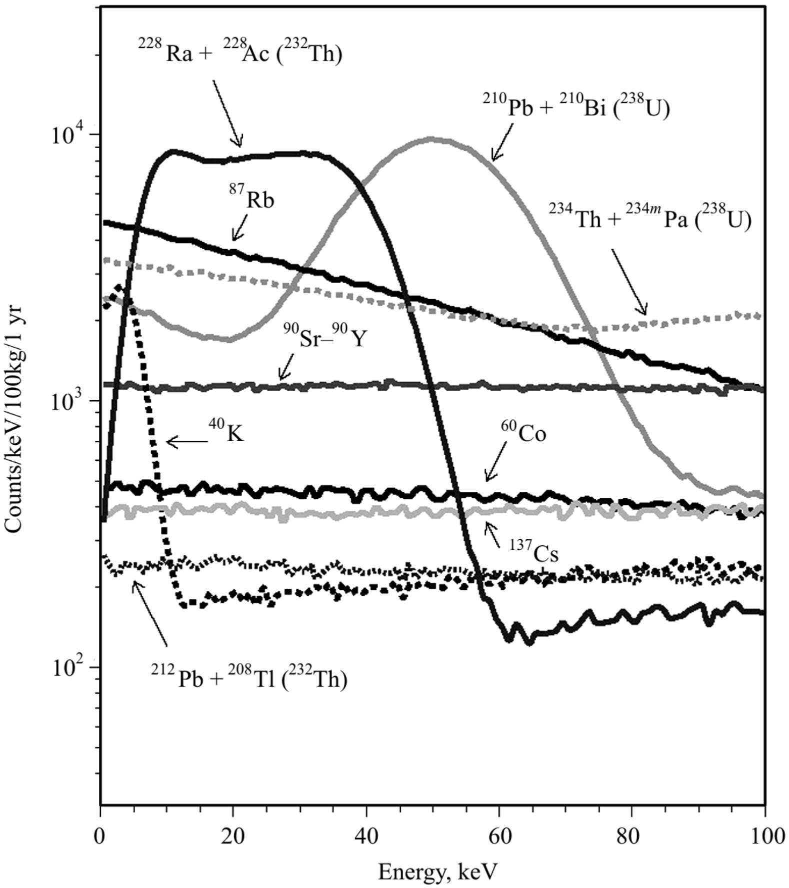

Fig. 7.27. Simulated energy spectra of a scintillation detector contaminated by ^{40}K, ^{60}Co, ^{87}Rb, ^{90}Sr—^{90}Y, ^{137}Cs, ^{232}Th, ^{238}U on the level of 0.1 mBq/kg by each radionuclide

Such an R&D should include the following principal steps [193, 195]:

1. Deep purification of raw materials is supposed to be the most important issue. Metal purification by vacuum distillation, zone melting, and filtering are very promising approaches [133], while further study is necessary for the purification of Ca and Li in order to achieve the required low levels of radioactive contamination.

2. Two to four step re-crystallization, involving screening and assessment of the produced scintillators after each step.

3. Testing at all stages through ultra-low background γ, α, β spectrometry compounds for crystal growing (choice of raw materials, quality control of purified elements and compounds).

4. All work should be done using highly pure reagents, lab-ware and water. All chemistry should be done in a clean room, and, as far as possible, in nitrogen atmosphere. Careful protection from radon should be foreseen.

The low-background scintillation measurements are currently the most appropriate methods of examining the performance of scintillators. R&D of ultra-low-radioactive instrumentation with the sensitivity at the level of 0.01 mBq/kg (able to operate at low, at least liquid nitrogen, temperatures) are necessary. In itself the problem of measurements of crystal scintillators' radiopurity on the level of 0.01 mBq/kg is rather complicated task. Detection of low energy β emitters (e.g., ^{87}Rb, ^{115}In, ^{138}La, ^{176}Lu, ^{187}Re, ^{210}Pb) is particularly difficult. Presence of these radionuclides on the levels dangerous for dark matter experiments can be detected only in produced crystal scintillators under very low background conditions. It should be stressed that measurements of low energy β active radionuclides in crystal scintillators were never realized at such a level of sensitivity.

In addition one should keep in mind also cosmogenic radionuclides. For instance, accumulation of radioactive ^{14}C ($Q_\beta = 156.475$ keV, $T_{1/2} = 5730$ yr), highly undesirable for dark matter experiments, was considered in [440]. The radioactive ^{14}C can be produced by hadronic component of cosmic rays in any materials composed of elements heavier than carbon. Another cosmogenic radionuclide, ^{65}Zn, was observed in comparatively radiopure $ZnWO_4$ scintillators [93,118]. An indication of cosmogenic ^{110m}Ag contamination in $^{116}CdWO_4$ crystal scintillators was reported in [77]. Underground production of detectors, in particular of crystal scintillators, can be requested by the next generation of low background experiments.

Zinc tungstate is a good example of radiopure scintillator (~0.2—1 mBq/kg level of radioactive contamination) [93, 192, 303]. Nevertheless, at least a ~20-fold improvement of $ZnWO_4$ radiopurity is still needed for the EURECA experiment, and this represents a significant challenge. Besides, optimization of light collection from crystal scintillators is highly desirable for cryogenic dark matter experiments. The scintillation properties of a zinc tungstate crystal, shaped as a hexagonal prism (height 40 mm, diagonal 40 mm) were determined. An energy resolution of 10.7 % for the 662 keV γ line of ^{137}Cs was measured with the scintillator placed in a light collection set-up similar to that used by the CRESST dark matter search. The light output and decay kinetics of $ZnWO_4$ were examined over the temperature range 7—300 K (see Fig. 7.28 where the temperature dependence is presented) and confirmed to be competitive with those of $CaWO_4$. The radioactive contaminations of the $ZnWO_4$ scintillator measured in the Solotvina underground laboratory do not exceed 0.1—10 mBq/kg (depending on radionuclide). Both scintillation measurements and Monte Carlo simulations show that a hexagonal shape of the scintillation detector provi-

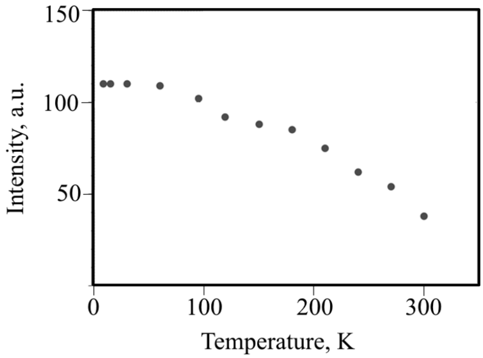

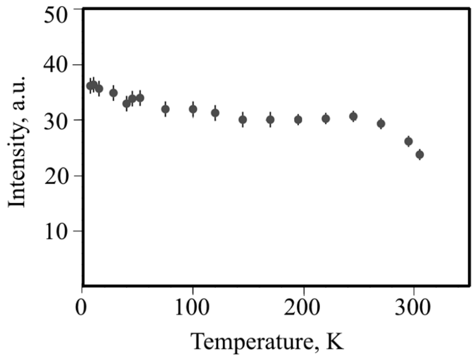

Fig. 7.28. Temperature dependence of the light output of $ZnWO_4$ crystal scintillator for excitation with ^{241}Am particles

Fig. 7.29. Temperature dependence of the light output of the $MgWO_4$ crystal scintillator for excitation with ^{241}Am α particles

des ~20 % better light output than a cylinder. This study demonstrates the excellent feasibility of $ZnWO_4$ scintillator for cryogenic dark matter experiments.

Calcium tungstate ($CaWO_4$) discovered as scintillator sixty years ago [250, 343] is an appropriate material for cryogenic scintillating bolometers currently used by the CRESST experiment to search for dark matter particles [29, 30, 308, 331, 428]. There is a noticeable variation of radioactive contamination of different $CaWO_4$ samples [175, 436]. The equilibrium of U radioactive chain is typically broken in calcium tungstate crystals, the activity of ^{210}Pb and its daughters dominates in radioactive contamination of $CaWO_4$. Development of radiopure $CaWO_4$ crystal scintillators would be a benefit both for the CRESST and EURECA dark matter experiments.

Recrystallization is expected to be an efficient way to decrease radioactive contamination of crystal scintillators. Effect of recrystallization on radioactive contamination was studied for $CaWO_4$ crystals. Seven samples of $CaWO_4$ crystals were fabricated from three ingots that have been grown using the recrystallization procedure [193]. The radioactive contamination of the crystals was investigated and it was found that ^{210}Po and ^{238}U are the main contributors to the intrinsic α background, the equilibrium of the ^{238}U chain in the crystals is broken. It was demonstrated that the recrystallization process causes significant changes of the radioactive contamination of $CaWO_4$ crystals. It leads to variation in the activity of ^{210}Po (in the range 0.03—1.32 Bq/kg), and ^{238}U (0.04—0.33 Bq/kg) in the crystals. Activity of uranium is decreased thanks to recrystallization. The increase of ^{210}Po activity with time evidenced that ^{210}Po is mainly produced due to ^{210}Pb decay. Therefore radioactive ^{210}Pb should be carefully screened and reduced in raw materials for crystal production. In addition, one needs to study effects of crystal production technology (crystal growth, annealing, cutting, surface treatment) on their radioactive contamination.

The feasibility of lead molybdate ($PbMoO_4$) and lead tungstate ($PbWO_4$) as detectors for rare event searches has been envisaged in [335] and [234], respectively. The prospects of radiopure $PbWO_4$ and $PbMoO_4$ crystal scintillators as target materials in cryogenic dark matter experiments have been discussed recently [346]. Scintillation properties of $PbWO_4$ and $PbMoO_4$ crystals, as potential cryogenic scintillators for rare event searches, have been studied. The light output and decay kinetics of $PbWO_4$ and $PbMoO_4$ crystals for excitation with ^{241}Am α particles were examined over the temperature range 7—300 K. The α/β ratio was measured with a $PbMoO_4$ crystal scintillator for 5.3 MeV α particles, and the ability to distinguish between signals induced by α particles and γ quanta by pulse shape discrimination was assessed for the $PbMoO_4$ crystal scintillator at 77 K. The energy dependence of the quenching factor for oxygen, molybdenum, tungsten and lead ions at low energy was calculated using a semi-empirical approach [412] with data from the α particle measurements. Both $PbWO_4$ and $PbMoO_4$ crystals are of particular interest for cryogenic experiments to search for dark matter due to the combination of heavy (W, Pb), middle (Mo) and light (O) elements. Nonetheless, the high intrinsic radioactivity due to ^{210}Pb is the main obstacle, limiting the usefullness of these materials for low-background experiments. However, the use of ancient lead for crystal growth should permit to produce lead tungstate and lead molybdate with substantially reduced intrinsic radioactivity to the level of a few mBq/kg [16, 17, 198].

Magnesium tungstate ($MgWO_4$) crystals of ~1 cm^3 volume were obtained for the first time using a flux growth technique. The crystal was subjected to comprehensive characterization that included room temperature measurements of the transmittance, X ray luminescence spectra, afterglow under X ray excitation, relative photoelectron output, energy resolution, non-proportionality of scintillation response to γ quanta, response to α particles, and pulse-shape for γ quanta and α particles. The light output and decay kinetics of $MgWO_4$ were studied over the temperature range 7—305 K. The variation with temperature of the $MgWO_4$ light output in the interval 7—305 K is shown in Fig. 7.29. Under X ray excitation the crystal exhibits an intense luminescence band peaking at a wavelength of 470 nm; the intensity of afterglow after 20 ms is 0.035 %. An energy resolution of 9.1 % for 662 keV γ quanta of ^{137}Cs was measured with a small (≈0.9 g) sample of the $MgWO_4$ crystal (see Fig. 7.30). The photoelectron output of the $MgWO_4$ crystal scintillator is 35 % of that for $CdWO_4$ and 27 % of that for NaI(Tl). The detector showed pulse-shape discrimination ability in measurements with α particles and γ quanta; and that enabled to assess the radioactive contamination of the scintillator. The results of these studies demonstrate the prospect of this material for a variety of scintillation applicati-

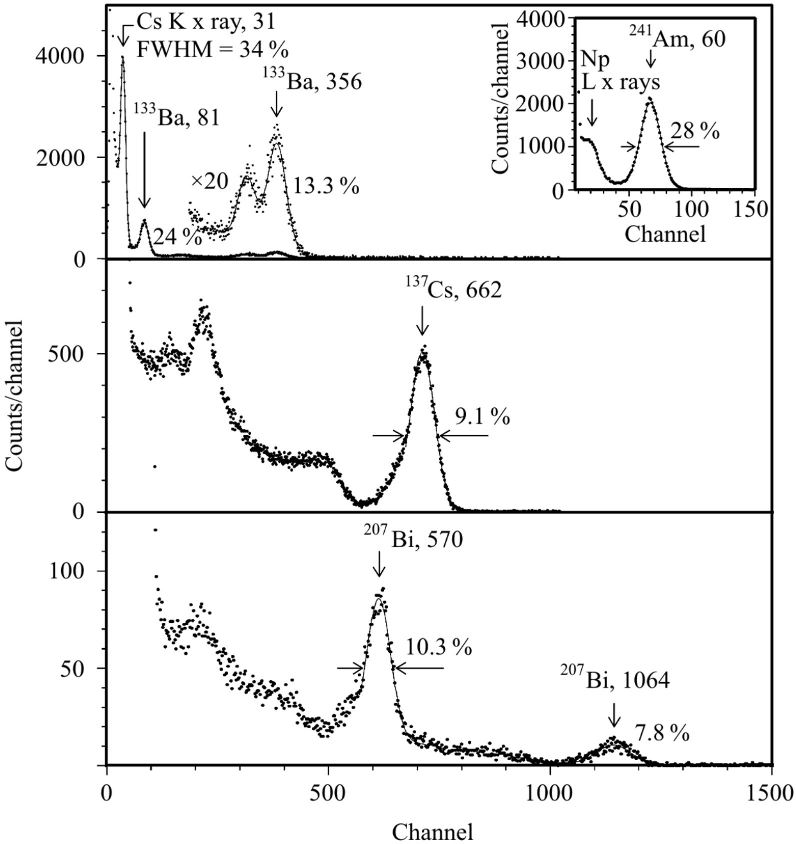

Fig. 7.30. Energy spectra of ^{133}Ba, ^{241}Am (inset), ^{137}Cs, and ^{207}Bi γ rays measured for the $MgWO_4$ scintillation crystal. Fits of the γ peaks are shown as solid lines. Energies of the γ and X ray lines are in keV

ons, including rare event searches [196]. The material can be used for instance in the EURECA project, which require a variety of scintillation targets to verify the nature of a detected signal.

7.9.4. Semi-empirical calculation of quenching factors for ions in scintillators

For a long time it is known that amount of light produced in scintillating material by highly ionizing particles (protons, α particles, heavy ions) is lower than that produced by electrons of the same energy [153]. Thus, in a scintillator calibrated with electron and/or γ sources (which is an usual practice), signals from ions will be seen at lower energies (sometimes up to 40 times) than their real values. Knowledge of these transformation coefficients —

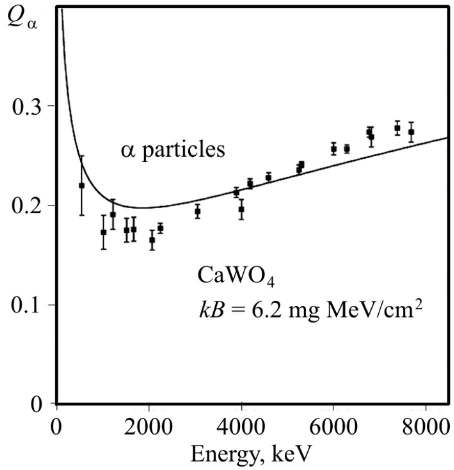

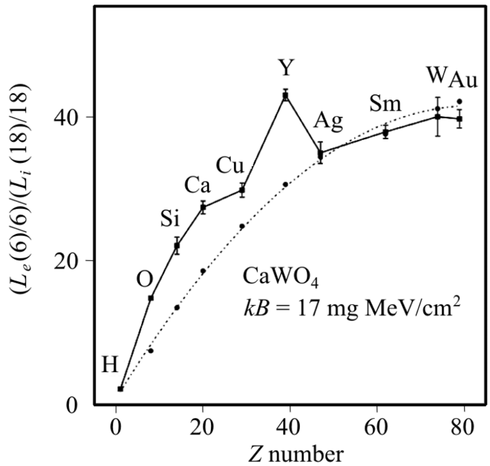

Fig. 7.31. Quenching factors for α particles in $CaWO_4$ and their fit with $kB =$ $= 6.2$ mg $MeV^{-1} \cdot cm^{-2}$

Fig. 7.32. Dependence of inverse of the relative light output at $E_i = 18$ keV, normalized to that for electrons at $E_e = 6$ keV on ion's Z number: squares are experimental points from [350], and circles are calculated values with $kB = 17$ mg $MeV^{-1} \cdot cm^{-2}$ found by equating experimental and theoretical values only at one point measured with protons in $CaWO_4$

quenching factors — is extremely important in prediction where the signal should be expected in searches for dark matter particles or in studies of rare α decays.

Semi-empirical method of calculation of quenching factors for scintillators is developed recently [412]. It is based on classical Birks formula [153] with using of the total stopping powers for electrons $(dE/dr)_e$ and ions $(dE/dr)_i$ calculated with the ESTAR [230] and SRIM [396] codes, respectively. The ion quenching factor Q_i at energy E is defined as the ratio of light yield of the ion to that of an electron of the same energy: $Q_i = L_i/L_e$, where

$$L_i = \int_0^E \frac{dE}{1 + kB(\frac{dE}{dr})_i}, \quad L_e = \int_0^E \frac{dE}{1 + kB(\frac{dE}{dr})_e}.$$

The method has only one fitting parameter (the Birks factor kB) which can have different values for the same material in different conditions of measurements and data treatment. A hypothesis is used that, once the kB value is obtained by fitting data for particles of one kind and in some energy region (e.g. for a few MeV α particles from internal contamination of a detector), it can be applied to calculate quenching factors for particles of other kind and for other energies (e.g. for low energy nuclear recoils) if all data are measured in the same experimental conditions and are treated in the same way. Applicability of the method was demonstrated on many examples including materials with different mechanisms of scintillation: organic scintillators (solid C_8H_8, and liquid $C_{16}H_{18}$, C_9H_{12}); crystal scintillators (pure $CdWO_4$, $PbWO_4$, $ZnWO_4$, $CaWO_4$, CeF_3, and doped CaF_2(Eu), CsI(Tl), CsI(Na), NaI(Tl)); liquid noble gases (LXe). Estimations of quenching factors for nuclear recoils are also given for some scintillators where experimental data are absent ($CdWO_4$, $PbWO_4$, CeF_3, $Bi_4Ge_3O_{12}$, LiF, ZnSe). Examples of calculations are given in Fig. 7.31 and 7.32.

BIBLIOGRAPHY

1. C.E. Aalseth et al., Experimental constraints on a dark matter origin for the DAMA annual modulation effect, Phys. Rev. Lett. **101**, 251301 (2008).
2. C.E. Aalseth et al., Results from a search for light-mass dark matter with a p-type point contact germanium detector, Phys. Rev. Lett. **106**, 131301 (2011).
3. C.E. Aalseth et al., The proposed Majorana ^{76}Ge double-beta decay experiment, Nucl. Phys. B (Proc. Suppl.) **138**, 217—220 (2005).
4. C.E. Aalseth, F.T. Avignone III, R.L. Brodzinski, J.I. Collar et al., Recent results from the IGEX double-beta decay experiment, Nucl. Phys. B. (Proc. Suppl.) **48**, 223—225 (1996).
5. C.E. Aalseth, F.T. Avignone III, R.L. Brodzinski et al. The IGEX ^{76}Ge neutrinoless double-beta decay experiment: prospect for next generation experiments, Phys. Rev. D **65**, 092007 (2002).
6. M. Ablikim et al., Search for invisible decays of η and η' in $J/\psi \to \phi\eta$ and $\phi\eta'$, Phys. Rev. Lett. **97**, 202002 (2006).
7. M. Ablikim et al., Search for the invisible decay of J/ψ in $\psi(2S) \to \pi^+\pi^- J/\psi$, Phys. Rev. Lett. **100**, 192001 (2008).
8. N. Ackerman et al., Observation of two-neutrino double-beta decay in ^{136}Xe with EXO-200 detector, Phys. Rev. Lett. **107**, 212501 (2011).
9. Y. Aharonov et al., New experimental limits for the electron stability, Phys. Lett. B **353**, 168—172 (1995).
10. Q.R. Ahmad et al., Direct evidence for neutrino flavor transformation from neutral-current interactions in the Sudbury Neutrino Observatory, Phys. Rev. Lett. **89**, 011301 (2002).
11. S.N. Ahmed et al., Constraints on nucleon decay via invisible modes from the Sudbury Neutrino Observatory, Phys. Rev. Lett. **92**, 102004 (2004).
12. Z. Ahmed et al., Search for weakly interacting massive particles with the first five-tower data from the cryogenic dark matter search at the Soudan Underground Laboratory, Phys. Rev. Lett. **102**, 011301 (2009).
13. S. Agostinelli et al., GEANT4 — a simulation toolkit, Nucl. Instrum. Meth. A **506**, 250—303 (2003).
14. D.V. Aleksandrov et al., Observation of the spontaneous emission of ^{14}C nuclei from ^{223}Ra, JETP Lett. **40**, 909—912 (1984).
15. A. Alessandrello et al., Bolometric measurements of the beta spectrum of ^{113}Cd, Nucl. Phys. B (Proc. Suppl.) **35**, 394—396 (1994).

16. A. Alessandrello et al., Measurements on radioactivity of ancient roman lead to be used as shield in searches for rare events, Nucl. Instr. Meth. B **61**, 106—117 (1991).
17. A. Alessandrello et al., The bolometers as nuclear recoil detectors, Nucl. Instr. Meth. A **409**, 451—453 (1998).
18. A. Alessandrello et al., Measurements of internal radioactive contamination in samples of Roman lead to be used in experiments on rare events, Nucl. Instr. Meth. B **142**, 163—172 (1998).
19. G. Alimonti et al., Measurement of the ^{14}C abundance in a low background liquid scintillator, Phys. Lett. B **422**, 349—358 (1998).
20. G.J. Alner et al., Limits on WIMP cross-sections from the NAIAD experiment at the Boulby Underground Laboratory, Phys. Lett. B **616**, 17—24 (2005).
21. R. Alonso, A. Lopez-Garcia, H. Vucetich, On the electron stability measured by the coincidence spectroscopy, Nucl. Instrum. Meth. A **383**, 451—453 (1996).
22. M. Alston-Garnjost, B.L. Dougherty, R.W. Kenney, R.D. Tripp et al., Experimental search for double-β decay of ^{100}Mo, Phys. Rev. C **55**, 474—493 (1997).
23. D. Akimov et al., EXO: an advanced Enriched Xenon double-beta decay Observatory, Nucl. Phys. B (Proc. Suppl.) **138**, 224—226 (2005).
24. J. Amare et al., Background understanding and improvement in NaI scintillators, J. Phys.: Conf. Series **39**, 201—201 (2006).
25. D.L. Anderson, *New Theory of the Earth* (Cambridge, 2007), 405 p.
26. E. Andreotti, C. Arnaboldi, F.T. Avignone III, M. Balata, I. Bandac et al., Search for β^+/EC double beta decay of ^{120}Te, Astropart. Phys. **34**, 643—648 (2011).
27. E. Andreotti et al., Half-life of the β decay $^{115}In(9/2+) \rightarrow {}^{115}Sn(3/2+)$, Phys. Rev. C **84**, 044605 (2011).
28. J. Angle et al. (XENON Collaboration), First results from the XENON10 dark matter experiment at the Gran Sasso National Laboratory, Phys. Rev. Lett. **100**, 021303 (2008).
29. G. Angloher et al., Commissioning run of the CRESST-II dark matter search, Astropart. Phys. **31**, 270—276 (2009).
30. G. Angloher et al., Limits on WIMP dark matter using scintillating $CaWO_4$ cryogenic detectors with active background suppression, Astropart. Phys. **23**, 325—339 (2005).
31. A.N. Annenkov et al., Development of $CaMoO_4$ crystal scintillators for a double beta decay experiment with ^{100}Mo, Nucl. Instr. Meth. A **584**, 334—345 (2008).
32. E. Aprile et al. (XENON100 Collaboration), First dark matter results from the XENON100 experiment, Phys. Rev. Lett. **105**, 131302 (2010).
33. T. Araki et al., Search for the invisible decay of neutrons with KamLAND, Phys. Rev. Lett. **96**, 101802 (2006).
34. J. Argyriades et al., Results of the BiPo-1 prototype for radiopurity measurements for the SuperNEMO double beta decay source foils, Nucl. Instr. Meth A **622**, 120—128 (2010).
35. J. Argyriades et al., Measurement of the double-β decay half-life of ^{150}Nd and search for neutrinoless decay modes with the NEMO-3 detector, Phys. Rev. C **80**, 032501 (2009).

36. J. Argyriades et al., Measurement of the two neutrino double beta decay half-life of Zr-96 with the NEMO-3 detector, Nucl. Phys. A **847**, 168—179 (2010).
37. N. Arkani-Hamed, S. Dimopoulos, G. Dvali, The hierarchy problem and new dimensions at a millimeter, Phys. Lett. B **429**, 263—272 (1998).
38. N. Arkani-Hamed, S. Dimopoulos, G. Dvali, Large extra dimensions: A new arena for particle physics, Phys. Today, February 2002, p. 35—40.
39. V. Artemiev et al., Half-life measurement of ^{150}Nd 2β decay in the time projection chamber experiment, Phys. Lett. B **345**, 564—568 (1995).
40. C. Arnaboldi et al., Physics potential and prospects for the CUORICINO and CUORE experiments, Astropart. Phys. **20**, 91—110 (2003).
41. C. Arnaboldi et al., Results from the CUORICINO $0\nu\beta\beta$-decay experiment, Phys. Rev. C **78**, 035502 (2008).
42. C. Arnaboldi et al., A calorimetric search on double beta decay of ^{130}Te, Phys. Lett. B **557**, 167—175 (2003).
43. R. Arnold et al., Measurement of the $\beta\beta$ decay half-life of ^{130}Te with the NEMO-3 detector, Phys. Rev. Lett. **107**, 062504 (2011).
44. R. Arnold et al., Double beta decay of ^{96}Zr, Nucl. Phys. A **658**, 299—312 (1999).
45. R. Arnold et al., Double-β decay of ^{82}Se, Nucl. Phys. A **636**, 209—223 (1998).
46. R. Arnold et al., First results of the search for neutrinoless double-beta decay with the NEMO 3 detector, Phys. Rev. Lett. **95**, 182302 (2005).
47. R. Arnold et al., Double-β decay of ^{116}Cd, Z. Phys. C **72**, 239—247 (1996).
48. R. Arnold et al., Measurement of double beta decay of ^{100}Mo to excited states in the NEMO 3 experiment, Nucl. Phys. A **781**, 209—226 (2007).
49. R. Arnold et al., Limits on different majoron decay modes of ^{100}Mo and ^{82}Se for neutrinoless double beta decays in the NEMO-3 experiment, Nucl. Phys. A **765**, 483—494 (2006).
50. V.D. Ashitkov, A.S. Barabash, S.G. Belogurov, G. Carugno et al., Double Beta Decay of ^{100}Mo, JETP Lett. **74**, 529—531 (2001).
51. S.J. Asztalos, L.J. Rosenberg, K. van Bibber et al., Searches for astrophysical and cosmological axions, Annu. Rev. Nucl. Part. Sci. **56**, 293—326 (2006).
52. F.T. Avignone III, G.S. King, Yu.G. Zdesenko, Next generation double-beta decay experiments: metrics for their evaluation, New J. Phys. **7**, 6—46 (2005).
53. F.T. Avignone III, S.R. Elliott, J. Engel, Double beta decay, Majorana neutrinos, and neutrino mass, Rev. Mod. Phys. **80**, 481—516 (2008).
54. F.T. Avignone III et al., New experimental limit on the stability of the electron, Phys. Rev. D **34**, 97—100 (1986).
55. B. Aubert et al., Search for B^0 decays to invisible final states and to $\nu\bar{\nu}\gamma$, Phys. Rev. Lett. **93**, 091802 (2004).
56. B. Aubert et al., Search for invisible decays of the $Y(1S)$, Phys. Rev. Lett. **103**, 251801 (2009).
57. G. Audi, A.H. Wapstra, C. Thibault, The AME2003 atomic mass evaluation (II). Tables, graphs and references, Nucl. Phys. A **729**, 337—676 (2003).
58. K.S. Babu, I. Gogoladze, K. Wang, Gauged baryon parity and nucleon stability, Phys. Lett. B **570**, 32—38 (2003).
59. H.O. Back et al., Search for electron decay mode $e \to \gamma + \nu$ with prototype of Borexino detector, Phys. Lett. B **525**, 29—40 (2002).

60. H.O. Back et al., New limits on nucleon decays into invisible channels with the BOREXINO counting test facility, Phys. Lett. B **563**, 23—34 (2003).
61. A. Badertscher et al., Improved limit on invisible decays of positronium, Phys. Rev. D **75**, 032004 (2007).
62. J.N. Bahcall, A.M. Serenelli, S. Basu, 10,000 standard solar models: a Monte Carlo simulation, Astrophys. J. Suppl. Ser. **165**, 400—431 (2006).
63. J.N. Bahcall, M.H. Pinsonneault, What do we (not) know theoretically about solar neutrino fluxes? Phys. Rev. Lett. **92**, 121301 (2004).
64. A.B. Balantekin, Neutrino magnetic moment, AIP Conf. Proc. **847**, 128—133 (2006).
65. A. Balysh, A. De Silva, V.I. Lebedev, K. Lou et al., Double beta decay of ^{48}Ca, Phys. Rev. Lett. **77**, 5186—5189 (1996).
66. A.Ya. Balysh et al., Radiochemical search for the decay of uranium-233 with the emission of neon-24 using a low-background semiconductor gamma-ray spectrometer, Sov. Phys. JETP **64**, 21—24 (1986).
67. A. Balysh et al., New experimental limits for electron decay and charge conservation, Phys. Lett. B **298**, 278—282 (1993).
68. A. Balysh et al., Radioactive impurities in crystals of bismuth germanate, Pribory i Tekhnika Eksperimenta **1**, 118—122 (1993) (in Russian).
69. I.R. Barabanov et al., Verification of the law of conservation of electric charge, JETP Lett. **32**, 359—361 (1980).
70. A.S. Barabash, Precise half-life values for two-neutrino double-β decay, Phys. Rev. C **81**, 035501 (2010).
71. A.S. Barabash et al., Two neutrino double-beta decay of ^{100}Mo to the first excited 0^+ state in ^{100}Ru, Phys. Lett. B **345**, 408—413 (1995).
72. A.S. Barabash et al., The extrapolation of NEMO techniques to future generation 2β-decay experiments, Phys. At. Nucl. **67**, 1984—1988 (2004).
73. A.S. Barabash, Ph. Hubert, A. Nachab, V. Umatov, Search for β^+EC and ECEC processes in ^{74}Se, Nucl. Phys. A **785**, 371—380 (2007).
74. A.S. Barabash et al., Search for β^+EC and ECEC processes in ^{112}Sn and $\beta^-\beta^-$ decay of ^{124}Sn to the excited states of ^{124}Te, Nucl. Phys. A **807**, 269—281 (2008).
75. A.S. Barabash, Double beta decay experiments, Phys. Part. Nucl. **42**, 613—627 (2011).
76. A.S. Barabash, Double beta decay: Historical review of 75 years of research, Phys. At. Nucl. **74**, 603—613 (2011).
77. A.S. Barabash et al., Low background detector with enriched $^{116}CdWO_4$ crystal scintillators to search for double β decay of ^{116}Cd, J. Instrumentation **06**, P08011 (2011).
78. A.S. Barabash et al., $2\nu\beta\beta$ decay of ^{100}Mo to the first 0^+ excited state in ^{100}Ru, Phys. At. Nucl. 62, 2039—2044 (1999).
79. A.S. Barabash, Ph. Hubert. A. Nachab, V.I. Umatov, Investigation of $\beta\beta$ decay in ^{150}Nd and ^{148}Nd to the excited states of daughter nuclei, Phys. Rev. C **79**, 045501 (2009).
80. A.S. Barabash, R.R. Saakyan, Experimental Limits on $2\beta^+$, Kβ^+, and 2K Processes for ^{130}Ba and on 2K Capture for ^{132}Ba, Phys. At. Nucl. **59**, 179—184 (1996).

81. O.P. Barinova et al, First test of Li_2MoO_4 crystal as a cryogenic scintillating bolometer, Nucl. Instrum. Meth. A **613**, 54—57 (2010).
82. O.P. Barinova et al., Intrinsic radiopurity of a Li_2MoO_4 crystal, Nucl. Instr. Meth. A **607**, 573—575 (2009).
83. R. Barloutaud, Status of the search for matter stability, Nucl. Phys. B (Proc. Suppl.) A **28**, 437—446 (1992).
84. J.C. Barton, J.A. Edgington, Analysis of alpha-emitting isotopes in an inorganic scintillator, Nucl. Instr. Meth. A **443**, 277—286 (2000).
85. N.V. Bashmakova et al., $Li_2Zn_2(MoO_4)_3$ crystal as a potential detector for ^{100}Mo 2β-decay search, Functional Materials **16**, 266—274 (2009).
86. L. Baudis et al., First results from the Heidelberg dark matter search experiment, Phys. Rev. D **63**, 022001 (2001).
87. M. Beck et al., Investigation of the Majoron-accompanied double-beta decay mode of ^{76}Ge, Phys. Rev. Lett. **70**, 2853—2855 (1993).
88. J.W. Beeman et al., A next-generation neutrinoless double beta decay experiment based on $ZnMoO_4$ scintillating bolometers, Phys. Lett. B **710**, 318—323 (2012).
89. N.F. Bell, V. Cirigliano, M.J. Ramsey-Musolf, P. Vogel, M.B. Wise, How magnetic is the Dirac neutrino? Phys. Rev. Lett. **95**, 151802 (2005).
90. P. Belli et al., First limits on neutrinoless resonant 2β captures in ^{136}Ce and new limits for other 2β processes in ^{136}Ce and ^{138}Ce isotopes, Nucl. Phys. A **824**, 101—114 (2009).
91. P. Belli et al., New observation of $2\beta2\nu$ decay of ^{100}Mo to the 0_1^+ level of ^{100}Ru in the ARMONIA experiment, Nucl. Phys. A **846**, 143—156 (2010).
92. P. Belli et al., Search for double-β decay processes in ^{108}Cd and ^{114}Cd with the help of the low-background $CdWO_4$ crystal scintillator, Eur. Phys. J. A **36**, 167—170 (2008).
93. P. Belli et al., Search for double beta decay of zinc and tungsten with low background $ZnWO_4$ crystal scintillators, Nucl. Phys. A **826**, 256—273 (2009).
94. P. Belli et al., New limits on spin-dependent coupled WIMPs and on 2β processes in ^{40}Ca and ^{46}Ca by using low radioactive CaF_2(Eu) crystal scintillators. Nucl. Phys. B **563**, 97—106 (1999).
95. P. Belli et al., Final result of experiment to search for 2β processes in zinc and tungsten with the help of radiopure $ZnWO_4$ crystal scintillators, J. Phys. G **38**, 115107 (2011).
96. P. Belli et al., Search for double-β decays of ^{96}Ru and ^{104}Ru by ultra-low background HPGe γ spectrometry, Eur. Phys. J. A **42**, 171—177 (2009).
97. P. Belli et al., Search for double β decays of ^{96}Ru and ^{104}Ru with high purity Ge γ spectrometry, Nucl. Phys. At. Energy **11**, 362—366 (2010).
98. P. Belli et al., New limits on $2\beta^+$ decay processes in ^{106}Cd, Astropart. Phys. **10**, 115—120 (1999).
99. P. Belli et al., First results of the experiment to search for 2β decay of ^{106}Cd with the help of $^{106}CdWO_4$ crystal scintillators, Proc. Int. Conf. NPAE-Kyiv2010, 7—12.06.2010, Kyiv, Ukraine — Kyiv, 2011, p. 428—431.
100. P. Belli et al., Search for 2β decay of cerium isotopes with $CeCl_3$ scintillator, J. Phys. G **38**, 015103 (2011).

101. P. Belli et al., First search for double β decay of dysprosium, Nucl. Phys. A **859**, 126—139 (2011).
102. P. Belli et al., First search for double β decay of platinum by ultra-low background HP Ge γ spectrometry, Eur. Phys. J. A **47**, 91 (2011).
103. P. Belli et al., Search for 2β processes in ^{64}Zn with the help of $ZnWO_4$ crystal scintillator, Phys. Lett. B **658**, 193—197 (2008).
104. P. Belli et al., Investigation of β decay of ^{113}Cd, Phys. Rev. C **76**, 064603 (2007).
105. P. Belli et al., Development of enriched $^{106}CdWO_4$ crystal scintillators to search for double β decay processes in ^{106}Cd, Nucl. Instr. Meth. A **615**, 301—306 (2010).
106. P. Belli et al., First results of the experiment to search for 2β decay of ^{106}Cd with the help of $^{106}CdWO_4$ crystal scintillators, AIP Conf. Proc. **1304**, 354—358 (2010).
107. P. Belli et al., ^{7}Li solar axions: Preliminary results and feasibility studies, Nucl. Phys. A **806**, 388—397 (2008).
108. P. Belli et al., Search for ^{7}Li solar axions using resonant absorption in LiF crystal: Final results, Phys. Lett. B **711**, 41—45 (2012).
109. P. Belli et al., Charge conservation and electron lifetime: Limits from a liquid xenon scintillator, Astropart. Phys. **5**, 217—219 (1996).
110. P. Belli et al., New experimental limit on the electron stability and non-paulian transitions in Iodine atoms, Phys. Lett. B **460**, 236—241 (1999).
111. P. Belli et al., Quest for electron decay $e^- \to \nu_e \gamma$ with a liquid xenon scintillator, Phys. Rev. D **61**, 117301 (2000).
112. P. Belli et al., New limits on the nuclear levels excitation of ^{127}I and ^{23}Na during charge nonconservation, Phys. Rev. C **60**, 065501 (1999).
113. P. Belli et al., Charge non-conservation restrictions from the nuclear levels excitation of ^{129}Xe induced by the electron's decay on the atomic shell, Phys. Lett. B **465**, 315—322 (1999).
114. P. Belli et al., Performances of a CeF_3 crystal scintillator and its application to the search for rare processes, Nucl. Instr. Meth. A **498**, 352—361 (2003).
115. P. Belli et al., Search for double-β decay processes in ^{106}Cd with the help of a $^{106}CdWO_4$ crystal scintillator, Phys. Rev. C **85**, 044610 (2012).
116. P. Belli et al., Search for α decay of natural europium, Nucl. Phys. A **789**, 15—29 (2007).
117. P. Belli et al., Intrinsic radioactivity of a $Li_6Eu(BO_3)_3$ crystal and α decays of Eu, Nucl. Instr. Meth. A **572**, 734—738 (2007).
118. P. Belli et al., Radioactive contamination of $ZnWO_4$ crystal scintillators, Nucl. Instr. Meth. A **626—627**, 31—38 (2011).
119. P. Belli et al., First observation of α decay of ^{190}Pt to the first excited level ($E_{exc} = 137.2$ keV) of ^{186}Os, Phys. Rev. C **83**, 034603 (2011).
120. G. Bellini al., High sensitivity 2β decay study of ^{116}Cd and ^{100}Mo with the BOREXINO counting test facility (CAMEO project), Eur. Phys. J. C **19**, 43—55 (2001).
121. G. Bellini et al., High sensitivity quest for Majorana neutrino mass with the BOREXINO counting test facility, Phys. Lett. B **493**, 216—228 (2000).
122. G. Bellini et al., Search for solar axions emitted in the M1-transition of $^{7}Li^*$ with Borexino CTF, Eur. Phys. J. C **54**, 61—72 (2008).

123. S. Belogurov et al., $CaMoO_4$ Scintillation Crystal for the Search of ^{100}Mo Double Beta Decay, IEEE Nucl. Sci. **52**, 1131—1135 (2005).
124. E. Bellotti et al., A new experimental limit on electron stability, Phys. Lett. B **124**, 435—438 (1983).
125. P. Benetti et al., First results from a dark matter search with liquid argon at 87 K in the Gran Sasso underground laboratory, Astropart. Phys. **28**, 495—507 (2008).
126. J. Benziger et al., A scintillator purification system for the Borexino solar neutrino detector, Nucl. Instr. Meth. A **587**, 277—291 (2008).
127. C. Berger et al., Lifetime limits on $(B - L)$-violating nucleon decay and dinucleon decay modes from the Frejus experiment, Phys. Lett. B **269**, 227—233 (1991).
128. L. Bergstrom, Non-baryonic dark matter: Observational evidence and detection methods, Rep. Prog. Phys. **63**, 793—842 (2000).
129. G. Bertone, D. Hooper, J. Silk, Particle dark matter: Evidence, candidates and constraints, Phys. Rept. **405**, 279—390 (2005).
130. R. Bernabei et al., On the investigation of possible systematics in WIMP annual modulation search, Eur. Phys. J. C **18**, 283 (2000).
131. R. Bernabei et al., The DAMA/LIBRA apparatus, Nucl. Instr. Meth. A **592**, 297—315 (2008).
132. R. Bernabei et al., First results from DAMA/LIBRA and the combined results with DAMA/NaI, Eur. Phys. J. C **56**, 333—355 (2008).
133. R. Bernabey et al., Production of high-pure Cd and ^{106}Cd for $CdWO_4$ and $^{106}CdWO_4$ scintillators, Metallofizika i Noveishije Tekhnologii **30**, 477—486 (2008) (in Russian).
134. R. Bernabei et al., The DAMA/LIBRA apparatus, Nucl. Instr. Meth. A **592**, 297—315 (2008).
135. R. Bernabei et al., Performances and potentialities of a $LaCl_3$:Ce scintillator, Nucl. Instr. Meth. A **555**, 270—281 (2005).
136. R. Bernabei et al., Performances of the ≈100 kg NaI(Tl) set-up of the DAMA experiment at Gran Sasso, Nuovo Cim. A **112**, 545—575 (1999).
137. R. Bernabei et al., Improved limits on WIMP — ^{19}F elastic scattering and first limit on the 2EC2ν ^{40}Ca decay by using a low radioactive CaF_2(Eu) scintillator, Astropart. Phys. **7**, 73—76 (1997).
138. R. Bernabei et al., A search for spontaneous emission of heavy clusters in the ^{127}I nuclide, Eur. Phys. J. A **24**, 51—56 (2005).
139. R. Bernabei et al., Search for charge non-conserving processes in ^{127}I by coincidence technique. Eur. Phys. J. C **72**, 1920 (2012).
140. R. Bernabei et al., The search for rare processes with DAMA/LXe, Proc. Int. Conf. "Beyond 2003", Tegernsee, Germany, 9—14 June 2003, Springer, 2004, p. 365—374.
141. R. Bernabei et al., Search for possible charge non-conserving decay of ^{139}La into ^{139}Ce with $LaCl_3$(Ce) scintillator, Ukr. J. Phys. **51**, 1037—1043 (2006).
142. R. Bernabei et al., Search for the nucleon and di-nucleon decay into invisible channels, Phys. Lett. B **493**, 12—18 (2000).
143. R. Bernabei et al., Search for rare processes with DAMA/LXe experiment at Gran Sasso, Eur. Phys. J. A **27**, s01, 35—41 (2006).

144. R. Bernabei et al., Search for axions by Primakoff effect in NaI crystals, Phys. Lett. B **515**, 6—12 (2001).
145. R. Bernabei et. al., Feasibility of $\beta\beta$ decay searches with Ce isotopes using CeF_3 scintillators, Nuovo Cim. A **110**, 189—195 (1997).
146. R. Bernabei, P. Belli, F. Cappella et al., Dark matter search, Riv. Nuovo Cim. **26**, No. 1, 1—73 (2003).
147. M. Berglund and M.E. Wieser, Isotopic compositions of the elements 2009 (IUPAC Technical Report), Pure Appl. Chem. **83**, 397—410 (2011).
148. R. Bernabei et al., Investigation of $\beta\beta$ decay modes in ^{134}Xe and ^{136}Xe, Phys. Lett. B **546**, 23—28 (2002).
149. J. Bernabeu, A. De Rujula, C. Jarlskog, Neutrinoless double electron capture as a tool to measure the electron neutrino mass, Nucl. Phys. B **223**, 15—28 (1983).
150. T. Bernatowicz, J. Brannon, R. Brazzle, R. Cowsik, C. Hohenberg, and F. Podosek, Neutrino mass limits from a precise determination of 2β-decay rates of ^{128}Te and ^{130}Te, Phys. Rev. Lett. **69**, 2341—2344 (1992).
151. *Particle dark matter. Observations, Models and Searches*, edited by G. Bertone (Cambridge University Press, 2010), 762 p.
152. K. van Bibber, Design for a practical laboratory detector for solar axions, Phys. Rev. D **39**, 2089—20993 (1989).
153. J.B. Birks, *Theory and Practice of Scintillation Counting* (Pergamon, London, 1964).
154. R.S. Boiko et al., Characterisation of scintillation crystals for cryogenic experimental search for rare events, Annual Rep. INR NASU 2008 — Kyiv, 2009, p. 79.
155. R. Bonetti et al., First observation of spontaneous fission and search for cluster decay of ^{232}Th, Phys. Rev. C **51**, 2530—2533 (1995).
156. R. Bonetti, A. Guglielmetti, Measurements on cluster radioactivity — present experimental status, in *Heavy Elements and Related New Phenomena*, ed. by W. Greiner, R.K. Gupta (World Sci., Singapore, 1999), Vol. 2, p. 643—672.
157. Borexino Collaboration, G. Alimonti et al., Light propagation in a large volume liquid scintillator, Nucl. Instrum. Meth. A **440**, 360—371 (2000).
158. Borexino Collaboration, G. Alimonti et al., Science and technology of Borexino: A real time detector for low energy solar neutrinos, Astropart. Phys. **16**, 205—234 (2002).
159. Borexino Collaboration, G. Alimonti et al., The Borexino detector at the Laboratori Nazionali del Gran Sasso, Nucl. Instrum. Meth. A **600**, 568—593 (2009).
160. Borexino Collaboration, C. Arpesella et al., Direct measurement of the ^{7}Be solar neutrino flux with 192 days of Borexino data, Phys. Rev. Lett. **101**, 091302 (2008).
161. Borexino Collaboration, M. Balata et al., Search for electron antineutrino interactions with the Borexino Counting Test Facility at Gran Sasso, Eur. Phys. J. C **47**, 21—30 (2006).
162. Borexino Collaboration, H.O. Back et al., New experimental limits on heavy neutrino mixing in ^{8}B decay obtained with the Borexino Counting Test Facility, JETP Lett. **78**, 261—266 (2003).
163. Borexino Collaboration, H.O. Back et al., Pulse-shape discrimination with the Counting Test Facility, Nucl. Instr. Meth. A **584**, 98—113 (2008).

164. Borexino Collaboration, H.O. Back et al., Study of the neutrino electromagnetic properties with the prototype of the Borexino detector, Phys. Lett. B **563**, 35—47 (2003).
165. A. Boyarsky, A. Neronov, O. Ruchayskiy, M. Shaposhnikov, I. Tkachev, Strategy for searching for a dark matter sterile neutrino, Phys. Rev. Lett. **97**, 261302 (2006).
166. L. De Braeckeleer et al., Measurement of the $\beta\beta$-Decay Rate of ^{100}Mo to the First Excited 0^+ State of ^{100}Ru, Phys. Rev. Lett. **86**, 3510—3513 (2001).
167. R.L. Brodzinski, F.T. Avignone III, J.I. Collar, H. Courant et al., Status report on the International Germanium Experiment, Nucl. Phys. B. (Proc. Suppl.) **31**, 76—81 (1993).
168. V.B. Brudanin, N.I. Rukhadze, Ch. Briancon, V.G. Egorov et al., Search for double beta decay of ^{48}Ca in the TGV experiment, Phys. Lett. B **495**, 63—68 (2000).
169. D.A. Bryman et al., Search for massive neutrinos in the decay $\pi \to e\nu$, Phys. Rev. Lett. **50**, 1546—1549 (1983).
170. E. Bukhner et al., Rare decays of mercury nuclei, Sov. J. Nucl. Phys. **52**, 193—197 (1990).
171. S.F. Burachas et al., A search for ^{160}Gd double beta decay using GSO scintillators, Phys. At. Nucl. **58**, 153—157 (1995).
172. B. Caccianiga, M.G. Giammarchi, Neutrinoless double beta decay with Xe-136 in BOREXINO and the BOREXINO Counting Test Facility, Astropart. Phys. **14**, 15—31 (2000).
173. C.M. Cattadori et al., Observation of β decay of ^{115}In to the first excited level of ^{115}Sn, Nucl. Phys. A **748**, 333—347 (2005).
174. C.M. Cattadori et al., Observation of β decay of ^{115}In to the first excited level of ^{115}Sn, Nucl. Phys. A **748**, 333—347 (2005).
175. S. Cebrian et al., Bolometric WIMP search at Canfranc with different absorbers, Astropart. Phys. **21**, 23—34 (2004).
176. R. Cerulli et al., Performances of a BaF_2 detector and its application to the search for $\beta\ \beta$ decay modes in ^{130}Ba, Nucl. Instr. Meth. A **525**, 535—543 (2004).
177. G.V. Chibisov, Astrophysical upper limits on the photon rest mass, Sov. Phys. Usp. **19**, 624—626 (1976).
178. M. Chen, The SNO liquid scintillator project, Nucl. Phys. B (Proc. Suppl.) **145**, 65—68 (2005).
179. H.-Y. Cheng, The strong CP problem revisited, Phys. Rep. **158**, 1—89 (1988).
180. Y. Chikashige, R.N. Mohapatra, and R.D. Peccei, Are there real goldstone bosons associated with broken lepton number? Phys. Lett. B **98**, 265—268 (1981).
181. Y. Chikashige, R.N. Mohapatra, and R.D. Peccei, Spontaneously broken lepton number and cosmological constraints on the neutrino mass spectrum, Phys. Rev. Lett. **45**, 1926—1929 (1980).
182. B.T. Cleveland et al., Measurement of the solar electron neutrino flux with the Homestake chlorine detector, Astrophys. J. **496**, 505—526 (1998).
183. N. Coron et al., Our -short- experience at IAS and within ROSEBUD with radioactive contaminations in scintillating bolometers: uses & needs, presented at the Workshop on Radiopure scintillators for EURECA (RPSCINT 2008), 9—10 September 2008, Kyiv, Ukraine, p. 12, arXiv:0903.1539 [nucl-ex].

184. C. Cozzini et al., Detection of the natural α decay of tungsten, Phys. Rev. C **70**, 064606 (2004).
185. F.A. Danevich, O.V. Ivanov, V.V. Kobychev, V.I. Tretyak, Heat flow of the Earth and resonant capture of solar ^{57}Fe axions, Kinemat. Phys. Cell. Bodies **25**, 102—106 (2009).
186. F.A. Danevich et al., α activity of natural tungsten isotopes, Phys. Rev. C **67**, 014310 (2003).
187. F.A. Danevich et al., $CdWO_4$, ZnSe and $ZnWO_4$ scintillators in studies of 2β-processes, Instr. Exp. R. **32**, 1059—1064 (1989).
188. F.A. Danevich, V.V. Kobychev, S.S. Nagorny, V.I. Tretyak, YAG:Nd crystals as possible detector to search for 2β and α decay of neodymium, Nucl. Instr. Meth. A **541**, 583—589 (2005).
189. F.A. Danevich et al., Investigation of β^+ β^+ and β^+/EC decay of ^{106}Cd, Z. Physik A **355**, 433—437 (1996).
190. F.A. Danevich et al., Application of $PbWO_4$ crystal scintillators in experiment to search for 2β decay of ^{116}Cd, Nucl. Instr. Meth. A **556**, 259—265 (2006).
191. F.A. Danevich, V.I. Tretyak, Radioactive contamination of scintillators, submitted to Astropart. Phys.
192. F.A. Danevich et al., $ZnWO_4$ crystals as detectors for 2β decay and dark matter experiments, Nucl. Instr. Meth. A **544**, 553—564 (2005).
193. F.A. Danevich et al., Effect of recrystallisation on the radioactive contamination of $CaWO_4$ crystal scintillators, Nucl. Instr. Meth. A **631**, 44—53 (2011).
194. F.A. Danevich et al., Two-neutrino 2β decay of ^{116}Cd and new half-life limits on 2β decay of ^{180}W and ^{186}W, Nucl. Phys. A **717**, 129—145 (2003).
195. F.A. Danevich, On R&D of radiopure crystal scintillators for low counting experiments, Proc. 1st Int. Workshop, Radiopure Scintillators for EURECA, RPScint'2008, 9—10 Sept. 2008, Institute for Nuclear Research, Kyiv, Ukraine, arXiv:0903.1539 [nucl-ex].
196. F.A. Danevich et al., $MgWO_4$ — A new crystal scintillator, Nucl. Instr. Meth. A **608**, 107—115 (2009).
197. F.A. Danevich et al., Feasibility study of $PbWO_4$ and $PbMoO_4$ crystal scintillators for cryogenic rare events experiments, Nucl. Instr. Meth. A **622**, 608—613 (2010).
198. F.A. Danevich et al., Ancient Greek lead findings in Ukraine, Nucl. Instr. Meth. A **603**, 328—332 (2009).
199. F.A. Danevich et al., Beta decay of ^{113}Cd, Phys. Atom. Nucl. 59 (1996) 1—5.
200. F.A. Danevich et al., Search for 2β decay of cadmium and tungsten isotopes: Final results of the Solotvina experiment, Phys. Rev. C **68**, 035501 (2003).
201. F.A. Danevich et al., Quest for double beta decay of ^{160}Gd and Ce isotopes, Nucl. Phys. A **694**, 375—391 (2001).
202. D. Dassie, R. Eschbach, F. Hubert, Ph. Hubert, Two-neutrino double-β decay measurement of ^{100}Mo, Phys. Rev. D **51**, 2090—2100 (1995).
203. J. Dawson et al., A search for various double beta decay modes of tin isotopes, Nucl. Phys. A **799**, 167—180 (2008).
204. A.V. Derbin et al., Search for solar axions emitted in an M1 transition in ^{7}Li* nuclei, JETP Lett. **81**, 365—370 (2005).

205. A.V. Derbin et al., Search for resonant absorption of solar axions emitted in M1 transition in ^{57}Fe nuclei, Eur. Phys. J. C **62**, 755—760 (2009).
206. A.V. Derbin et al., New limit on the mass of 14.4-keV solar axions emitted in an M1 transition in ^{57}Fe nuclei, Phys. At. Nucl. **74**, 596—602 (2010).
207. A.V. Derbin et al., Search for resonant absorption of solar axions emitted in an M1 transition in ^{57}Fe nuclei, JETP Lett. **85**, 12—16 (2007).
208. A.V. Derbin, O.Ju. Smirnov, Search for the neutrino radiative decay with the prototype of the Borexino detector, JETP Lett. **76**, 483—487 (2002).
209. A.V. Derbin et al., Experiment on antineutrino scattering by electrons at a reactor of the Rovno nuclear power plant, JETP Lett. **57**, 768—772 (1993).
210. A. Derbin, A. Ianni, O. Smirnov, Comment on the statistical analysis in "A new experimental limit for the stability of the electron" by H.V. Klapdor-Kleingrothaus, I.V. Krivosheina and I.V. Titkova, arXiv:0704.2047v1 [hep-ex].
211. L. Devis jr., A.S. Goldhaber, M.M. Nieto, Limit on the photon mass deduced from Pioneer-10 observation of Jupiter's magnetic field, Phys. Rev. Lett. **35**, 1402—1405 (1975).
212. M. Dine, W. Fischler, M. Srednicki, A simple solution to the strong CP problem with a harmless axion, Phys. Lett. B **104**, 199—202 (1981).
213. F.E. Dix, Ph. D. Thesis (Case Western Reserve University, 1970).
214. S. Dodelson, L. Widrow, Sterile neutrinos as dark matter, Phys. Rev. Lett. **72**, 17—20 (1994).
215. C. Dörr, H.V. Klapdor-Kleingrothaus, New Monte-Carlo simulation of the Heidelberg—Moscow double beta decay experiment, Nucl. Instr. Meth. A **513**, 596—621 (2003).
216. U. Dore, D. Orestano, Experimental results on neutrino oscillations, Rep. Prog. Phys. **71**, 106201 (2008).
217. S.L. Dubovsky, V.A. Rubakov, P.G. Tinyakov, Brane world: Disappearing massive matter, Phys. Rev. D **62**, 105011 (2000).
218. S.L. Dubovsky, V.A. Rubakov, P.G. Tinyakov, Is the electric charge conserved in brane world? JHEP **08**, 041 (2000).
219. S.L. Dubovsky, Tunneling into extra dimension and high-energy violation of Lorentz invariance, JHEP **01**, 012 (2002).
220. H. Ejiri et al., Limit on the Majorana neutrino mass and right-handed weak current by neutrinoless double β-decay of ^{100}Mo, Phys. Rev. C **63**, 065501 (2001).
221. H. Ejiri, K. Fushimi, T. Kamada, H. Kinoshita et al., Double beta decay of ^{100}Mo, Phys. Lett. B **258**, 17—23 (1991).
222. H. Ejiri, K. Fushimi, R. Hazama, M. Kawasaki, Double beta decays of ^{116}Cd, J. Phys. Soc. Jpn. **64**, 339—343 (1995).
223. H. Ejiri et al., Search for exotic K X-rays from neutral iodine atoms and limits on charge non-conservation, Phys. Lett. B **282**, 281—287 (1992).
224. H. Ejiri et al., Limits on charge nonconservation studied by nuclear excitation of ^{127}I, Phys. Rev. C **44**, 502—505 (1991).
225. H. Ejiri, Double beta decays and neutrino masses, J. Phys. Soc. Japan **74**, 2101—2127 (2005).
226. S. Eliseev et al., Resonant enhancement of neutrinoless double-electron capture in ^{152}Gd, Phys. Rev. Lett. **106**, 052504 (2011).
227. S.R. Elliot, J. Engel, Double-beta decay, J. Phys. G **30**, R183—R215 (2004).

228. S.R. Elliot, A.A. Hahn, M.K. Moe, M.A. Nelson, M.A. Vient, Double beta decay of ^{82}Se, Phys. Rev. C **46**, 1535—1537 (1992).
229. S.R. Elliot, P. Vogel, Double beta decay, Ann. Rev. Nucl. Part. Sci. **52**, 115—151 (2002).
230. http://physics.nist.gov/PhysRefData/Star/Text/contents.html.
231. J.C. Evans Jr., R.I. Steinberg, Nucleon stability: A geochemical test independent of decay mode, Science **197**, 989—991 (1977).
232. G. Feinberg, M. Goldhaber, Microscopic tests of symmetry principles, Proc. Nat. Acad. Sci. U.S. **45**, 1301—1312 (1959).
233. G. Fiorentini, M. Lissia, F. Mantovani, Geo-neutrinos and Earth's interior, Phys. Rep. **453**, 117—172 (2007).
234. E. Fiorini, CUORE: a cryogenic underground observatory for rare events, Phys. Rep. **307**, 309—317 (1998).
235. E.L. Fireman, The depth dependence of ^{37}Ar from ^{39}K and the backgound in solar neutrino studies, Proc. Int. Conf. "Neutrino'77", Baksan Valley, USSR, 18—24 June 1977, Moscow, Nauka, 1978, v. 1, p. 53—59; R.I. Steinberg, J.C. Evans Jr., Decay-mode-independent tests of nucleon stability, Proc. Int. Conf. "Neutrino'77", Baksan Valley, USSR, 18—24 June 1977, Moscow, Nauka, 1978, v. 2, p. 321—326.
236. R.B. Firestone et al., *Table of isotopes* (John Wiley, New York, 1996).
237. G.N. Flerov et al., Spontaneous fission of Th^{232} and stability of nucleons, Sov. Phys. Dokl. **3**, 79—81 (1958).
238. A. Friedland, M. Giannotti, Astrophysical bounds on photons escaping into extra dimensions, Phys. Rev. Lett. **100**, 031602 (2008).
239. K. Fujikawa, R.E. Shrock, Magnetic moment of a massive neutrino and neutrino-spin rotation, Phys. Rev. Lett. **45**, 963—966 (1980).
240. W.H. Furry, On transition probabilities in double beta-disintegration, Phys. Rev. **56**, 1184—1193 (1939).
241. S. Gales et al., Exotic nuclear decay of ^{223}Ra by emission of ^{14}C nuclei, Phys. Rev. Lett. **53**, 759—762 (1984).
242. GALLEX Collaboration, W. Hampel et al., GALLEX solar neutrino observations: Results for GALLEX IV, Phys. Lett. B **447**, 127—133 (1999).
243. A. Gando et al., Measurement of the double-β decay half-life of ^{136}Xe with the KamLAND-Zen experiment, Phys. Rev. C **85**, 045504 (2012).
244. Yu.M. Gavriljuk et al., New stage of search for 2K(2ν) capture of ^{78}Kr, Phys. Atom. Nucl. **69**, 2124—2128 (2006).
245. Yu.M. Gavriljuk, A.M. Gangapshev, V.V. Kuzminov, S.I. Panasenko and S.S. Ratkevich, Results of a search for 2β decay of ^{136}Xe with high-pressure copper proportional counters in Baksan Neutrino Observatory, Phys. Atom. Nucl. **69**, 2129—2133 (2006).
246. G.B. Gelmini, M. Roncadelli, Left-handed neutrino mass scale and spontaneously broken lepton number, Phys. Lett. B **99**, 411—415 (1981).
247. A.Sh. Georgadze et al., Evaluation of activities of impurity radionuclides in cadmium tungstate crystals, Instr. Exp. Technique **39**, 191—198 (1996).
248. H. Georgi, L. Randall, Charge conjugation and neutrino magnetic moments, Phys. Lett. B **244**, 196—202 (1990).

249. Gemma Collaboration, A.G. Beda et al., GEMMA experiment: Three years of the search for the neutrino magnetic moment, Phys. Part. Nucl. Lett. **7**, 406—409 (2010).
250. R.H. Gillette, Calcium and cadmium tungstate as scintillation counter crystals for gamma-ray detection, Rev. Sci. Instr. **21**, 294—301 (1950).
251. L. Gironi, et al., Performance of $ZnMoO_4$ crystal as cryogenic scintillating bolometer to search for double beta decay of molybdenum, JINST **5**, P11007 (2010).
252. L. Gironi et al., $CdWO_4$ bolometers for double beta decay search, Opt. Mat. **31**, 1388—1392 (2008).
253. A. Giuliani, Searches for neutrinoless double beta decay, Acta Phys. Pol. B **41**, 1447—1468 (2010).
254. A. Giuliani, Searches for neutrinoless double beta decay, Acta Phys. Pol. B **41**, 1447—1468 (2010).
255. J.-F. Glicenstein, New limits on nucleon decay modes to neutrinos, Phys. Lett. B **411**, 326—329 (1997).
256. GNO Collaboration, M. Altmann et al., Complete results for five years of GNO solar neutrino observations, Phys. Lett. B **616**, 174—190 (2005).
257. M. Goeppert-Mayer, Double Beta-Disintegration, Phys. Rev. **48**, 512—516 (1935).
258. G. Goessling et al., Experimental study of ^{113}Cd β decay using CdZnTe detectors, Phys. Rev. C **72**, 064328 (2005).
259. J.J. Gomez-Cadenas, J. Martin-Albo, M. Mezzetto, F. Monrabal, M. Sorel, The search for neutrinoless double beta decay, Riv. Nuovo Cim. **35**, 29—98 (2012).
260. W.E. Greth et al., Beta instability in ^{113}Cd, J. Inorg. Nucl. Chem. **32**, 2113—2117 (1970).
261. M. Gunther et al., Heidelberg—Moscow $\beta\beta$ experiment with ^{76}Ge: Full setup with five detectors, Phys. Rev. D **55**, 54—67 (1997).
262. A. Guglielmetti et al., Nonobservation of ^{12}C cluster decay of ^{114}Ba, Phys. Rev. C **56**, 2912—2916 (1997).
263. W.C. Haxton, K.Y. Lee, Red-giant evolution, metallicity, and new bounds on hadronic axions, Phys. Rev. Lett. **66**, 2557—2560 (1991).
264. C. Hagner et al., Experimental search for the neutrino decay $\nu_3 \to \nu_j + e^+ + e^-$ and limits on neutrino mixing, Phys. Rev. D **52**, 1343—1352 (1995).
265. H. Hidaka, C.V. Ly, K. Suzuki, Geochemical evidence of the double β decay of ^{100}Mo, Phys. Rev. C **70**, 025501 (2004).
266. M. Hirsch et al., Nuclear structure calculation of $\beta^+\beta^+$, β^+/EC and EC/EC decay matrix elements, Z. Phys. A **347**, 151—161 (1994).
267. S. Holjevic, B.A. Logan, A. Ljubicic, Nuclear level excitation during charge nonconservation, Phys. Rev. C **35**, 341—343 (1987).
268. G. 't Hooft, Symmetry breaking through Bell-Jackiw anomalies, Phys. Rev. Lett. **37**, 8—11 (1976).
269. J.C. Huang, Stability of the electron in the SU(5) and GWS models, J. Phys. G **13**, 273—284 (1987).
270. F. Iachello, J. Barea, Proc. XIV Int. Workshop on "Neutrino Telescopes", Venice, Italy, March 2011, in press.
271. The ILIAS database on radiopurity of materials, http://radiopurity.in2p3.fr/.

272. A.S. Iljinov, M.V. Mebel, S.E. Chigrinov, Properties of nuclear radioactivity induced by nucleon instability, Sov. J. Nucl. Phys. **37**, 18—26 (1983).
273. L.I. Ivleva et al., Growth and properties of $ZnMoO_4$ single crystals, Crystallography Reports **53**, 1087—1090 (2008).
274. K. Jakovcic et al., A search for solar hadronic axions using ^{83}Kr, Rad. Phys. Chem. **71**, 793—794 (2004).
275. Kamiokande Collaboration, K. S. Hirata et al., Observation of ^{8}B solar neutrinos in the Kamiokande-II detector, Phys. Rev. Lett. **63**, 16—19 (1989).
276. KamLAND Collaboration, S. Abe et al., Precision measurement of neutrino oscillation parameters with KamLAND, Phys. Rev. Lett. **100**, 221803 (2008).
277. KamLAND Collaboration, K. Eguchi et al., High sensitivity search for $\tilde{\nu}_e$'s from the Sun and other sources at KamLAND, Phys. Rev. Lett. **92**, 071301 (2004).
278. K2K Collaboration, M.H. Ahn et al., Measurement of neutrino oscillation by the K2K experiment, Phys. Rev. D **74**, 072003 (2006).
279. M. Kauer (on behalf of the SuperNEMO Collaboration), Calorimeter R&D for the SuperNEMO double beta decay experiment, J. Phys.: Conf. Ser. **160**, 012031 (2009).
280. A. Kawashima, K. Takahashi, A. Masuda, Geochemical estimation of the half-life for the double beta decay of ^{96}Zr, Phys. Rev. C **47**, R2452 (1993).
281. M.F. Kidd, J.H. Esterline, W. Tornow, A.S. Barabash, V.I. Umatov, New results for double-beta decay of ^{100}Mo to excited final states of ^{100}Ru using the TUNL-ITEP apparatus, Nucl. Phys. A **821**, 251—261 (2009).
282. J.E. Kim, G. Carosi, Axions and the strong CP problem, Rev. Mod. Phys. **82**, 557—601 (2010).
283. J.E. Kim, Light pseudoscalars, particle physics and cosmology, Phys. Rep. **150**, 1—177 (1987).
284. J.E. Kim, Weak-interaction singlet and strong CP invariance, Phys. Rev. Lett. **43**, 103—107 (1979).
285. H.J. Kim, et al., Proc. of New View in Particle Physics (VIETNAM'2004), August 5—11, 2004, p. 449.
286. H.J. Kim et al., Neutrino-less double beta decay experiment using $Ca^{100}MoO_4$ scintillation crystals, IEEE Trans. Nucl. Sci. **57**, 1475—1480 (2010).
287. T. Kirsten, H. Richter, E. Jessberger, Rejection of evidence for nonzero neutrino rest mass from double beta decay, Phys. Rev. Lett. **50**, 474—477 (1983).
288. H.V. Klapdor-Kleingrothaus, A. Dietz, H.L. Harney, I.V. Krivosheina, Evidence for neutrinoless double beta decay, Mod. Phys. Lett. A **16**, 2409—2420 (2001).
289. H.V. Klapdor-Kleingrothaus, I.V. Krivosheina, A. Dietz, O. Chkvorets, Search of neutrinoless double beta decay ^{76}Ge in Gran Sasso 1990—2003, Phys. Lett. B **586**, 198—212 (2004).
290. H.V. Klapdor-Kleingrothaus, I.V Krivosheina, The evidence for the observation of $0\nu\beta\beta$ decay: the identification of $0\nu\beta\beta$ events from the full spectra, Mod. Phys. Lett. A **21**, 1547—1556 (2006).
291. H.V. Klapdor-Kleingrothaus et al., Latest results from the Heidelberg—Moscow double beta decay experiment, Eur. Phys. J. A **12**, 147—154 (2001).
292. H.V. Klapdor-Kleingrothaus, A. Staudt, *Non-accelerator Particle Physics* (IoP, Philadelphia, 1995), 531 p.

293. H.V. Klapdor-Kleingrothaus, I.V. Krivosheina, I.V. Titkova, A new experimental limit for the stability of the electron, Phys. Lett. B **644**, 109—118 (2007).
294. H.V. Klapdor-Kleingrothaus et al., GENIUS-TF: A test facility for the GENIUS project, Nucl. Instr. Meth. A **481**, 149—159 (2002).
295. A.A. Klimenko et al., Search for annual and daily dark matter modulations with Ge detectors at Baksan, Phys. At. Nucl. **61**, 1129—1136 (1998).
296. A.A. Klimenko et al., Experimental limit on the charge non-conserving β decay of ^{73}Ge, Phys. Lett. B **535**, 77—84 (2002).
297. M. Kobayashi, S. Kobayashi, Neutrinoless double-beta decay of ^{160}Gd, Nucl. Phys. A **586**, 457—465 (1995).
298. M. Kortelainen, J. Suhonen, Nuclear matrix elements of $0\nu2\beta$ decay with improved short-range correlations, Phys. Rev. C **76**, 024315 (2007).
299. E.L. Koval'chuk, A.A. Pomanskii, A.A. Smol'nikov, A new experimental limit of the $e^- \to \nu_e + \gamma$ decay, JETP Lett. **29**, 145—148 (1979).
300. G.P. Kovtun, A.P. Shcherban', D.A. Solopikhin, V.D. Virich, Z.I. Zelenskaja et al., Production of radiopure natural and isotopically enriched cadmium and zinc for low background scintillators, Functional Materials **18**, 121—127 (2011).
301. H. Kraus et al., EURECA — The European future of cryogenic dark matter searches, J. Phys.: Conf. Series **39**, 139—141 (2006).
302. H. Kraus et al., EURECA — the European future of dark matter searches with cryogenic detectors, Nucl. Phys. B (Proc. Suppl.) **173**, 168—171 (2007).
303. H. Kraus et al., $ZnWO_4$ scintillators for cryogenic dark matter experiments, Nucl. Instr. Meth. A **600**, 594—598 (2009).
304. H. Kraus et al., EURECA — setting the scene for scintillators, Proc. 1st Int. Workshop, Radiopure Scintillators for EURECA, RPScint'2008, 9—10 Sept. 2008, Institute for Nuclear Research, Kyiv, Ukraine, arXiv:0903.1539 [nucl-ex].
305. M. Krcmar et al., Search for solar axions using ^{7}Li, Phys. Rev. D **64**, 115016 (2001).
306. M. Krcmar et al., Search for solar axions using ^{57}Fe, Phys. Lett. B **442**, 38—42 (1998).
307. M.I. Krivoruchenko, F. Simkovic, D. Frekers, A. Faessler, Resonance enhancement of neutrinoless double electron capture, Nucl. Phys. A **859**, 140—171 (2011).
308. R.F. Lang, W. Seidel, Search for dark matter with CRESST, New J. Phys. **11**, 105017 (2009).
309. P. Langacker, Grand unified theories and proton decay, Phys. Rep. **72**, 185—385 (1981).
310. J. Learned, F. Reines, A. Soni, Limits on nonconservation of Baryon Number, Phys. Rev. Lett. **43**, 907—910 (1979).
311. V.N. Lebedenko et al., Result from the First Science Run of the ZEPLIN-III Dark Matter Search Experiment, Phys. Rev. D **80**, 052010 (2009).
312. H.S. Lee et al., Limits on interactions between weakly interacting massive particles and nucleons obtained with CsI(Tl) crystal detectors, Phys. Rev. Lett. **99**, 091301 (2007).
313. H.S. Lee et al., Development of low background CsI(Tl) crystals for WIMP search, Nucl. Instr. Meth. A **571**, 644—650 (2007).

314. S.J. Lee et al., The Development of a Cryogenic Detector with $CaMoO_4$ Crystals for Neutrinoless Double Beta Decay Search, Astropart. Phys. **34**, 732—737 (2011).
315. B.W. Lee, R.E. Shrock, Natural suppression of symmetry violation in gauge theories: Muon- and electron-lepton-number nonconservation, Phys. Rev. D **16**, 1444—1473 (1977).
316. S.T. Lin et al., New limits on spin-independent and spin-dependent couplings of low-mass WIMP dark matter with a germanium detector at a threshold of 220 eV, Phys. Rev. D **79**, 061101 (2009).
317. W.J. Lin et al., Double beta-decay of tellurium-128 and tellurium-130, Nucl. Phys. A **481**, 484—493 (1988).
318. W.J. Lin et al., Geochemically measured half-lives of ^{82}Se and ^{130}Te, Nucl. Phys. A **481**, 477—483 (1988).
319. A. Ljubicic, In search for axions, Rad. Phys. Chem. **74**, 443—453 (2005).
320. LSD Collaboration, M. Aglietta et al., Upper limit on the solar anti-neutrino flux according to LSD data, JETP Lett. **63**, 791—795 (1996).
321. LSND Collaboration, A. Aguilar et al., Evidence for neutrino oscillations from the observation of $\tilde{\nu}_e$ appearance in a $\tilde{\nu}_\mu$ beam, Phys. Rev. D **64**, 112007 (2001).
322. R.A. Lyttleton, H. Bondi, On the physical consequences of a general excess of charge, Proc. Roy. Soc. London A **252**, 313—333 (1959).
323. E. Majorana, Teoria simmetrica dell'elettrone e del positrone, Nuovo Cimento **14**, 171—184 (1937).
324. W.J. Marciano, A.I. Sanda, Exotic decays of the muon and heavy leptons in gauge theories, Phys. Lett. B **67**, 303—305 (1977).
325. P. de Marcillac, N. Coron, G. Dambier, J. Leblanc, J.P. Moalic, Experimental detection of α-particles from the radioactive decay of natural bismuth, Nature **422**, 876—878 (2003).
326. P.D. Marcillac, private communication (2008).
327. E. der Mateosian and M. Goldhaber, Limits for lepton-nonconserving double beta decay of Ca 48, Phys. Rev. **146**, 810—815 (1966).
328. A.P. Meshik et al., Weak decay of ^{130}Ba and ^{132}Ba: Geochemical measurements, Phys. Rev. C **64**, 035205 (2001).
329. A.P. Meshik et al., ^{130}Te and ^{128}Te double beta decay half-lives, Nucl. Phys. A **809**, 275—289 (2008).
330. V.B. Mikhailik et al., Cryogenic scintillators in searches for extremely rare events, J. Phys. D **39**, 1181—1191 (2006).
331. V.B. Mikhailik, H. Kraus, Performance of scintillation materials at cryogenic temperatures, Phys. Stat. Sol. B **247**, 1583—1599 (2010).
332. H.S. Miley, F.T. Avignone III, R.L. Brodzinski, J.I. Collar et al., Suggestive evidence for the two-neutrino double-β decay of ^{76}Ge, Phys. Rev. Lett. **65**, 3092—3095 (1990).
333. MiniBooNE Collaboration, A.A. Aguilar-Arevalo et al., Event excess in the MiniBooNE search for $\tilde{\nu}_\mu \to \tilde{\nu}_e$ oscillations, Phys. Rev. Lett. **105**, 181801 (2010).
334. MINOS Collaboration, P. Adamson et al., Measurement of neutrino oscillations with the MINOS detectors in the NuMI beam, Phys. Rev. Lett. **101**, 131802 (2008).

335. M. Minowa, K. Itakura, S. Moriyama, W. Ootani, Measurement of the property of cooled lead molybdate as a scintillator, Nucl. Instr. Meth. A **320**, 500—503 (1992).
336. O.G. Miranda, T.I. Rashba, A.I. Rez, J.F.W. Valle, Constraining the neutrino magnetic moment with anti-neutrinos from the sun, Phys. Rev. Lett. **93**, 051304 (2004).
337. A. Mirizzi, D. Montanino, P.D. Serpico, Revisiting cosmological bounds on radiative neutrino lifetime, Phys. Rev. D **76**, 053007 (2007).
338. L.W. Mitchel et al., Rare decays of cadmium and tellurium, Phys. Rev. C **38**, 895—899 (1988).
339. M.K. Moe, F. Reines, Charge conservation and the lifetime of the electron, Phys. Rev. B **140**, 992—998 (1965).
340. R.N. Mohapatra, Possible nonconservation of electric charge, Phys. Rev. Lett. **59**, 1510—1512 (1987).
341. R.N. Mohapatra et al., Theory of neutrinos: a white paper, Rep. Prog. Phys. **70**, 1757—1867 (2007).
342. R.N. Mohapatra et al., Neutrino mass, bulk majoron and neutrinoless double beta decay, Phys. Lett. B **491**, 143—147 (2000).
343. R.J. Moon, Inorganic crystals for the detection of high energy particles and quanta, Phys. Rev. **73**, 1210—1210 (1948).
344. A. Morales et al., Improved constraints on WIMPs from the international germanium experiment IGEX, Phys. Lett. B **532**, 8—14 (2002).
345. B.J. Mount et al., Q value of ^{115}In $\rightarrow$ ^{115}Sn(3/2+): The lowest known energy β decay, Phys. Rev. Lett. **103**, 122502 (2009).
346. L.L. Nagornaya et al., Tungstate and molybdate scintillators to search for dark matter and double beta decay, IEEE Trans. Nucl. Sci. **56**, 2513—2518 (2009).
347. K. Nakamura et al. (Particle Data Group), The Review of Particle Physics, J. Phys. G **37**, 075021 (2010).
348. T. Namba, Results of a search for monochromatic solar axions using ^{57}Fe, Phys. Lett. B **645**, 398—401 (2007).
349. P. Nath, P.F. Perez, Proton stability in grand unified theories, in strings and in branes, Phys. Rep. **441**, 191—317 (2007).
350. J. Ninkovic et al., New technique for the measurement of the scintillation efficiency of nuclear recoils, Nucl. Instrum. Meth. A **564**, 567—578 (2006).
351. E.B. Norman, J.N. Bahcall, M. Goldhaber, Improved limit on charge conservation derived from ^{71}Ga solar neutrino experiments, Phys. Rev. D **53**, 4086—4088 (1996).
352. E.B. Norman, A.G. Seamster, Improved test of nucleon charge conservation, Phys. Rev. Lett. **43**, 1226—1229 (1979).
353. I. Ogawa, R. Hazama, H. Miyawaki et al., Search for neutrino-less double beta decay of ^{48}Ca by CaF_2 scintillator, Nucl. Phys. A **730**, 215—223 (2004).
354. I. Ogawa et al., Double beta decay study of ^{48}Ca by CaF_2 scintillator, Nucl. Phys. A **721**, C525—C528 (2003).
355. L.B. Okun, Note on testing charge conservation and the Pauli exclusion principle, Phys. Rev. D **45**, VI.10—VI.14 (1992).
356. L.B. Okun, *Lepton and Quarks* (North-Holland, Amsterdam, 1982), p. 181—183.

357. L.B. Okun, Tests of electric charge conservation and the Pauli principle, Sov. Phys. Usp. **32**, 543—547 (1989).
358. L.B. Okun, Ya.B. Zeldovich, Paradoxes of unstable electron, Phys. Lett. B **78**, 597—600 (1978).
359. R.D. Peccei, H.R. Quinn, Constraints imposed by CP conservation in the presence of pseudoparticles, Phys. Rev. D **16**, 1791—1797 (1977).
360. R.D. Peccei, H.R. Quinn, CP conservation in the presence of pseudoparticles, Phys. Rev. Lett. **38**, 1440—1443 (1977).
361. D.H. Perkins, Proton decay experiments, Ann. Rev. Nucl. Part. Sci. **34**, 1—52 (1984).
362. F. Piquemal, The SuperNEMO project, Phys. Atom. Nucl. **69**, 2096—2100 (2006).
363. S. Pirro et al., Development of bolometric light detectors for double beta decay searches, Nucl. Instr. Meth. A **559**, 361—363 (2006).
364. S. Pirro et al., Scintillating double-beta-decay bolometers, Phys. Atom. Nucl. **69**, 2109—2116 (2006).
365. D.N. Poenaru, M. Ivascu, Estimation of the alpha decay half-lives, Journal de Physique, **44**, 791—796 (1983).
366. D.N. Poenaru, W. Greiner, New island of cluster emitters, Phys. Rev. C **47**, 2030—2037 (1993).
367. A.A. Pomansky, Proc. Int. Neutrino Conf., Aachen, Germany, 1976, Braunschweig, Vieweg, 1977, p. 671.
368. G.G. Raffelt, Axions — motivation, limits and searches, J. Phys. A **40**, 6607—6620 (2007).
369. G.G. Raffelt, *Stars as Laboratories for Fundamental Physics* (University Chicago Press, Chicago, 1997), 664 p.
370. G.G. Raffelt, Neutrino radiative-lifetime limits from the absence of solar γ rays, Phys. Rev. D **31**, 3002—3004 (1985).
371. S. Rahaman et al., Q values of the ^{76}Ge and ^{100}Mo double-beta decays, Phys. Lett. B **662**, 111—116 (2008).
372. F. Reines, C.L. Cowan, Conservation of the number of nucleons, Phys. Rev. **96**, 1157—1158 (1954).
373. D. Reusser et al., Limits on cold dark matter from the Gotthard Ge experiment, Phys. Lett. B **255**, 143—145 (1991).
374. W. Rodejohann, Neutrino-less double beta decay and particle physics, Int. J. Mod. Phys. E **29**, 1833—1930 (2011).
375. H.J. Rose, G.A. Jones, A new kind of natural radioactivity, Nature **307**, 245—247 (1984).
376. A. Roy et al., Further experimental test of nucleon charge conservation through the reaction $^{113}\mathrm{Cd} \to {}^{113m}\mathrm{In}$ + neutrals, Phys. Rev. D **28**, 1770—1772 (1983).
377. V.A. Rubakov, Large and infinite extra dimensions, Phys. Usp. **44**, 871—893 (2001).
378. N.I. Rukhadze et al., New limits on double beta decay of ^{106}Cd, Nucl. Phys. A **852**, 197—206 (2011).
379. N.I. Rukhadze et al., Search for double beta decay of ^{106}Cd in TGV-2 experiment, J. Phys.: Conf. Ser. **203**, 012072 (2010).

380. SAGE Collaboration, J.N. Abdurashitov et al., Measurement of the solar neutrino capture rate by SAGE and implications for neutrino oscillations in vacuum, Phys. Rev. Lett. **83**, 4686—4689 (1999).
381. A. Sandulescu, D.N. Poenaru, F. Greiner, A new decaying mode of heavy nuclei intermediate between nuclear fission and α decay, Sov. J. Part. Nucl. **11**, 528—541 (1980).
382. V. Sanglard et al. (EDELWEISS Collaboration), Final results of the EDELWEISS-I dark matter search with cryogenic heat-and-ionization Ge detectors, Phys. Rev. D **71**, 122002 (2005).
383. J. Schechter, J.W.F. Valle, Neutrino masses in SU(2)$\times$U(1) theories, Phys. Rev. D **22**, 2227—2235 (1980).
384. M.A. Shifman, A.I. Vainstein, V.I. Zakharov, Can confinement ensure natural CP invariance of strong interaction? Nucl. Phys. B **166**, 493—506 (1980).
385. S. Schönert et al., The GERmanium Detector Array (Gerda) for the search of neutrinoless $\beta\beta$ decays of ^{76}Ge at LNGS, Nucl. Phys. B (Proc. Suppl.) **145**, 242—245 (2005).
386. R.E. Shrock, General theory of weak processes involving neutrinos. II. Pure leptonic decays, Phys. Rev. D **24**, 1275—1309 (1981).
387. A. De Silva, M.K. Moe, M.A. Nelson, M.A. Vient et al., Double β decays of ^{100}Mo and ^{150}Nd, Phys. Rev. C **56**, 2451—2467 (1997).
388. F. Simkovic, A. Faessler, V. Rodin, P. Vogel, J. Engel, Anatomy of the $0\nu2\beta$ nuclear matrix elements, Phys. Rev. C **77**, 045503 (2008).
389. F. Simkovic, M.I. Krivoruchenko and A. Faessler, Neutrinoless double-beta decay and double-electron capture, Prog. Part. Nucl. Phys. **66**, 446—451 (2011).
390. SNO Collaboration, B. Aharmim et al., Determination of the ν_e and total ^{8}B solar neutrino fluxes using the Sudbury Neutrino Observatory phase I data set, Phys. Rev. C **75**, 045502 (2007).
391. SNO Collaboration, Q.R. Ahmad et al., Measurement of the rate of $\nu_e + d \to$ $\to p{+}p{+}e^-$ interactions produced by ^{8}B solar neutrinos at the Sudbury Neutrino Observatory, Phys. Rev. Lett. **87**, 071301 (2001).
392. SNO Collaboration, B. Aharmim et al., Electron antineutrino search at the Sudbury Neutrino Observatory, Phys. Rev. D **70**, 093014 (2004).
393. N.J.C. Spooner, Direct dark matter searches, J. Phys. Soc. Japan **76**, 111016 (2007).
394. S.D. Steffen, Dark-matter candidates. Axions, neutralinos, gravitinos, and axinos, Eur. Phys. J. C **59**, 557—588 (2009).
395. R.I. Steinberg et al., Experimental test of charge conservation and the stability of the electron, Phys. Rev. D **12**, 2582—2586 (1975).
396. http://www.srim.org.
397. F. Suekane, T. Iwamoto, H. Ogawa, O. Tajima and H. Watanabe (for the KamLAND RCNS Group), An overview of the KamLAND 1-kiloton liquid scintillator, arXiv:physics/0404071.
398. Z. Sujkowski, S. Wycech, Neutrinoless double electron capture: A tool to search for Majorana neutrinos, Phys. Rev. C **70**, 052501 (2004).
399. A.W. Sunyar, M. Goldhaber, K-electron capture branch of Sr^{87m}, Phys. Rev. **120**, 871—873 (1960).

400. SuperKamiokande Collaboration, J.P. Cravens et al., Solar neutrino measurements in Super-Kamiokande-II, Phys. Rev. D **78**, 032002 (2008).
401. Super-Kamiokande Collaboration, Y. Fukuda et al., Evidence for oscillation of atmospheric neutrinos, Phys. Rev. Lett. **81**, 1562—1567 (1998).
402. SuperKamiokande Collaboration, Y. Gando et al., Search for $\tilde{\nu}_e$ from the Sun at Super-Kamiokande-I, Phys. Rev. Lett. **90**, 171302 (2003).
403. Y. Suzuki et al., Study of invisible nucleon decay, $n \to \nu\nu\bar{\nu}$, and a forbidden nuclear transition in the Kamiokande detector, Phys. Lett. B **311**, 357—361 (1993).
404. N. Takaoka, Y. Motomura, K. Nagao, Half-life of ^{130}Te double-β decay measured with geologically qualified samples, Phys. Rev. C **53**, 1557—1561 (1996).
405. A. Terashima et al., R&D for possible future improvements of KamLAND, J. Phys. Conf. Ser. **120**, 052029 (2008).
406. M. Torres, H. Vucetich, Limits on charge non-conservation from possible seasonal variations of the solar neutrino experiments, Mod. Phys. Lett. A **19**, 639—644 (2004).
407. V.I. Tretyak, V.Yu. Denisov, Yu.G. Zdesenko, New limits on dinucleon decay into invisible channels, JETP Lett. **79**, 106—108 (2004).
408. V.I. Tretyak, Yu.G. Zdesenko, Experimental limits on the proton life-time from the neutrino experiments with heavy water, Phys. Lett. B **505**, 59—63 (2001).
409. V.I. Tretyak, False starts in history of searches for 2β decay, or Discoverless double beta decay, AIP Conf. Proc. **1417**, 129—133 (2011).
410. V.I. Tretyak, Yu.G. Zdesenko, Tables of double beta decay data, At. Data Nucl. Data Tables **6**, 43—90 (1995).
411. V.I. Tretyak, Yu.G. Zdesenko, Tables of double beta decay data — an update, At. Data Nucl. Data Tables **80**, 83—116 (2002).
412. V.I. Tretyak, Semi-empirical calculation of quenching factors for ions in scintillators, Astropart. Phys. **33**, 40—53 (2010).
413. V.I. Tretyak et al., The NEMO-3 results after completion of data taking, AIP Conf. Proc. **1471**, 125—128 (2011).
414. S.P. Tretyakova, G.A. Pik-Pichak, A.A. Ogloblin, The present state and prospects of cluster radioactivity research, Prog. Theor. Phys. Suppl. **146**, 530—535 (2002).
415. A.L. Turkevich, T.E. Economou, G.A. Cowan, Double beta decay of ^{238}U, Phys. Rev. Lett. **67**, 3211—3214 (1991).
416. S. Umehara, T. Kishimoto, I. Ogawa et al., Neutrino-less double-β decay of ^{48}Ca studied by CaF_2(Eu) scintillators, Phys. Rev. C **78**, 058501 (2008).
417. S.C. Vaidya et al., Experimental limit for nucleon stability against charge-nonconserving decay, Phys. Rev. D **27**, 486—492 (1983).
418. A.A. Vasenko, I.V. Kirpichnikov, V.A. Kuznetsov, A.S. Starostin et al., New results in the ITEP/YePI double beta-decay experiment with enriched germanium detectors, Mod. Phys. Lett. A **5**, 1299—1306 (1990).
419. S.I. Vasil'ev, A.A. Klimenko, S.B. Osetrov, A.A. Pomanskii, A.A. Smol'nikov, Observation of the excess of events in the experiment on the search for a two-neutrino double beta decay of ^{100}Mo, JETP Lett. **51**, 622—626 (1990).
420. J.D. Vergados, H. Ejiri, F. Simkovic, Theory of neutrinoless double beta decay, Rep. Prog. Phys. **75**, 106301 (2012).
421. J.D. Vergados, The neutrinoless double beta decay from a modern perspective, Phys. Rept. **361**, 1—56 (2002).

422. M.B. Voloshin, G.V. Mitselmakher, R.A. Eramzhyan, Conversion of an atomic electron into a positron and double $\beta+$ decay, JETP Lett. **35**, 656—659 (1982).
423. M.B. Voloshin, L.B. Okun, Conservation of electric charge, JETP Lett. **28**, 145—149 (1978).
424. J.-C. Vuilleumier, J. Busto, J. Farine, V. Jurgens et al., Search for neutrinoless double-β decay in ^{136}Xe with a time projection chamber, Phys. Rev. D **48**, 1009—1020 (1993).
425. S.C. Wang, H.T. Wong, M. Fujiwara, Measurement of intrinsic radioactivity in a GSO crystal, Nucl. Instr. Meth. A **479**, 498—510 (2002).
426. S. Weinberg, A new light boson? Phys. Rev. Lett. **40**, 223—226 (1978).
427. S. Weinberg, Photons and gravitons in S-matrix theory: Derivation of charge conservation and equality of gravitational and inertial mass, Phys. Rev. B **135**, 1049—1056 (1964).
428. W. Westphal et al., Dark-matter search with CRESST, Czech. J. Phys. **56**, 535—542 (2006).
429. M.E. Wieser, J.R. De Laeter, Evidence of the double β decay of zirconium-96 measured in 1.8×10^9 year-old zircons, Phys. Rev. C **64**, 024308 (2001).
430. J.S.E. Wieslander et al., Smallest known Q value of any nuclear decay: The rare β^- decay of ^{115}In(9/2+) $\rightarrow$ ^{115}Sn(3/2+), Phys. Rev. Lett. **103**, 122501 (2009).
431. F. Wilczek, Problem of strong P and T invariance in the presence of instantons, Phys. Rev. Lett. **40**, 279—282 (1978).
432. R.G. Winter, Double K capture and single K capture with positron emission, Phys. Rev. **100**, 142—144 (1955).
433. S. Yoshida et al., CANDLES project for double beta decay of ^{48}Ca, Nucl. Phys. B (Proc. Suppl.) **138**, 214—216 (2005).
434. Yu.G. Zdesenko, V.I. Tretyak, To what extent does the latest SNO result guarantee the proton stability? Phys. Lett. B **553**, 135—140 (2003).
435. Yu.G. Zdesenko, The future of double β decay research, Rev. Mod. Phys. **74**, 663—684 (2002).
436. Yu.G. Zdesenko et al., Scintillation properties and radioactive contamination of $CaWO_4$ crystal scintillators, Nucl. Instr. Meth. A **538**, 657—667 (2005).
437. Yu.G. Zdesenko et al., Lead molybdate as a low-temperature scintillator in the experimental search for the neutrinoless double beta-decay of ^{100}Mo, Instr. Exp. Technique **39**, 364—368 (1996).
438. Yu.G. Zdesenko, F.A. Danevich, V.I. Tretyak, Sensitivity and discovery potential of the future 2β decay experiments, J. Phys. G **30**, 971—981 (2004).
439. Yu.G. Zdesenko et al., CARVEL experiment with $^{48}CaWO_4$ crystal scintillators for the double β decay study of ^{48}Ca, Astropart. Phys. **23**, 249—263 (2005).
440. Yu.G. Zdesenko, O.A. Ponkratenko, V.I. Tretyak, High sensitivity GEM experiment on 2β decay of ^{76}Ge, J. Phys. G **27**, 2129—2146 (2001).
441. A.R. Zhitnitskii, On possible suppression of the axion-hadron interactions, Sov. J. Nucl. Phys. **31**, 260—267 (1980).
442. Y.F. Zhu et al., Measurement of the intrinsic radiopurity of ^{137}Cs/^{235}U/^{238}U/^{232}Th in CsI(Tl) crystal scintillators, Nucl. Instr. Meth. A **557**, 490—500 (2006).
443. K. Zioutas, S. Andriamonje, V. Arsov et al., First results from the CERN axion solar telescope, Phys. Rev. Lett. **94**, 121301 (2005).
444. K. Zuber, Nd double beta decay search with SNO+, AIP Conf. Proc. **942**, 101—104 (2007).